



THE UNIVERSITY
of ADELAIDE



**DEEP EXPLORATION
TECHNOLOGIES CRC**
Uncovering the future

**The Mesozoic sediments around Andamooka, South Australia; Stratigraphy, geochemistry and
IOCG exploration potential**

Oliver Hughes

Discipline of Geology and Geophysics, School of Earth and Environmental Sciences

University of Adelaide, Adelaide SA 5005 Australia

Supervisor: Dr Robert Dart

Co-Supervisor: Dr Steven Hill

Abstract

The Gawler Craton, South Australia hosts the Olympic Dam Iron Oxide Copper Gold deposit as well as a number of other IOCG, copper, gold, and iron ore deposits. In the Stuart Shelf region (eastern Gawler Craton), primary mineralisation is generally hosted within basement granites and volcanics of the Hiltaba Suite. Basement rock, potentially containing mineralisation, on the Stuart Shelf is often overlain and concealed by Adelaidean sequences as well as highly weathered, altered and complex Mesozoic cover sequences. These sedimentary basin sediments can conceal mineralisation and are a major frontier for mineral explorers to overcome. Identification of key physical, chemical and biological interfaces, such as basal gravels, redox zones and palaeosols, within the cover sequences and understanding the processes which have led to their formation can be a useful tool in exploration.

Andamooka, South Australia lies on the Stuart Shelf near the southern margin of the Eromanga Basin. Exposed Mesozoic sediments of the Eromanga basin at Andamooka are in close proximity to the Olympic Dam IOCG deposit and are therefore important in understanding dispersion patterns within the cover sequences of elements and minerals associated with IOCG type mineral systems. This understanding can be used for further exploration in the area, where mineralisation may be concealed by Mesozoic sediments.

The purpose of this paper is to describe the Mesozoic sediments around Andamooka, identifying any key interfaces and to devise a geochemical footprint of the Mesozoic sediments in this area, which can be used to aid exploration. Gold, nickel, zinc, lead and copper are found to be elevated in multiple regions within the Mesozoic stratigraphy. Several geochemical conceptual models are presented, including; a detrital source of gold and base metals in the basal region of the Algebuckina Sandstone, and a relationship between base metal accumulation and a major redox zone in the Cadna-owie Formation. Other outcomes of this study include; A proposed structural framework of the region, where extensional block faulting has impacted the landscape structure and the relative

positions of Mesozoic sequences, and a revision of previous geological mapping. As well as, a possible mechanism for the formation and distribution of opals within the Bulldog Shale, as a direct result of oxidation of pyrite and organic material causing the breakup of aluminosilicates.

Key words: Andamooka, Mesozoic, IOCG, mineral exploration, cover sequence, redox, ferruginisation, opal

Contents

1. INTRODUCTION	7
1.1. IOCG exploration on the Stuart Shelf	7
1.2. Key interfaces	8
1.3. Project aims	9
1.4. Significance	9
2. BACKGROUND INFORMATION	10
2.1. The study area	10
2.2. Geological setting	10
2.3. Landscape setting	11
2.4. Previous work	11
3. METHODOLOGY	16
3.1. Geological and regolith mapping	16
3.2. Sampling	16
3.3. Sample descriptions	17
3.4. Stratigraphic logging	17
3.5. Geochemical assays	17
3.6. HyLogger	18
4. RESULTS	18

4.1. Stratigraphic logging of exposed sections	18
4.1.1. HyLogger	19
4.1.2. Thin section	19
4.1.3. Stratigraphic logs	20
4.2. Geochemistry	24
4.2.1. Gold anomalies	24
4.2.2. Base metal anomalies	24
4.3. Geological mapping	25
4.4. Bedding readings	26
5. DISCUSSION	26
5.1. Locating the redox controlled ferruginous zones	26
5.2. Determination of rock formation, comparison with type sections	28
5.3. Depositional environments and paleoflow directions	30
5.4. Geochemistry	31
5.4.1. Detrital gold anomaly	31
5.4.2. Base metal anomalies	32
5.5. Source of iron rich fluids	33
5.6. Faulting	35
5.7. Thoughts about opal formation	35

6. CONCLUSIONS	36
7. ACKNOWLEDGEMENTS	37
8. REFERENCES	38
9. FIGURE CAPTIONS	40
10. FIGURES	42
11. TABLES	61
12. APPENDICES	64

1. INTRODUCTION

1.1. IOCG exploration on the Stuart Shelf

The Gawler Craton (Figure 1) in South Australia hosts the Olympic Dam Iron Oxide Copper Gold (IOCG) deposit as well as a number of other IOCG, copper, gold, and iron ore deposits (Hand *et al.* 2007) such as; Prominent Hill, and Carapateena (IOCG)(Belperio *et al.* 2007), Oak Dam (IOCG) (Davidson *et al.* 2007), Mt Gunson (copper) (Knutson *et al.* 1983), Challenger (gold) (Tomkins *et al.* 2004), and Peculiar Knob (iron ore) (Schmidt *et al.* 2007).

In the Stuart Shelf region (eastern Gawler Craton), primary mineralisation is generally hosted within basement granites and volcanics of the Hiltaba Suite. Whilst many other events have affected the Gawler Craton and makeup of the basement geology e.g. Gawler Range Volcanics (1595-1590 Ma), the emplacement of the Hiltaba Suite (1595-1575 Ma) is considered the main source of mineralisation in the region (Budd *et al.* 1998, Hand *et al.* 2007). A distinct mineral system, the Olympic Cu, Au province has been defined in the eastern part of the Gawler Craton (Figure 2)(Bastrakov *et al.* 2007).

Basement rock, potentially containing mineralisation, is often overlain and concealed by Mesozoic 'cover sediments' throughout the Stuart Shelf. Many Australian landscapes have an origin of up to 300 Ma, and during this long history cover sequences have been subjected to a wide range of climates and tectonic events (Smith 1996). As a result, cover sequences can be highly weathered, altered and complex in their stratigraphy and associated chemical and mineralogical properties (Smith 1996). Surface expressions of ore deposits are commonly altered beyond visual recognition throughout these terrains (Smith 1996). Hence cover sediments are often regarded as a barrier to mineral exploration, and are a major frontier for mineral explorers to overcome.

In terms of exploration, some key geochemical questions which are currently facing the Australian mineral exploration industry include (Smith 1996):

- What is the geochemical footprint of a concealed ore body in the overlying cover sediments?
- Do buried ore deposits have a measurable surface or near surface geochemical expression?
- Can large ore systems be distinguished from minor systems at prospect stage?

1.2. Key interfaces

To successfully overcome the cover sediment barrier, and ultimately use this barrier to our advantage, a thorough understanding of the cover sequences is first required. Identification of key interfaces within the cover sequence is one way in which to guide this process of understanding the materials and geochemical signatures within the cover, and the geological processes behind them. Key interfaces within cover sediments can be physical, chemical and/or biological.

- Physical interfaces: Such as associated with unconformities. They include, basal gravels, lags, and accumulations of detrital resistate minerals
- Chemical interfaces: Such as groundwater interfaces, redox fronts and indurations
- Biological interfaces: Such as palaeosols, hydrocarbons and concentrations of microorganisms

Understanding the processes controlling the formation of these key interfaces and characterising the geochemical signatures within them can aid in exploration. Therefore making cover sequences an aid for exploration rather than a hindrance.

Geochemical data obtained from cover sediments can be used to detect target and pathfinder elements, distinguish sediment and regolith materials, estimate the degree of weathering/leaching and locate ferruginous zones/redox fronts, which are potential sites for the accumulation or fixation of target or pathfinder elements (McQueen 2006).

1.3. Project aims

The aims of this project are to describe and define the geochemical characteristics of the Mesozoic sediments (Algebuckina Sandstone, Cadna-owie Formation, Bulldog Shale) around Andamooka, South Australia. These sediments form part of a 'cover' sequence which overlies potential basement mineralisation in the region of the Olympic Cu, Au province. A better geochemical understanding of these cover sediments will aid future exploration for IOCG type mineralisation on the Stuart Shelf of South Australia (Figure 1a). This work is aligned with current research being undertaken by the Deep Exploration Technologies Cooperative Research Centre (DET CRC) project 3.3, entitled 'Geochemical Sampling of Deep Cover'. The objective of this project is to develop geochemical methods for exploration within deep cover materials and integrate such into exploration workflows in drilling, logging and sampling.

1.4. Significance

The Mesozoic sediments of Andamooka are the closest exposed Mesozoic sediments to the Olympic Dam IOCG deposit, and thus have importance in terms of understanding dispersion patterns within cover sediments of elements and minerals associated with IOCG type mineral systems. The geochemical footprint of these sediments can be used to aid future exploration in the cover sediment dominated terrain of the Stuart Shelf. The Mesozoic sequences at Andamooka have not been fully described or differentiated in the past, and geological maps of the area are basic and inaccurate.

To achieve the aims of this study, the Mesozoic sequences at Andamooka were mapped, fully described and stratigraphically logged. Spectral data was used to identify mineralogy, and geochemical data was used to build up a geochemical footprint of cover sequences in this region.

2. BACKGROUND INFORMATION

2.1. The study area

The historic opal mining town of Andamooka is located ~640 km north of Adelaide (Figure 1b) (Direen & Lyons 2007), near the western margin on Lake Torrens. The region has an arid climate with low erratic rainfall with a mean of 194.5 mm/yr with minimal marked seasonal influence, and a high evaporation rate (Carr *et al.* 1979). The area of focus can be seen in Figure 3.

2.2. Geological setting

Andamooka lies within the Stuart Shelf, a province of the Gawler Craton (Houseman *et al.* 1989). The Gawler Craton is a large poorly exposed Archean to Neoproterozoic terrain in South Australia (Belperio *et al.* 2007) (Figure 1). The Neoproterozoic (Adelaidean) Stuart Shelf occupies the eastern margin of the Gawler Craton and is separated from the Adelaide Geosyncline to the east, by the Torrens Hinge Zone (Figure 1). During the Adelaidean, the Stuart Shelf was a stable platform on which only a few hundred metres of sedimentary cover accumulated (Lambert *et al.* 1987). The Adelaidean sediments are generally sub-horizontal and have remained relatively undisturbed since deposition (Rattigan *et al.* 1977). At Andamooka the basal Hiltaba Suite Volcanics are thought to underlie the Adelaidean Arcoona Quartzite from magnetic interpretation, but are not exposed at the surface in the area (Fairclough 2009). Mesozoic sequences, Algebuckina Sandstone, Cadna-owie Formation and Bulldog Shale, lie unconformably over an erosional surface of the Adelaidean Arcoona Quartzite in most of the Andamooka area, except to the north and north east, where the Cambrian Andamooka Limestone overlies the Adelaidean rocks (Figure 3 & 4). The Mesozoic sediments are part of the Eromanga Basin, the largest and most central of three epicontinental depressions which together comprise the Great Artesian Basin (Krieg *et al.* 1995). The Great Artesian Basin is a non-marine to marine Jurassic-Cretaceous super-basin, which covers around a fifth of the Australian continent (Krieg *et al.* 1995) (Figure 5).

2.3. Landscape setting

The topography at Andamooka is typically a single dissected tableland elevated ~130 m above sea level. Well defined channels dissect the landscape exposing lower surfaces and drain eastward into Lake Torrens (Carr *et al.* 1979). Residual Mesozoic sediment material forms prominent mesas and buttes in the area, which are key landscape features.

Extensive longitudinal dune fields cover undissected plateau areas. Most dunes are vegetated however small areas of mobile sand are present (Carr *et al.* 1979).

Vegetation in the area is largely controlled by the land-form. The dissected tablelands mainly support grasses and saltbush, whereas the dune fields host a variety of Acacias, Callitris, Casuarinas and ephemerals. Small trees and shrubs grow in larger drainage depressions (Carr *et al.* 1979).

2.4. Previous work

Limited geological work has been undertaken at Andamooka and the majority of this work focussed on the occurrence of opal in the Bulldog Shale. More extensive geological work on the Mesozoic sequences, particularly the Algebuckina Sandstone and Cadna-owie Formation, has been undertaken in other areas of the Stuart Shelf (Wopfner *et al.* 1970, Wopfner 2010). This work was focused on exposures further to the north in areas such as Mt. Anna (Figure 6).

A study by Carr *et al.* (1979) was aimed at increasing geological knowledge of the Andamooka area in order to improve opal exploration. This document contains useful observations of the Mesozoic sequences around Andamooka but the Algebuckina Sandstone, Cadna-owie Formation and Bulldog Shale are not fully differentiated as separate units.

Wopfner *et al.* (1970) describes the basal Jurassic-Cretaceous rocks of the Eromanga Basin. Basal Jurassic-Cretaceous rocks of the Eromanga Basin described in this study include the Algebuckina

Sandstone, the Cadna-owie Formation and the Mt Anna Sandstone Member. A brief summary of these three formations described by Wopfner *et al.* (1970) is below.

The Mesozoic sedimentary rocks of the Eromanga Basin represent a change from a terrestrial fluvial, fluvio-lacustrine depositional regime in the Late Jurassic to a marine environment in the Early Cretaceous (Wopfner *et al.* 1970). The sequence consists of the Algebuckina Sandstone, Cadna-owie Formation and associated Mt Anna Sandstone Member, and is overlain by the uniform marine Bulldog Shale (Wopfner *et al.* 1970).

The Algebuckina Sandstone is interpreted as a terrestrial, fluvial deposit. It is defined as a formation of medium-grained to conglomeritic arenite beds unconformably overlying pre-Jurassic rocks and overlain, generally disconformably, by the Cadna-owie Formation (Wopfner *et al.* 1970). The type section (Figure 7) locality is a low escarpment south-west of Algebuckina Hill (Figure 6). It is typically white to very light grey due to abundance of kaolin, but secondary ferruginisation has produced some dark-brown discolourations. A key feature of the Algebuckina Sandstone is the decrease in kaolinite content from the base to the top, with the lower parts containing very high levels of kaolinite, grading up to a pure sandstone with no kaolinite at the top (Wopfner *et al.* 1970). The other key features of the Algebuckina Sandstone include; Angular current bedding in the lower two thirds of the sequence, and the absence of detrital feldspar throughout the formation. A basal conglomerate is frequently present consisting of predominantly well-rounded quartz pebbles embedded in kaolinitic sandstone (Wopfner *et al.* 1970). Local silicification has occurred in the upper units of well-sorted sandstones, and these zones typically preserve or host plant fossils. Dating of these fossils, have placed the Algebuckina Sandstone in the Upper Jurassic (Wopfner *et al.* 1970).

At Andamooka, Carr *et al.* (1979) briefly describe the Algebuckina Sandstone as coarse grained, fluvial sediments which are frequently cross-bedded, sometimes bioturbidated, and generally consist almost entirely of quartz grains. Prominent thin, black ferruginous sandstone and grit are locally present at the base.

The Cadna-owie Formation marks the onset of a marine transgression, and is considered the mappable interval between the Algebuckina Sandstone, and the younger Bulldog Shale (Wopfner *et al.* 1970). The type section (Figure 8) is located near Algebuckina Hill (Figure 6). The composition of the Cadna-owie Formation is extremely heterogeneous due to its marginal marine setting, so sections through this unit vary greatly (Wopfner *et al.* 1970). At the type section, the lowest third of the sequence is composed of brown-weathered sandstone of fine to medium grain size, and bedding is poorly defined. The upper units are generally fine to very fine grained sandstone with laminated to very thin bedding. They are generally feldspathic, and grey when fresh. Calcareous beds are characteristic of the upper part of the formation. Carbonate cement is present in varied amounts in several sandstone intervals (Wopfner *et al.* 1970). Other key features include minor feldspar, unorientated muscovite, opaque heavy mineral grains and pyrite concretions. Upper parts of the section are permeated with iron oxides and ferruginous sandstones have formed. Gypsum crystals are also infused in some upper parts (Wopfner *et al.* 1970).

The Mt. Anna Sandstone Member occurs within the upper half of the Cadna-owie Formation in some areas. It is defined as a medium to coarse grained sandstone with abundant red to purple porphyritic rhyolite pebbles (Wopfner *et al.* 1970). This unit is discussed in more detail later.

Wopfner (2010) describes the surface of Gondwana during the Jurassic, termed the 'Gondwana Surface', before deposition of Mesozoic sequences, and the burial history of this surface over time. During the Jurassic, large parts of Gondwana were exposed causing intense weathering and alteration of near surface rocks and development of the Gondwana Surface (Wopfner 2010). The Gondwana surface around the Eromanga Basin occurs on a number of different rocks of different ages depending on what was exposed in each region during that particular period (Wopfner 2010). At Andamooka, it is represented by the Adelaidean Arcoona Quartzite. At other localities, such as Algebuckina Hill near Oodnadatta the surface is on intensely folded Palaeoproterozoic Peake Metamorphics (Wopfner 2010). In summary, the Gondwana Surface is considered a thick weathering

mantle of kaolinised basement which reflects the crustal stability experienced in Gondwana at the time, which followed the termination of the Pangaea depositional phase in the mid-Triassic and the commencement of dispersion of Gondwana fragments in the Late Jurassic to Early Cretaceous (Wopfner 2010).

The first sediments to cover the Gondwana Surface were the fluvial deposits of the Algebuckina Sandstone. These were deposited by large, moderate energy, high volume river systems (Wopfner 2010). Algebuckina Sandstone was deposited in topographic lows, filling in low lying areas.

Algebuckina Sandstone was not initially deposited on palaeo-highs and so some of these highs were not covered until the Early Cretaceous marine transgression (Wopfner 2010).

The sediments of the Cadna-owie Formation were next to be deposited, as a result of the Early Cretaceous marine transgression (Wopfner 2010). The Cadna-owie Formation is considered to have been deposited in a marginal marine type setting. Due to the nature of marginal marine systems, the sequence is highly variable depending local depositional environments (Wopfner 2010). The deposition of the Cadna-owie Formation coincided with expansion of the rift system along the southern margin of Australia related to the break-up of Gondwana fragments (Wopfner 2010). The Mt Anna Sandstone Member occurs within the upper half of the Cadna-owie Formation and contains pebbles of the Gawler Range porphyry (Figure 6) which indicates the formation of a new rift shoulder simultaneous with the marine transgression (Wopfner 2010).

Wopfner (2010) and Wopfner et al. (1970) do not discuss the youngest of the Mesozoic sequences the Bulldog Shale. Carr et al. (1979) doesn't recognize the Cadna-owie Formation as a separate formation, and it is not clear if sediments of this unidentified unit have been lumped together with the older Algebuckina Sandstone, or the younger Bulldog Shale. The Cretaceous sediments are lumped together and termed the Marree Formation. The Marree Formation is described as undifferentiated Cretaceous sediments (Johns 1968). Johns (1968) and Tyler et al. (1990) provide an

overall description of the Marree Formation. A comparison of previous descriptions of the Mesozoic sequences at Andamooka and nearby areas can be seen in Figure 9.

Carr et al. (1979) divides the Marree Formation sediments at Andamooka into three main sub-units. The upper most sub-unit, called *Kopi*, estimated to have been at least 30 m in thickness before erosion, comprising of mainly white, slightly sandy clays with large sub-rounded boulders scattered throughout. A conglomerate band up to 0.2 m thick marks the boundary with the middle sub-unit. This is where opalisation is considered most common. The middle-sub unit, called *mud*, is a light brown, grey or yellow claystone with low sand content and is up to 4 m thick. The basal sub-unit is comprised of up to 4 m of pale yellow to red and brown pebbly silt referred to as *Bulldust* and contains boulders of pre-Mesozoic quartzites up to 1 m in diameter.

The Bulldog Shale has since been identified and mapped at Andamooka (Fairclough 2009). On a regional scale it is considered a grey to black organic-carbon-rich mudstone (Moore & Pitt 1982), deposited in a restricted epicontinental seaway that occupied central Australia in the Early Cretaceous (Frakes & Francis 1988, De Lurio & Frakes 1999).

Tyler et al. (1990) describe the Bulldog Shale as a dark grey shaley mudstone with silty and very fine sand phases with small constituents of shell fragments, flecks of carbonate matter and disseminated patches of sulphide minerals. The basal part contains large water-worn Permian boulders and large fossil logs. The upper parts contain limestone layers occasionally with abundant shell fragments and commonly rich in microfossils (Tyler *et al.* 1990). They suggest the Bulldog Shale is mainly an offshore shelf mud deposit from suspension. The lowest part represents restricted, stagnant marginal marine conditions and the upper part represents a more open oxygenated marine environment indicated by the abundance and diversity of fossil remains (Tyler *et al.* 1990).

Cretaceous and Jurassic sediments at Andamooka have undergone extensive weathering during the Tertiary, and as a result have been highly kaolinised and bleached in places, and extensive silcrete cappings have developed (Carr *et al.* 1979).

3. METHODOLOGY

To aid in further exploration of this and other similar areas a number of outcomes are required, including; Full descriptions of the Mesozoic geology, distributions of rock types and the mechanisms controlling this distribution, and a geochemical footprint of these sediments. A number of methods were undertaken to achieve this including geological and regolith-landform mapping, sampling, sample descriptions, stratigraphic logging, geochemical assaying and HyLogger mineral mapping.

3.1. Geological and regolith mapping

Field descriptions and mapping of the Mesozoic units at Andamooka was undertaken. Several sections were identified and logged where outcrop was available. Surface materials were also noted to give insight into rock types that were once stratigraphically above the current land surface, or materials that have been transported to their current location. The older (Adelaidean) Arcoona Quartzite was also mapped and described as it unconformably underlies the Mesozoic sediments over most of the area. Similarly, the Cambrian Andamooka Limestone was noted in the northern area where it underlies the Mesozoic sediments. As surface exposures are scarce in the region, mapping was achieved by taking point or section locations, and then photo interpreting the approximate boundaries of each mapping unit.

3.2. Sampling

Samples were taken from 6 exposed sections through Mesozoic sequences, as well as numerous point location samples. Rock chips or loose sediment were collected from each rock unit of interest

with care taken to collect material evenly from different parts of the unit. The very outside of the exposed surface was often discarded where possible, and samples were taken from the cleaned surface to reduce the risk of contamination from foreign materials. Approximately 1 kg of material was collected for each sample and stored in plastic sample bags.

3.3. Sample descriptions

The samples taken from exposed sections were described thoroughly, including; grain size and shape, bedding and sedimentary structures, rock strength, rock fabric, degree of sorting, porosity, pH, colour, mottling, induration, segregations, degree of weathering and weathering types and the occurrences of veins and clasts.

Thin sections of selected samples were attempted in the laboratory. Although success was limited due to the soft and/or loose nature of the sample material. One hard rock sample however, was successfully made into a thin section and was viewed using a petrographic microscope.

3.4. Stratigraphic logging

Field logging combined with descriptions in the laboratory were used to produce six profile sections of the Mesozoic sediments around Andamooka labelled AP1 to AP6. Several amendments/variants of these were then constructed from further field observations and further logging of unexposed parts of the initial sections. Logs were first constructed by hand and later digitalized. GPS and tape measurements were used to obtain an accurate distance between samples for logging purposes.

3.5. Geochemical assays

Multi-element geochemical analysis was performed on 47 samples including 5 repeats from profiles AP2, AP3 and AP4, by ACME Laboratories in Canada. The 5 repeat samples were used to determine the precision of the analysis. The samples were prepared by pulverising 250 g of sample to 85% passing 200 mesh. Rare earth and refractory elements were determined by ICP mass spectrometry

following a lithium metaborate / tetraborate fusion and nitric acid digestion of 0.2 g of sample. In addition, a separate 0.5 g split was digested in Aqua Regia and analysed by ICP mass spectrometry to determine precious and base metals.

A full list of elements analysed for, and their units of measure and detection limits can be seen in Appendix 1. Total carbon and total sulphur content was also determined as a percentage. Loss on ignition (LOI) was also recorded as a percentage, and is the weight difference after ignition at 1000°C.

3.6. HyLogger

The HyLogger system characterises dominant mineral species in drill core or rock chips and couples this with a high resolution digital image (Mauger *et al.* 2004). The system uses continuous visible and short-wave infrared spectroscopy to identify minerals. Fifty-seven rock chip samples were logged and imaged at the Primary Industries and Resources South Australia (PIRSA) Glenside Core Library at a spatial resolution of approximately 1 cm (spectral data) and 0.11 mm (image data). These samples correspond to the 57 samples taken in the first four profiles AP1 to AP4. The Hylogger software produces a mineral map of the samples, indicates the dominant minerals in each sample, links this to a digital image and plots the data on an X-Y table.

4. RESULTS

4.1. Stratigraphic logging of exposed sections

The locations of six profiles analysed for this study can be seen in Figure 3 and 16. Profile AP1 and AP2 were taken from a low escarpment near Blue Dam just west of the Andamooka township, previously mapped as undifferentiated Jurassic-Cretaceous sediments of the Algebuckina Sandstone and Cadna-owie Formation (Fairclough 2009). Profile AP3 and AP5 were taken from exposures on a

lower plain just to the west of profile AP1 and AP2, previously mapped as Adelaidean Arcoona Quartzite (Fairclough 2009), however resembling Mesozoic sediments. Profile AP4 was taken from Trigg Bluff, a prominent landscape feature approximately 4 km south-west of the Andamooka township, previously mapped as Algebuckina Sandstone (Carr *et al.* 1979). Profile AP6 was taken from an exposure on a low hill approximately 3.5 km south of the Andamooka township, previously mapped as Bulldog Shale (Fairclough 2009).

A full description of each sample collected from the six profiles can be seen in Appendix 2.

4.1.1. HYLOGGER

The HyLogger system can identify minerals with strong absorption features, such as aluminosilicates, but cannot identify silicate minerals due to high reflectance of the Si-O bond, and lack of strong absorption features. For this reason, quartz and feldspars do not appear on the analyses.

The HyLogger mineral plots (Appendix 3-6) described in Table 1 show plots of samples from profiles AP1 to AP4, starting from the base of the profile (oldest sediments on the left) at depth 0 m, and increasing depth towards the top of the profile (youngest sediments on the right). The depth indicators shown in the HyLogger images are not actual depth of the exposed section, rather a requirement of the software to process the samples. A grey colour indicates that the HyLogger system has not recognised any minerals in that zone.

Discussions of notable mineral occurrences obtained from the HyLogger system can be seen in Table 2.

4.1.2. THIN SECTION

Images of a thin section made of sample 016 at the top of profile AP4 can be seen in Appendix 7. The thin section shows an abundance of sub-rounded quartz grains with minor kaolin cement matrix, possibly containing smaller quartz grains as well as some iron oxide.

4.1.3. STRATIGRAPHIC LOGS

Colours in stratigraphic logs below are based on the actual colour of the exposed rock. The logs include information gathered from field work, laboratory work, geochemical assays and the HyLogger system. GPS co-ordinates of the profiles are given below; the datum used was GDA 94.

Profile AP1, shown in Figure 10 is located at 0712173 mE 6629548 mN. The material in profile AP1 is predominantly white kaolin rich sands ranging from fine to coarse with the majority being medium-sized, and generally rounded to sub-rounded in shape. Secondary ferruginisation has caused colour changes to brown, red and yellow in some instances. Bedding is poorly defined throughout the profile. The rock strength throughout the profile is generally very weak, and material is loose and friable, with the exception of a slight hardening at around 4 m depth. Pyrite concretions occur at various intervals throughout the profile.

The lower part of the profile contains around 5% kaolin. Overprinting of hematite and goethite commonly occurs in intervals or lenses, which tend to follow or are constrained by minor bedding or lamination features. Modern calcite veining is evident. Kaolin content increases to 10% for the interval 8-8.4 m.

A more consolidated region in the upper half of the profile occurs at around 4 m depth. This area has been affected by ferruginisation to a higher degree than the sediments below. Kaolin content drops to around 3%. Sub-angular quartz of coarse grain size occurs in this region. Quartz grains are a mixture of clear and dark red coloured.

A fine, kaolin rich (5%), sub-rounded sand occurs in the upper 2 m of the profile. This region is not greatly affected by ferruginisation and so colours remain light, pale browns. Some fine grained laminated mud is present, and forms hard, brittle thin sheets. Some rounded quartz pebbles (1-2 cm diameter) are present at a depth of 1 m.

Profile AP2, shown in Figure 11 is located at 0712155 mE 6629265 mN. Profile AP2 is highly variable in terms of materials, colours and sedimentary structures. Kaolin is present throughout the profile.

The lower 6.5 m (23-16.5 m) consist of mainly clays with a minor rounded sand interval at a depth of 20 m. Colours range from green to orange to dark red/purple. Kaolin is dominant, with minor gypsum. Laminations and a minor occurrence of cross-bedding are preserved in the lower section.

From a depth of 16.5 m to the surface (0 m), material is generally fine to medium sized rounded to sub-rounded sands, with varying iron oxide and kaolin content. Colours are generally white to pale browns and oranges. Bedding is generally poorly defined. A layer (approximately 1.5 m thick) of ferricrete (Appendix 8) occurs at a depth of around 14 m. This consists of porous sub-rounded, medium-size sand, with a kaolin and iron oxide cement. The unit is bedded, and highly ferruginised. The unit is dark red to purple coloured with minor yellow and red bands. This layer stands out as a bench structure on the side of the hill. The profile is offset laterally approximately 20 m above this layer (Appendix 8). Two carbonaceous beds occur at depths 12-13 m and 0-1.5 m. These beds are finer grained than their surroundings; the lower carbonaceous bed consists of a fine sand, and the upper bed consists of silt. Pyrite concretions occur towards the top of the profile. A small layer of gypsum and kaolin rich material occurs at depth 5-6 m. Large scale cross bedding is seen at round 7 m depth, where beds of up to 0.5 m width cross-cut one another. Some modern calcite veining is present near the top. Quartz grains are generally clear, but in places a mixture of clear and dark red iron-oxide stained grains are present.

Profile AP3, shown in Figure 12 is located at 0712167 mE 6629035 mN. A Photograph of the exposed section is shown in Appendix 9. Profile AP3 is a clay and gypsum rich section. Material is generally homogenous in terms of material, however the colour is variable. Laminations are preserved throughout. Kaolinite and gypsum are the dominant minerals, with minor hematite and goethite.

The lower unit consists of a green to grey clay containing minor red iron-oxide mottles. On top of this is a red hematite stained layer. Red mottling increases in this region. A yellow goethite stained layer is on top of the red layer. This layer contains minor cross-laminations, and mottling is slightly less than the red layer below. The upper layer is green coloured with minor red mottling. Overall, red hematite mottling is present to a degree throughout the entire profile, but increases in the red layer at depth 0.5-0.8 m. Iron-oxide content is relatively low (1-3%), however it has caused significant staining of these clay rich sediments.

Profile AP4, shown in Figure 13a is located at 0714782 mE 6627140 mN. A photograph of the exposed section is shown in Appendix 10. For the purposes of the geochemical analysis below, Figure 13b shows a stratigraphic log of profile AP4 before it was finalised by further field work. This figure only shows stratigraphic units which were sampled for geochemistry.

The lower part of the profile up to 10 m depth contains an abundance of kaolin with minor sands and gypsum. The basal unit consists of green, red and purple laminated clays. A ferruginous band occurs at 19.5-20 m containing about 63% iron-oxide. Gypsum is present at multiple intervals in the lower part of the profile. Pyrite concretions are present at 16 m. A major iron-oxide stained zone occurs from 10.5-14 m. The upper part of this zone is purple coloured and hematite rich and has increased iron-oxide levels (19%), the lower part is yellow coloured and goethite rich but iron-oxide content is only slightly above background levels (4%). Sand intervals are generally sub-rounded to sub-angular and fine grained.

From 10 m to the top of the Algebuckina Sandstone sequence (0 m) material is much sandier and less affected by secondary ferruginisation. Kaolin content decreases from the bottom to the top of this part of the profile. A minor conglomeritic textured bed occurs from 9-10 m, containing small weathered rounded quartz pebbles (1-2 cm) and medium to coarse grained rounded quartz in a kaolin rich matrix. A gypsum rich layer occurs at 8 m. From 8-2 m material is bedded to massive medium grained, rounded sands. Kaolin is present, reducing upwards. A red coloured medium

grained, cross-bedded, rounded sand unit occurs from 1-2 m. This unit contains clear sands, with a hematite stained, kaolin cement. The upper unit of the Algebuckina Sandstone sequence (0-1 m) is a clean sandstone, containing very minor kaolin content. This unit contains fine to medium grained rounded sands, and has been silicified. Large scale cross-bedding is present, with beds of up to 0.5 m cross-cutting one another. This unit hosts fern and bark fossils as shown in Appendix 11.

Profile AP5, shown in Figure 14 is located at 0712142 mE 6629078 mN. A photograph of the exposed section is shown in Appendix 12. Profile AP5 is located 2 m vertically above and 30 m laterally offset from profile AP3.

The basal unit consists of poorly sorted, rounded, medium to coarse sized sands in a kaolin matrix. Sub-angular fine sand is also present in parts. It is a pale cream colour with minor red hematite stained segregations. Sand content varies from 80-90% in sandy segregations to 5% or less in other parts. Kaolinite is the dominant mineral.

A dark purple to red layer occurs between 1.5 and 1.75 m depth. Similar to the unit below, but stained by iron-oxide. A very coarse sand fraction is present.

Above the purple layer is a 40 cm layer consisting of mainly clays. Some layering/laminations are present. This unit is grey coloured with thin layers (1-2 cm) of goethite stained (yellow) or hematite stained (red) clays.

Between 0.3 and 1.1 m sub-angular to sub-rounded sands are dominant, varying from fine to coarse grain size. Kaolin makes up the matrix material. Segregations of varying shape, size and composition occur throughout this zone and include; Sandy red hematite nodules (2-10 cm), grey sandy nodules (2-10 cm), and pure kaolin nodules (1-5 cm). Gypsum is present at a depth of around 0.75 m. The top unit is almost pure kaolinite, with minor segregations of clear sands.

Profile AP6, shown in Figure 15 is located at 0708845 mE 6626004 mN. A Photograph of the exposed section is shown in Appendix 13.

The profile is dominated by highly fractured white carbonaceous shale. The basal unit consists of fine, sub-rounded sand embedded in a kaolin rich cement. The material fines up from a silty, fine sand to a shale from 4.5 -3.5 m depth. This sand-shale interbedded unit is white and kaolinitic. The profile is dominated by mainly white carbonaceous shale from 3.5 m to the surface. A prominent red hematite staining occurs at 3 m, particularly on and around fracture surfaces of the rock. Yellow, goethite staining occurs at 2 m depth. Bedding is well preserved in the upper shale part of the profile, and kaolin is present in places. Gypsum is present at a depth of around 3 m.

4.2. Geochemistry

Although 56 elements were tested for by geochemical analysis, not all were included in the discussion, as it is not practical to do so. Elements that were emitted were those with most values at or below the analytical detection limit. Generally if less than 20% of the samples were above the detection limit then that element would also be ignored. The following elements: Au, Cu, Pb, Zn, Ni, Co, As, In, Mo and W were focussed on, due to their importance in Au and base metal exploration in sediment covered terrains (Smith *et al.* 2000).

4.2.1. GOLD ANOMALIES

Some anomalous Au values (up to 4.9 ppb) occur in the lower third of profile AP4 (Appendix 14). These high Au values do not necessarily correspond to ferruginous zones (Appendix 15). Minor anomalous Au values (up to 6.4 ppb) occur in profile AP2 (Appendix 16). However, again these values do not correspond with ferruginous zones (Appendix 17). Gold was not particularly anomalous in profile AP3, and Au concentration showed no relationship with ferruginisation.

4.2.2. BASE METAL ANOMALIES

Some anomalous values of Ni, Pb, Zn and Cu occur throughout the samples. Nickel shows a very strong positive relationship with Zn (Appendix 18), and Zn shows quite a strong positive relationship

with Pb (Appendix 19). However, no strong relationships are seen between Cu and Zn, Ni, or Pb. Gold shows no strong relationship with any of these base metals.

High values of Ni (up to 102.6 ppm), Zn (up to 364 ppm), Pb (up to 63 ppm) and Cu (up to 36.9 ppm) generally occur in two main regions. Firstly the basal region of profile AP4 (Appendix 20), where Co and Mo are also elevated, and secondly the region under and including the ferricrete layer (14 m depth) in profile AP2 (Appendix 21). The anomalies in the base of AP4 do not necessarily correspond with ferruginous zones; however some influence may be apparent. The anomalies in AP2 show a strong relationship with the ferruginous zone, as they all occur at or below the ferruginous zone.

In profile AP3 some anomalous values occur, particularly Cu, which compared to the other profiles is quite high relative to Ni, Zn and Pb (Appendix 22).

4.3. Geological mapping

A simplified geological map of the study area can be seen in Figure 16. A cross-section through part of this region showing interpreted faulting and field relationships of the outcropping rocks at Andamooka is seen in Figure 17.

An annotated photograph taken facing towards the west on an erosional plain of Bulldog Shale, towards a low hill of Cadna-owie Formation (background), which is near the location of profiles AP1 and AP2 is provided in Appendix 23. A small outcrop of Bulldog Shale can be seen in the mid-ground. Profiles AP3 and AP5 are located at this outcrop.

Other than the relative positions of the Mesozoic sequences throughout the landscape, the only other evidence of faulting is seen in the underlying Adelaidean Arcoona Quartzite. The Arcoona Quartzite in the region is typically flat lying and well bedded (Appendix 24). In an observed faulted region it is very steeply dipping, highly fractured and folded (Appendix 25). The orientation of these faulted zones in the Arcoona Quartzite strike approximately NE-SW.

Differences of the geological map produced to the current map include the differentiation of the Algebuckina Sandstone and the Cadna-owie Formation, interpretation of extensional block faulting, and some minor variations in the distribution of the Arcoona Quartzite and the Bulldog Shale.

4.4. Bedding readings

The number of bedding readings taken was limited, due to the nature and minimal amount of exposed bedrock in the area. A list of the readings acquired is provided in Appendix 26. The overall trend of bedding orientations for the Algebuckina Sandstone and Cadna-owie Formation were gently dipping towards the west.

5. DISCUSSION

5.1. Locating the redox controlled ferruginous zones

Ferruginisation is a key chemical interface. It is controlled by oxidation and reduction of Fe in solution (McQueen 2006). The mobilisation of Fe^{2+} in groundwater under reducing conditions followed by oxidation to Fe^{3+} (i.e. redox reaction) and precipitation causes the formation of ferruginous zones. Resulting iron oxides and iron hydroxides, commonly hematite and goethite, overprint other materials (McQueen 2006). Therefore, ferruginisation can indicate the position of redox boundaries within a sequence which are considered important chemical transition zones. Groundwater movement is one of the main mechanisms of metal dispersion from an ore body through transported overburden (Aspandiar 2004). Metals (such as As, Ba, Bi, Cu, Pb, Sb, Zn) travel in the groundwater and may precipitate due to redox reactions (i.e. oxidation) at the redox front and are adsorbed or incorporated into the chemical structure of minerals such as goethite and hematite (McQueen 2006). Thus, ferruginisation is an important control on the accumulation of target and pathfinder elements and a useful interface for geochemical exploration.

Ferruginisation and the location of redox boundaries can be estimated visually in the field, however this approach is prone to error due to the ability of a small amount of hematite to strongly colour clay-rich sediment (McQueen 2006). A potential indicator of ferruginisation is iron oxide (Fe_2O_3), however this is relative to the abundance of quartz and other iron-free minerals (McQueen 2006). The Fe_2O_3 content of samples taken from profile AP2 can be seen in Appendix 27. The Fe_2O_3 plot indicates two separate ferruginous zones. However field observations suggest only one main ferruginous zone at a depth of around 14 m is present.

Comparing Fe_2O_3 content against an 'immobile' or 'near immobile' element can provide a more precise indicator of ferruginisation (McQueen 2006). Near immobile elements in the regolith include titanium (Ti), zirconium (Zr) and aluminium (Al).

Zirconium is probably the least mobile, as it is concentrated in zircon, a resistate mineral that is extremely stable under most weathering conditions (McQueen 2006). The problem with zircon is that it is not distributed uniformly in sedimentary rocks where sediments have undergone sorting (McQueen 2006). Appendix 27 also shows the ratio of $\text{Fe}_2\text{O}_3/\text{Zr}$ for samples from profile AP2.

Noticeably, there is now only one ferruginous zone. The second zone which appears in the straight Fe_2O_3 plot is possibly due to the higher clay content and reduced quartz content of this part of the profile.

Titanium is also a relatively immobile element and is more abundant and widely hosted than Zr, although in sedimentary rocks most Ti is hosted in rutile and ilmenite, which can also be affected by sedimentary sorting (McQueen 2006). The ratio of $\text{Fe}_2\text{O}_3/\text{TiO}_2$ of samples from profile AP2 is seen in Appendix 27. This figure also supports a single ferruginous zone, and 'smoothes off' many of the minor fluctuations seen in the Fe_2O_3 plot.

Aluminium is also considered a relatively immobile element, and comparison of Al and Fe_2O_3 can be particularly useful for detecting ferruginous zones in weathered sedimentary rocks with highly

variable quartz content. The ratio of $\text{Fe}_2\text{O}_3/\text{Al}_2\text{O}_3$ of samples from profile AP2 is seen in Appendix 27. This ratio also works well, however the plot becomes somewhat misleading towards the top.

Similar observations are observed in samples from profile AP4 (Appendix 28) and AP3 (Appendix 29).

5.2. Determination of rock formation, comparison with type sections

Andamooka lies very near to the margin of the Eromanga Basin, near the south-eastern most extent of the late Jurassic and Cretaceous sediments (Figure 5) (Pewklian *et al.* 2008), which may explain significant differences observed in the stratigraphy of the Mesozoic sequences in this study to those described for the type sections. The Algebuckina Sandstone quite often wedges out in this region (Carr *et al.* 1979), supporting that this area is near the extremities of the basin. Figure 18 shows the rock formations of each profile, and how the profiles relate to each other stratigraphically.

Profile AP1 and AP2 are deemed to be part of the same rock sequence, due to their closeness in position and similar materials and characteristics. Profile AP1 is likely to be the same as the upper part of profile AP2 above the ferricrete layer observed at a depth of 14 m in profile AP2. These two profiles most closely resemble the type section and descriptions of Cadna-owie Formation (Figure 8). Profile AP2 contains multiple carbonaceous beds, and overall the sandstones of profile AP2 and AP1 are highly kaolinitic. Profile AP2 contains ferruginous sandstones, such as the ferricrete layer at 14 m depth and gypsum is present near the top. Pyrite concretions are also present in profile AP2 and AP1 and bedding is poor and not well defined. The ferricrete layer observed (Appendix 8) is quite a laterally extensive unit and is seen in multiple regions where the Cadna-owie Formation was exposed (Appendix 30).

The key differences of profiles AP1 and AP2 to the Cadna-owie Formation type section (Figure 8) described by Wopfner (1970) include; a lack of feldspar, no conglomerate unit near the base and a lack of muscovite grains.

In the subsurface, the Cadna-owie Formation has been described as a single coarsening upwards sequence grading from grey siltstone at the base, to fine or occasionally medium grained calcareous sandstone at the top (Moore & Pitt 1985). The profiles AP1 and AP2 observed at Andamooka fit this description well.

A silicified boulder conglomerate is seen on the land surface above profile AP2, the Cadna-owie Formation profile (Appendix 31). This conglomerate unit may indicate the boundary between the Cadna-owie Formation and the overlying Bulldog Shale. This transition zone contains silicified material at the top of the Cadna-owie Formation (Wopfner *et al.* 1970) and in the basal portion of the Bulldog Shale, large rounded pebbles of Adelaidean Quartzite up to very large boulder size (Krieg & Rogers 1995) and/or Permian aged boulders (Tyler *et al.* 1990). A pebbly conglomerate unit was seen at multiple *in-situ* areas at Andamooka where the Cadna-owie Formation contacted with the Bulldog Shale. It is likely that this lag deposit on the surface of profile AP2 is also part of this conglomerate contact unit.

Profile AP3, AP5 and AP6 are most likely all part of Bulldog Shale sequence, due to their shale and mud-like nature with abundant gypsum and kaolinite. It is also seen in contact with the underlying Cadna-owie Formation in many locations, and a basal conglomeritic unit is often present at this interface. A key difference to Bulldog Shale seen in other areas is a very white colour due to intense weathering. In comparison to the three sub-units of the Marree Formation described above (Carr *et al.* 1979), profile AP6 resembles the upper sub-unit (*Kopi*). Profiles AP3 and AP5 resemble the middle sub-unit (*Mud*), but profile AP3 could possibly be at least in part, the basal sub-unit (*Bulldust*). The surface lag deposit of silicified conglomerate above profile AP2 is likely to be part of the *Bulldust* sub-unit.

Profile AP4 resembles the Algebuckina Sandstone (Figure 7). This profile supports previous descriptions at Trigg Bluff of Algebuckina Sandstone. It contains a lower region of kaolinitic sands, grading up to a relatively clean sandstone on top. The very top unit is silicified and contains fern and

bark fossils (Appendix 11) as described by Carr et al. (1979), Wopfner et al. (1970) and Wopfner (2010). The upper part of profile AP4 is likely to be the Cadna-owie Formation. This zone contains highly kaolinitic sands, as well as rounded quartzite pebbles (1-4 cm).

Wopfner (2010) suggests that the prominence of the Mt. Anna Sandstone Member relative to the Cadna-owie Formation increases towards the source area of the Gawler Ranges where its participation on the total Cadna-owie section is 100 percent (Figure 6). The current directions shown on Figure 6 also suggest that the Mt. Anna Sandstone Member should be significant in the Andamooka area. It would be expected therefore, that the Mt. Anna Sandstone member would participate a higher percentage of the Cadna-owie Formation at Andamooka (near the NW shores of Lake Torrens) than at Mt. Anna, as Andamooka is considerably closer to the source. No rhyolite pebbles were observed in the field area Andamooka and thus the Mt. Anna Sandstone Member was not identified. It is possible that the relative percentage of Mt. Anna Sandstone Member is more of a locally controlled feature, rather than just a feature of how proximal or distal the location is from the Gawler Ranges. Mt. Anna Sandstone Member material may have accumulated in drainage channels or deltas causing local variations in relative Mt. Anna Sandstone Member participation. Even though Wopfner (2010) has not identified the presence of Cadna-owie Formation (Figure 6) at Andamooka, it would still be expected that Mt. Anna Sandstone Member would be present at Andamooka if this hypothesis was correct.

5.3. Depositional environments and paleoflow directions

At the beginning of deposition the environment is interpreted as being a moderate to high energy braided river system environment, due to the occurrence of rounded pebbles at the base of the Algebuckina (Wopfner 2010). The direction of paleoflow would therefore be highly affected by the changes in direction of the braided rivers and this may explain the reason why we see multiple apparent paleoflow directions from the limited bedding readings and field observations. The Cadna-owie Formation also provides complex paleoflow flow directions. This formation is a transgressive

marginal marine formation and thus has many different depositional systems affecting the flow direction (e.g. beach sands, fans and deltas, and shallow marine), which would all have unique flow directions within a relatively close proximity of each other. Fans and deltas would be affected by the direction of flow from topographic highs into the ocean. Beach sands are affected by wind direction, as well as wave motion. Shallow marine sediments are affected by current direction.

The Cadna-owie Formation was deposited in a complex of local environments associated with the marine transgression (Wopfner *et al.* 1970, Tyler *et al.* 1990, Wopfner 2010). Tyler *et al.* (1990) suggest that the occurrence of quiet backwater lagoons and swamps would have been present in this environment and they could have produced chemically reducing conditions. These conditions would allow for the formation of pyrite and carbonaceous beds within the Cadna-owie Formation, as seen at Andamooka (Figure 11).

5.4. Geochemistry

5.4.1. DETRITAL GOLD ANOMALY

Since the Au anomaly observed in profile AP4 has no relationship with ferruginisation and occurs at the base of the unit; it is likely that this is a detrital type Au anomaly.

An important consideration with this type of anomaly is the land surface and depositional environment, as this type of anomaly forms simultaneously with deposition. Wopfner (2010) describes the surface at the time of deposition as being very old and weathered. Exposed rocks varied depending on what was exposed in a particular area. It is likely that basement rock containing mineralisation, such as the Hiltaba Suite or Adelaidean rocks may have been exposed in areas nearby to Andamooka. As the Algebuckina Sandstone began to deposit, erosion of this material containing Au mineralisation could have taken place, and the prominent regolith profile of the time stripped by these large river systems, causing a detrital Au anomaly within the basal units.

In terms of exploration, an interesting but highly difficult and complex technique would be to try and locate some of these palaeochannels of Algebuckina Sandstone and measure palaeoflow in an attempt to trace the Au anomaly upstream to the source. This is where the identification of key interfaces becomes important when trying to track particular units over considerable distances. This type of exploration involves building up a knowledge of a palaeosurface in order to track metal anomalies and determine the positions of source materials within the palaeo-landscape.

5.4.2. BASE METAL ANOMALIES

The base metal anomalies (Zn, Pb, Ni, Cu) which occur at the base of Algebuckina Sandstone (Appendix 20) may be related to detrital processes where basement rock containing mineralisation has been reworked and deposited by the river systems of the Algebuckina Formation. In Africa, stratiform Cu, Pb, Zn mineralisation occurs in detrital sediments at the base of the Cretaceous at several locations (Caia 1976). Best known deposits include Merija (Cu-Pb) and Bou-Sellam (Pb-Zn) (Van Eden 1978). These basal sediments are equivalent to the basal sediments of the Eromanga basin and were deposited during the break-up of Gondwana (Wopfner 2010). These deposits are hosted in conglomerates, sandstones and siltstones, and mineral occurrences are locally controlled by palaeochannels of highly variable size and composition which have deposited on the boundary between the basement rocks and the sedimentary basins (Caia 1976). Base metals were sourced from the basement rock and transported considerable distance. The base metals have undergone further remobilisation in places after consolidation (Caia 1976). A detrital source of base metals at Andamooka is a strong possibility.

Some of this anomaly however, may be a result of the abundance of clay minerals where the anomalies occur (Figure 13). Clay-sized minerals play a vital role in the dispersion of base metals in kaolinite dominated terrains (Le Gleuher *et al.* 2008). These clay minerals such as vermiculite, smectite and corrensite, are generally low in abundance, and thus remain undetected in spectral analysis of bulk samples (Le Gleuher *et al.* 2008). This may be why the HyLogger data does not show

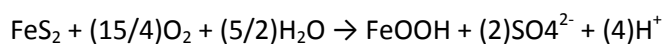
all of these base metal host clay minerals. In comparison to these layer silicates, kaolinite incorporates minimal base metals and can dilute geochemical anomalies (Le Gleuher *et al.* 2008). So for the abundance of clay minerals to have a significant effect on the base metal accumulation, minerals such as vermiculite, smectite and corrensite would have to be present, not just kaolinite. Smectite was seen in varying amounts at Andamooka, so this may be a contributing factor to the base metal accumulation.

The base metals which have accumulated at the redox zone within the Cadna-owie Formation (Appendix 21) may have been remobilised by groundwater processes from the underlying Algebuckina Sandstone basal anomaly and concentrated at the redox interface, and just below the water table. The anomalies are not as high as those in the Algebuckina Sandstone, suggesting the primary anomaly accumulated in the Algebuckina Sandstone, and was then remobilised somewhat and accumulated in the redox zone of the Cadna-owie Formation as a secondary process.

Alternatively, the anomaly may be caused by hydromorphic leakage directly from a base metal deposit in the basement rocks (Smith *et al.* 2000).

5.5. Source of iron rich fluids

The Bulldog Shale is potentially a major source of iron rich fluids which have caused ferruginisation of underlying sediments. Supergene enrichment is generally defined as an inorganic near-surface process where oxidation produces acidic solutions which leach metals, carry them downward, and re-precipitate them resulting in an enrichment of minerals already present (Kelley *et al.* 2006). The Bulldog Shale contains high levels of sulphide minerals such as pyrite (Tyler *et al.* 1990), (Simon-Coincon *et al.* 1996), and when oxidised, the sulphide from the pyrite produces acidic solutions (Coker 2010) and dissolved sulphate solutions, leaving behind iron oxide which is then available to be concentrated in solution or remain in-situ as iron oxide or jarosite (Postma 1983). The overall reaction for complete pyrite oxidation is as follows;



The acidic solution produced is then able to leach other elements and metals. This process would also encourage the formation of gypsum, which is in great abundance in the Bulldog Shale, as a source of sulphur would then be available even though much is transported away as dissolved sulphates (Postma 1983). This may explain the occurrence of gypsum in some of the older sediments below the Bulldog Shale, as sulphate solutions may have flowed from the overlying Bulldog Shale into the older Cadna-owie Formation and Algebuckina Sandstone and formed gypsum deposits. The same process may be linked to the formation of opal as discussed below. Iron discolouration occurs throughout fractures within the Bulldog Shale at Andamooka where oxidation and iron-oxide formation has occurred (Appendix 32), further supporting that the Bulldog Shale may be a major source of the iron rich fluids at Andamooka. The question remains, whether the Bulldog Shale contains sufficient base metal abundances to be responsible for any of the base metal anomalies seen in the underlying sediments. Other possible sources of iron rich fluids need to be considered.

Another possible source of iron rich fluids may be from below. Fault regions within the underlying Arcoona Quartzite often exhibit ferruginous zones, and fractured rock surfaces are often coated in what appears to be an iron rich cement which formed as a result of iron rich fluids flowing through fractures (Appendix 33). Fluids permeating upwards through these fault structures could be a source of iron as well as base metals seen in the ferruginous zones of the Mesozoic sediments. This is especially the case, since it is concluded that these fault structures are likely to have been active post-Mesozoic, due to the current landscape positions of the Mesozoic units, as described above and below. An iron-rich fluid source from the Arcoona Quartzite is particularly evident in the basal region of the Algebuckina Sandstone (AP4) where a rock layer (sample 004) contains around 63% iron-oxide. This iron rich band may have been a fluid pathway at the time iron-rich fluids entered the Algebuckina Formation. This fluid source would be more likely the source of base metal anomalies seen in the basal region of the Algebuckina Sandstone (Appendix 20) and the redox zone of the

Cadna-owie Formation (Appendix 21) since these anomalies are relatively high, and these fluids may have come from areas within the basement which may contain mineralisation e.g. Hiltaba Suite Volcanics which underlie the Arcoona Quartzite at Andamooka (Fairclough 2009). Whereas, the iron rich fluids sourced from the Bulldog Shale are likely to not accumulate such high base metal anomalies simply by permeating down the profile, through sediments not particularly rich in base metals. However, these fluids may be responsible for many of the ferruginous/iron oxide stained zones seen throughout the sequences.

5.6. Faulting

The NE-SW orientation of faulting seen in the Arcoona Quartzite (Figure 16) suggests a possible reactivation of these older faults causing the movement of the younger Mesozoic sediments observed in the region. The Mesozoic outcrops align well with the fault positions and orientations seen in the Arcoona Quartzite (Figure 16, 17). This suggests that these fault structures were reactivated post-Mesozoic. This tectonic model allows for oxidation of parts of the Bulldog Shale producing iron rich fluids, as described above, as post-Mesozoic faulting would have exposed uplifted regions to oxygen.

5.7. Thoughts about opal formation

The formation of opal at Andamooka may be heavily influenced by the post-Mesozoic faulting as well as the composition of the rock. The Bulldog Shale is rich in pyrite, a sulphide mineral. It is also very rich in organic matter and aluminosilicates (Tyler *et al.* 1990, Krieg & Rogers 1995). Faulting in the Andamooka region has uplifted parts of the Bulldog Shale and exposed them to oxidation. The acidic solutions produced from the oxidation of sulphide minerals and organic materials have the ability to break down aluminosilicates (Postma 1983), essentially stripping the aluminium and precipitating gibbsite or similar minerals, leaving free silica in solution. There is now a clear source of silica, and with the combination of this and the oxidation of iron producing discolouration of the

silica, a mechanism for the formation of multicoloured opal becomes apparent. It is no coincidence that opal workings at Andamooka tend to be concentrated on the relatively higher plains of Bulldog Shale, more prone to oxidation, rather than the lower plains. There is a distinct pattern of opal workings which trend along the fault NE-SW trending fault traces where the Bulldog Shale would have been exposed and oxidised.

All sites containing opal at Andamooka are heavily kaolinised (Carr *et al.* 1979). Carr *et al.* (1979) suggest that no significant opal has been discovered in the Jurassic, Cambrian or Adelaidean sequences because no suitable permeability interface is known in these rocks. They fail to recognise however, that the composition of the rock and the oxidation mechanisms (i.e. faulting) can play a vital role in the formation of opal, as mentioned above, and it is not just a product of a permeable zone within a rock sequence.

6. CONCLUSIONS

Multiple interfaces that could possibly be used as key interfaces for exploration purposes within the Mesozoic stratigraphy at Andamooka have been identified, including: a basal clay-rich unit of the Algebuckina Sandstone containing substantial base metal anomalies; a laterally extensive ferricrete layer within the Cadna-owie Formation which may indicate the position of a former water table, and where base metals have accumulated, and a conglomerate unit which is often silicified where the top of the Cadna-owie Formation contacts the base of the Bulldog Shale.

An apparent detrital Au and base metal anomaly is present at the base of the Algebuckina Sandstone. A redox associated base metal anomaly is also present in the Cadna-owie Formation possibly sourced and re-mobilised from the underlying anomaly at the base of the Algebuckina Sandstone and/or hydrothermal leakage from a buried deposit.

Base metals which have accumulated particularly in the Algebuckina Sandstone and Cadna-owie Formation possibly have three different sources; leaching by acidic solutions from and through the overlying Bulldog Shale, exposed basement rocks containing mineralisation during the early stages of deposition of the Algebuckina Sandstone forming detrital deposits, and fluids which have moved upwards through faults in the underlying Arcoona Quartzite.

Iron rich fluids causing ferruginisation in the region have two possible sources; oxidation of pyrite within the Bulldog Shale, and iron rich solutions that have moved upwards through faults in the underlying Arcoona Quartzite.

The Mt. Anna Sandstone Member was not identified at Andamooka posing questions about the controls over its deposition and participation within the Cadna-owie Formation as well as where the materials were sourced.

A structural regime (faulting) affecting the Mesozoic sequences and current landscape has been suggested. This regime has been applied to models of the formation of opal and gypsum in the area, as well as the formation of iron rich fluids.

7. ACKNOWLEDGEMENTS

I would like to extend my thanks to Robert Dart for all his patience, hard work and sense of humour throughout the year, and to Steven Hill for his thoughts and expertise. I would also like to thank the DET CRC for funding part of the project, and Georgina Gordon for helping with, and allowing me to use the HyLogger facilities at the PIRSA Core Library, as well as processing the HyLogger data. I would also like to thank Mathew Kavanagh for companionship in the field and thoughts about the Andamooka geology.

8. REFERENCES

- ASPANDIAR M. F. 2004. Potential mechanisms of metal transfer through transported overburden within the Australian regolith: a review. *Regolith*, 17-20.
- BASTRAKOV E. N., SKIRROW R. G. & DAVIDSON G. J. 2007. Fluid Evolution and Origins of Iron Oxide Cu-Au Prospects in the Olympic Dam District, Gawler Craton, South Australia. *Economic Geology* **102**, 1415-1440.
- BELPERIO A., FLINT R. & FREEMAN H. 2007. Prominent Hill: A Hematite-Dominated, Iron Oxide Copper-Gold System. *Economic Geology* **102**, 1499-1510.
- BUDD A., WYBORN L. & BASTRAKOVA I. 1998. Exploration significance of the Hiltaba Suite, South Australia. *AGSO Research Newsletter* **29**.
- CAIA J. 1976. Paleogeographical and sedimentological controls of copper, lead, and zinc mineralizations in the lower Cretaceous sandstones of Africa. *Economic Geology* **71**, 409-422.
- CARR S. G., OLLIVER J. G., CONOR C. H. H. & SCOTT D. C. 1979. Andamooka Opal Fields. The Geology of the Precious Stones Field and the Results of the Subsidised Mining Program. *Report of Investigations Department of Mines and Energy Geological Survey of South Australia* **51**.
- COKER W. B. 2010. Future research directions in exploration geochemistry. *Geochemistry: Exploration, Environment, Analysis* **10**, 75-80.
- DAVIDSON G. J., PATERSON H., MEFFRE S. & BERRY R. F. 2007. Characteristics and Origin of the Oak Dam East Breccia-Hosted, Iron Oxide Cu-U-(Au) Deposit: Olympic Dam Region, Gawler Craton, South Australia. *Economic Geology* **102**, 1471-1498.
- DE LURIO J. L. & FRAKES L. A. 1999. Glendonites as a paleoenvironmental tool: implications for early Cretaceous high latitude climates in Australia. *Geochimica et Cosmochimica Acta* **63**, 1039-1048.
- DIREEN N. G. & LYONS P. 2007. Regional Crustal Setting of Iron Oxide Cu-Au Mineral Systems of the Olympic Dam Region, South Australia: Insights from Potential-Field Modeling. *Economic Geology* **102**, 1397-1414.
- FAIRCLOUGH M. C. 2009. *Andamooka Map Sheet*. Department of Primary Industries and Resources South Australia, Adelaide.
- FRAKES L. A. & FRANCIS J. E. 1988. A guide to Phanerozoic cold polar climates from high-latitude ice-rafting in the Cretaceous. *Nature* **333**, 547-549.
- HAND M., REID A. & JAGODZINSKI L. 2007. Tectonic Framework and Evolution of the Gawler Craton, Southern Australia. *Economic Geology* **102**, 1377-1395.
- HOUSEMAN G. A., CULL J. P., MUIR P. M. & PATERSON H. L. 1989. Geothermal signatures and uranium ore deposits on the Stuart Shelf of South Australia. *Geophysics* **54**, 158-170.
- JOHNS R. K. 1968. *Geology and Mineral Resources of the Andamooka-Torrens area*. Australia D. o. M. S. **41**: 103. Govt. Printer, Adelaide.
- KELLEY D. L., KELLEY K. D., COKER W. B., CAUGHLIN B. & DOHERTY M. E. 2006. Beyond the Obvious Limits of Ore Deposits: The Use of Mineralogical, Geochemical, and Biological Features for the Remote Detection of Mineralization. *Economic Geology* **101**, 729-752.
- KNUTSON J., DONNELLY T. H. & TONKIN D. G. 1983. Geochemical constraints on the genesis of copper mineralization in the Mount Gunson area, South Australia. *Economic Geology* **78**, 250-274.
- KRIEG W. G., ALEXANDER E. M. & ROGERS P. A. 1995. Eromanga Basin. *The Geology of South Australia* **2**, 101-127.
- KRIEG W. G. & ROGERS P. A. 1995. Eromanga Basin: Stratigraphy-marine succession. *The Geology of South Australia* **2**, 112-122.
- LAMBERT I. B., KNUTSON J., DONNELLY T. H. & ETMINAN H. 1987. Stuart Shelf-Adelaide Geosyncline copper province, South Australia. *Econ Geol* **82**, 108-123.
- LE GLEUHER M., ANAND R. R., EGGLETON R. A. & RADFORD N. 2008. Mineral hosts for gold and trace metals in regolith at Boddington gold deposit and Scuddles massive copper-zinc sulphide

- deposit, Western Australia: an LA-ICP-MS study. *Geochemistry: Exploration, Environment, Analysis* **8**, 157-172.
- MAUGER A. J., HUNTINGTON J. F. & KEELING J. L. 2004. Mineral mapping and spectral logging of the Gawler Craton. *Regolith*, 234.
- MCQUEEN K. G. 2006. Unravelling the Regolith with Geochemistry. *CRC LEME Regolith 2006 - Consolidation and Dispersion of Ideas*.
- MOORE P. S. & PITT G. M. 1982. Cretaceous of the southwestern Eromanga Basin: Stratigraphy, facies variation and petroleum potential. In *Eromanga Basin Symposium Summary Papers* (ed. P. S. Moore and T. J. Mount). *Petroleum Exploration Society of Australia and Geological Society of Australia*, 127-144.
- MOORE P. S. & PITT G. M. 1985. Cretaceous subsurface stratigraphy of the southwestern Eromanga Basin: a review. *Special Publication. South Australian Dept. Mines & Energy* **5**, 269-286.
- PEWKLIANG B., PRING A. & BRUGGER J. 2008. The formation of precious opal: clues from the opalization of bone. *The Canadian Mineralogist* **46**, 139-150.
- POSTMA D. 1983. Pyrite and siderite oxidation in swamp sediments. *Journal of Soil Science* **34**, 163-182.
- RATTIGAN J. H., GERSTELING R. W. & TONKIN D. G. 1977. Exploration geochemistry of the Stuart Shelf, South Australia. *Journal of Geochemical Exploration* **8**, 203-217.
- SCHMIDT P. W., MCENROE S. A., CLARK D. A. & ROBINSON P. 2007. Magnetic properties and potential field modeling of the Peculiar Knob metamorphosed iron formation, South Australia: An analog for the source of the intense Martian magnetic anomalies? *J. Geophys. Res.* **112**, B03102.
- SIMON-COINCON R., MILNES A. R., THIRY M. & WRIGHT M. J. 1996. Evolution of landscapes in northern South Australia in relation to the distribution and formation of silcretes. *Journal of the Geological Society* **153**, 467-480.
- SMITH R. E. 1996. Regolith research in support of mineral exploration in Australia. *Journal of Geochemical Exploration* **57**, 159-173.
- SMITH R. E., ANAND R. R. & ALLEY N. F. 2000. Use and implications of paleoweathering surfaces in mineral exploration in Australia. *Ore Geology Reviews* **16**, 185-204.
- TOMKINS A. G., DUNLAP W. J. & MAVROGENES J. A. 2004. Geochronological constraints on the polymetamorphic evolution of the granulite-hosted Challenger gold deposit: implications for assembly of the northwest Gawler Craton*. *Australian Journal of Earth Sciences* **51**, 1-14.
- TYLER M. J., TWIDALE C. R., DAVIES M. & WELLS C. B. (Editors) 1990. *Natural History of the North East Deserts*. Royal Society of South Australia Inc., Adelaide.
- VAN EDEN J. G. 1978. Stratiform copper and zinc mineralization in the Cretaceous of Angola. *Economic Geology* **73**, 1154-1161.
- WOPFNER H. 2010. Burial history of Jurassic Gondwana Surface west and southwest of Lake Eyre, central Australia. *Coruna* **35**, 221-242.
- WOPFNER H., FREYTAG I. B. & HEATH G. R. 1970. Basal Jurassic-Cretaceous rocks of western Great Artesian Basin, South Australia; stratigraphy and environment. *AAPG Bulletin* **54**, 383-416.

9. FIGURE CAPTIONS

Figure 1: a) Geological setting of Andamooka, showing Gawler Craton, Stuart Shelf, Torrens Hinge Zone, Andamooka and Olympic Dam. b) Locality map showing Andamooka and regional copper prospects and deposits in the region (edited from Direen & Lyons, 2007 & Houseman et al., 1989).

Figure 2: Location and simplified geology of the Gawler Craton, showing Olympic Cu, Au province (Bastrakov et al., 2007).

Figure 3: Geological map of Andamooka region showing the study area outlined in red. Blue=Andamooka Limestone, beige with red dots=Arcoona Quartzite, bright green=undifferentiated Cadna-owie Formation and Algebuckina Sandstone, pale green=Bulldog Shale, pale yellow=sand dunes, pale blue=Lake Torrens. Shows location of profiles AP1-AP6, and Blue Dam and Trigg Bluff. Edited from Fairclough (2009). A Google Earth image of the study area outlined in red is shown below.

Figure 4: Stratigraphic columns of central Andamooka and northern Andamooka. Shows the presence of the Andamooka Limestone and lack of Algebuckina Sandstone and Cadna-owie Formation in the northern region.

Figure 5: Map showing Great Artesian Basin and the three depressions which it is comprised (Eromanga Basin, Carpentaria Basin, Surat Basin). Also indicates the extents of the Cretaceous sediments and the Quaternary – Tertiary sediments, as well as the position of Andamooka along with other precious opal fields and deposits (edited from Pewkliang et al. 2008).

Figure 6: Isopach map of Cadna-owie Formation in feet of area between Peake and Denison inliers and Gawler Ranges, southwestern Eromanga Basin, showing location of Mt. Anna, Algebuckina Hill, and Andamooka. Thickness of Mt. Anna Sandstone Member, expressed as a percentage of total Cadna-owie Formation thickness, demonstrates increased dominance of Mt Anna Sandstone proximal to the Gawler Range Massif (edited from Wopfner (2010).

Figure 7: Type section of Algebuckina Sandstone, south-west of Algebuckina Hill (Wopfner, 1970).

Figure 8: Type section of Cadna-owie Formation, near Algebuckina Hill (Wopfner, 1970).

Figure 9: Comparison of previous descriptions of Mesozoic sequences at Andamooka and nearby regions.

Figure 10: Stratigraphic log of profile AP1. Located at 0712173 mE 6629548 mN.

Figure 11: Stratigraphic log of profile AP2. Located at 0712155 mE 6629265 mN.

Figure 12: Stratigraphic Log of profile AP3. Located at 0712167 mE 6629035 mN.

Figure 13a: Stratigraphic log of profile AP4. Located at 0714782 mE 6627140 mN.

Figure 13b: Stratigraphic log of profile AP4 before amendments made by further field work. Indicates stratigraphic units that samples were taken from for geochemical analysis.

Figure 14: Stratigraphic log of profile AP5. Located at 0712142 mE 6629078 mN.

Figure 15: Stratigraphic log of profile AP6. Located at 0708845 mE 6626004 mN.

Figure 16. Geological map of study area. Includes bedding readings, faulting, cross-section line and locations of all six profiles (AP1-AP6).

Figure 17. Cross-section of line A-B shown on geological map (Figure 16).

Figure 18: Schematic diagram showing the stratigraphic relationships of the six profiles (AP1-AP6) of Mesozoic sequences at Andamooka, indicating the rock formation of each profile. Gaps in between profiles indicate zones within the stratigraphy that the profile sections do not cover.

Table 1: Descriptions of HyLogger mineral plots for profiles AP1-AP4. Refer to Appendices 3-6 for mineral plots.

Table 2: Discussion of notable/unusual mineral occurrences obtained by the HyLogger system. Refer to Appendices 3-6 for mineral plots.

10. FIGURES

Figure 1: a) Geological setting of Andamooka, showing Gawler Craton, Stuart Shelf, Torrens Hinge Zone, Andamooka and Olympic Dam. b) Locality map showing Andamooka and regional copper prospects and deposits in the region (edited from Direen & Lyons, 2007 & Houseman et al., 1989).

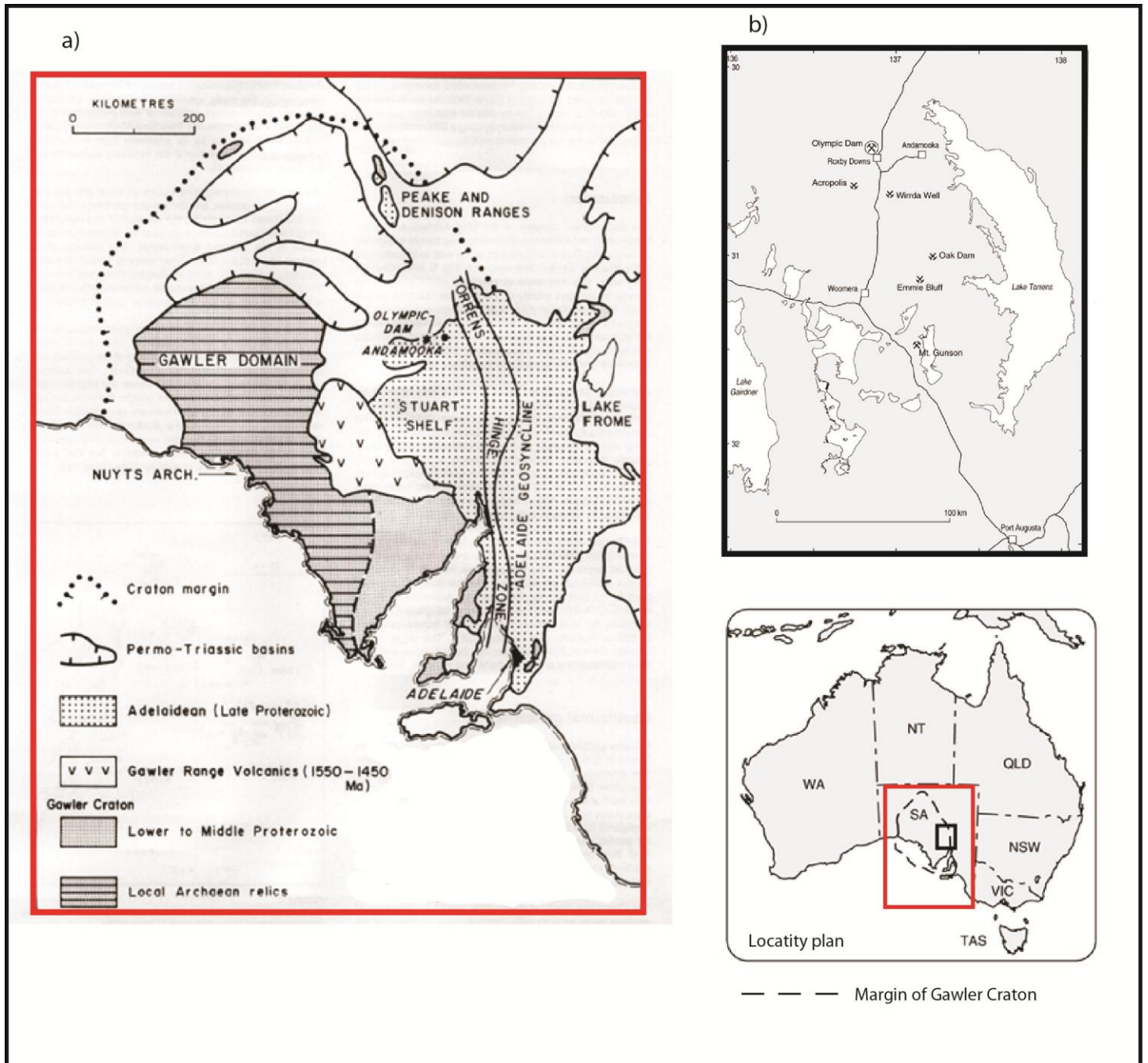


Figure 2: Location and simplified geology of the Gawler Craton, showing Olympic Cu, Au province (Bastrakov et al., 2007).

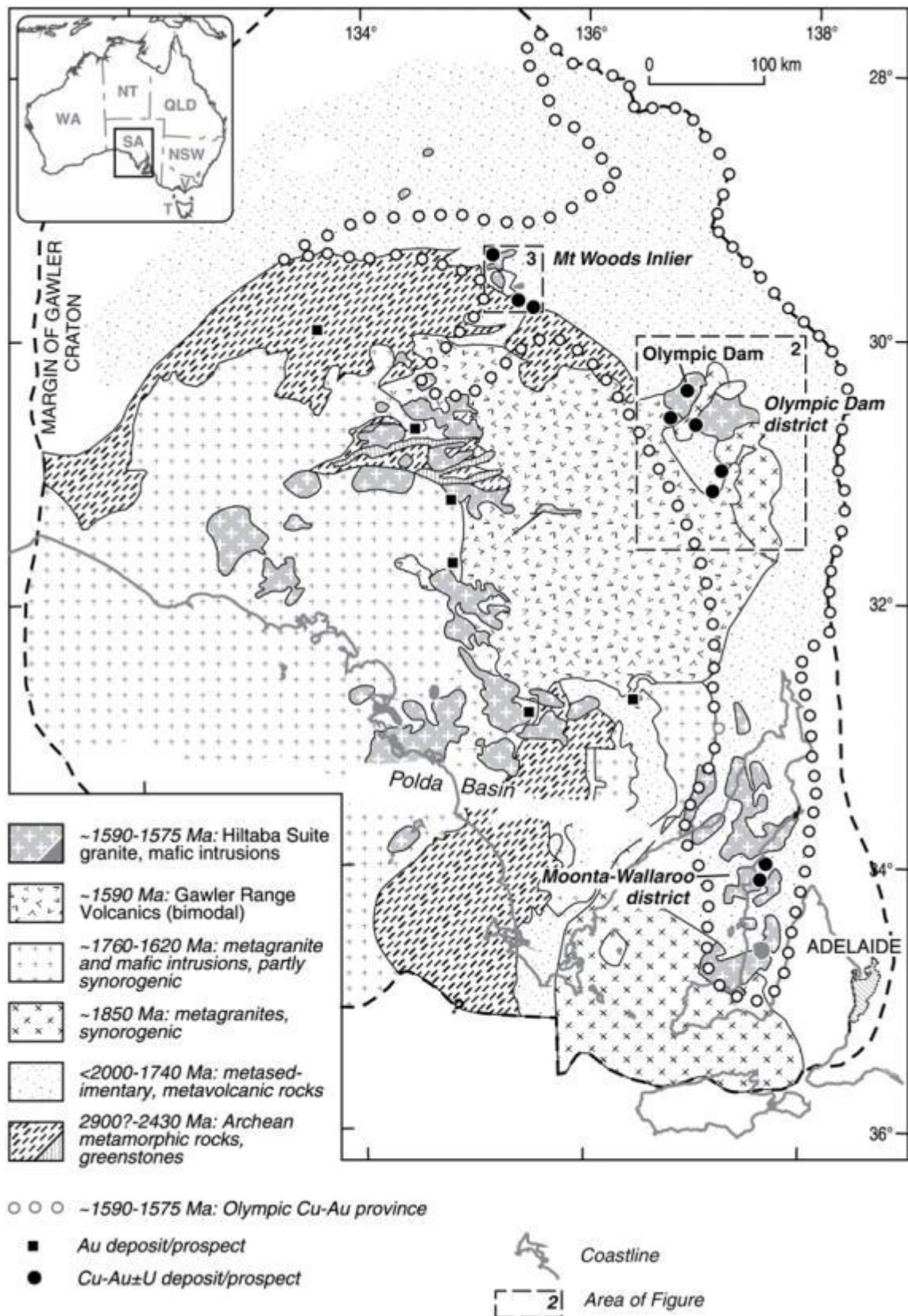


Figure 3: Geological map of Andamooka region showing the study area outlined in red. Blue=Andamooka Limestone, beige with red dots=Arcoona Quartzite, bright green=undifferentiated Cadna-owie Formation and Algebuckina Sandstone, pale green=Bulldog Shale, pale yellow=sand dunes, pale blue=Lake Torrens. Shows location of profiles AP1-AP6, and Blue Dam and Trigg Bluff. Edited from Fairclough (2009). A Google Earth image of the study area outlined in red is shown below.

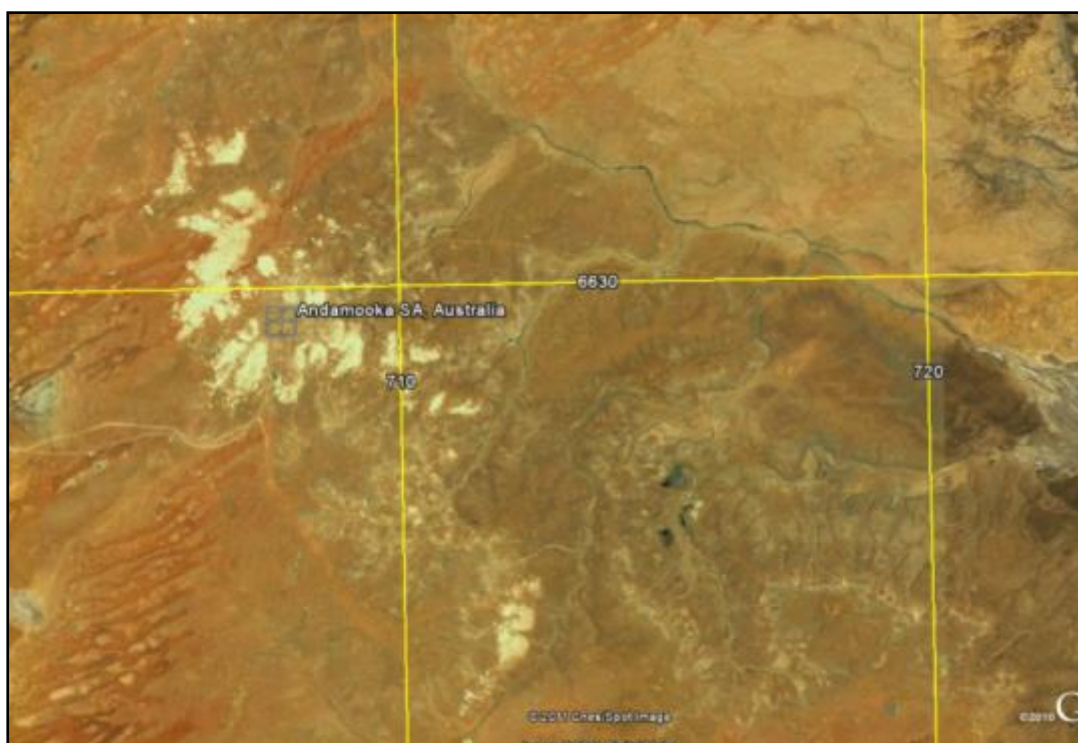
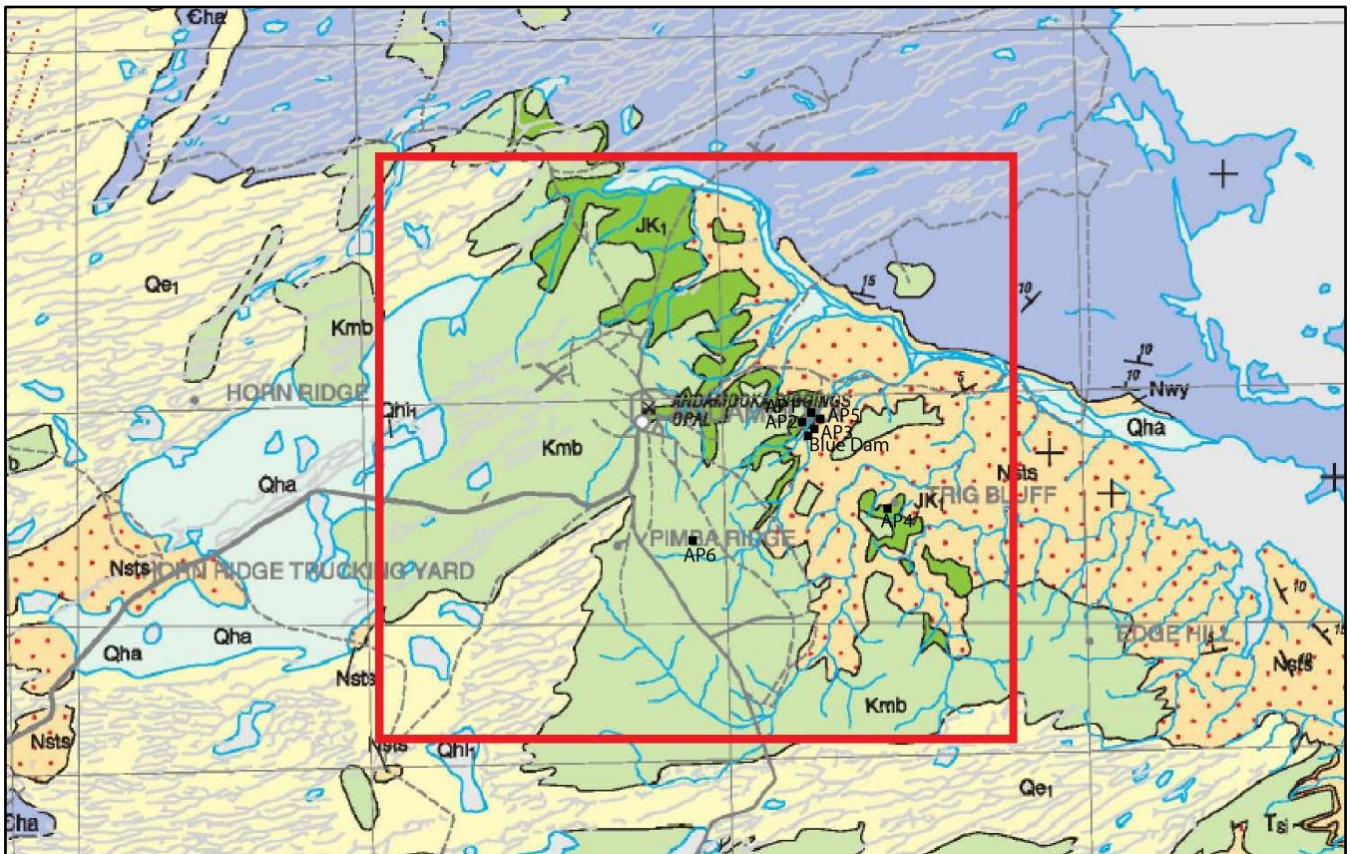


Figure 4: Stratigraphic columns of central Andamooka and northern Andamooka. Shows the presence of the Andamooka Limestone and lack of Algebuckina Sandstone and Cadna-owie Formation in the northern region.

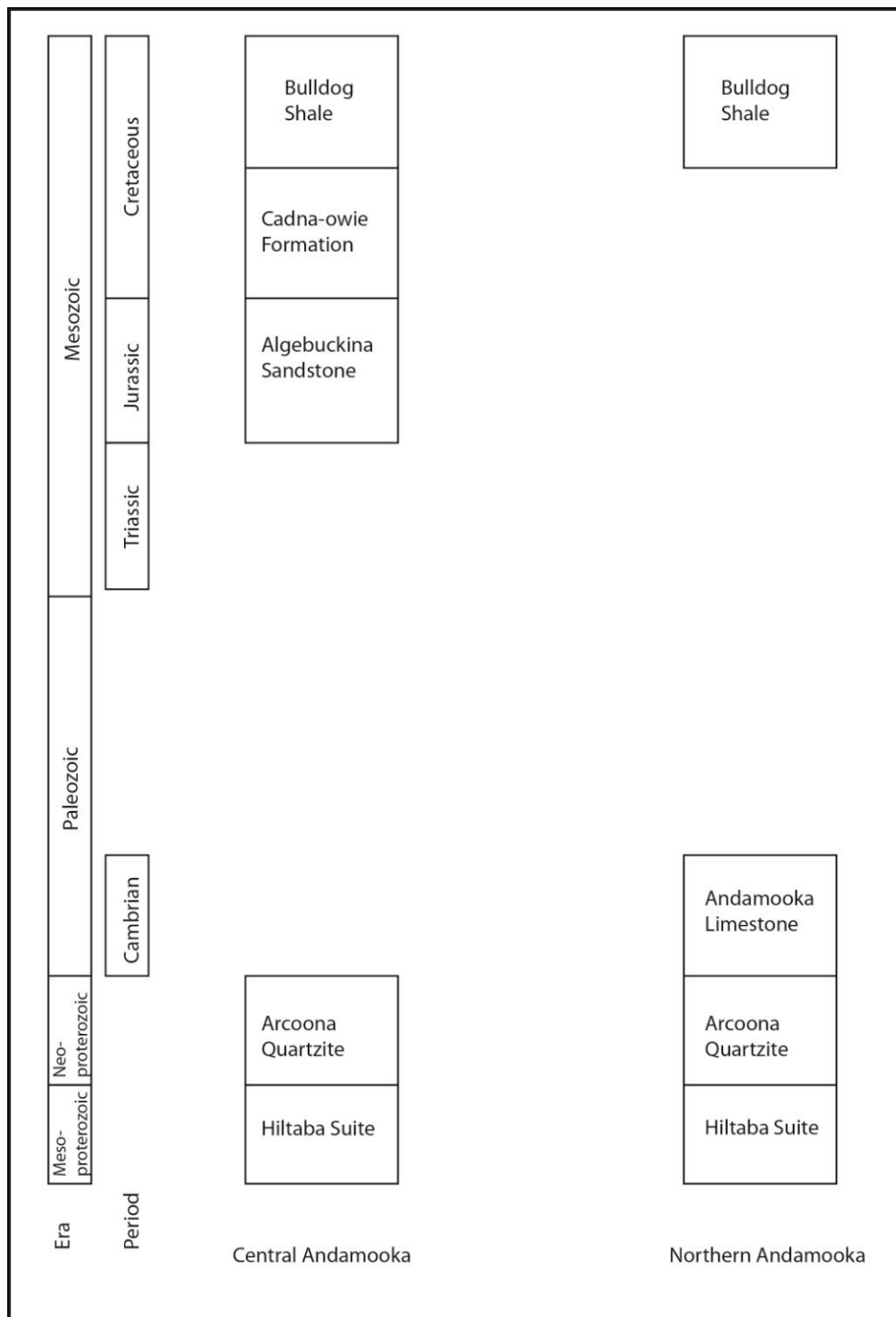


Figure 5: Map showing Great Artesian Basin and the three depressions which it is comprised (Eromanga Basin, Carpentaria Basin, Surat Basin). Also indicates the extents of the Cretaceous sediments and the Quaternary – Tertiary sediments, as well as the position of Andamooka along with other precious opal fields and deposits (edited from Pewkliang et al. 2008).

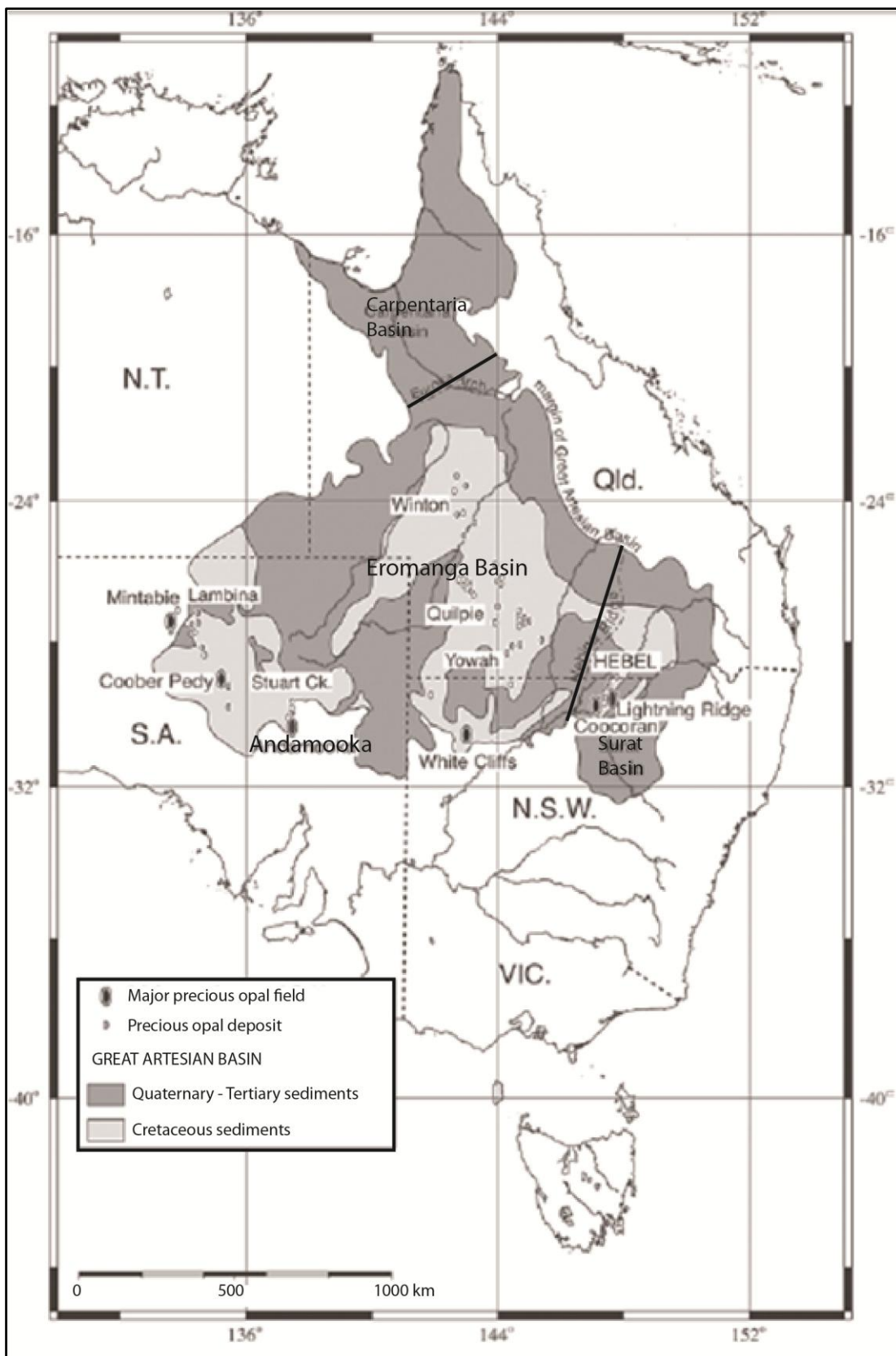


Figure 6: Isopach map of Cadna-owie Formation in feet of area between Peake and Denison inliers and Gawler Ranges, southwestern Eromanga Basin, showing location of Mt. Anna, Alge buckina Hill, and Andamooka. Thickness of Mt. Anna Sandstone Member, expressed as a percentage of total Cadna-owie Formation thickness, demonstrates increased dominance of Mt Anna Sandstone proximal to the Gawler Range Massif (edited from Wopfner (2010)).

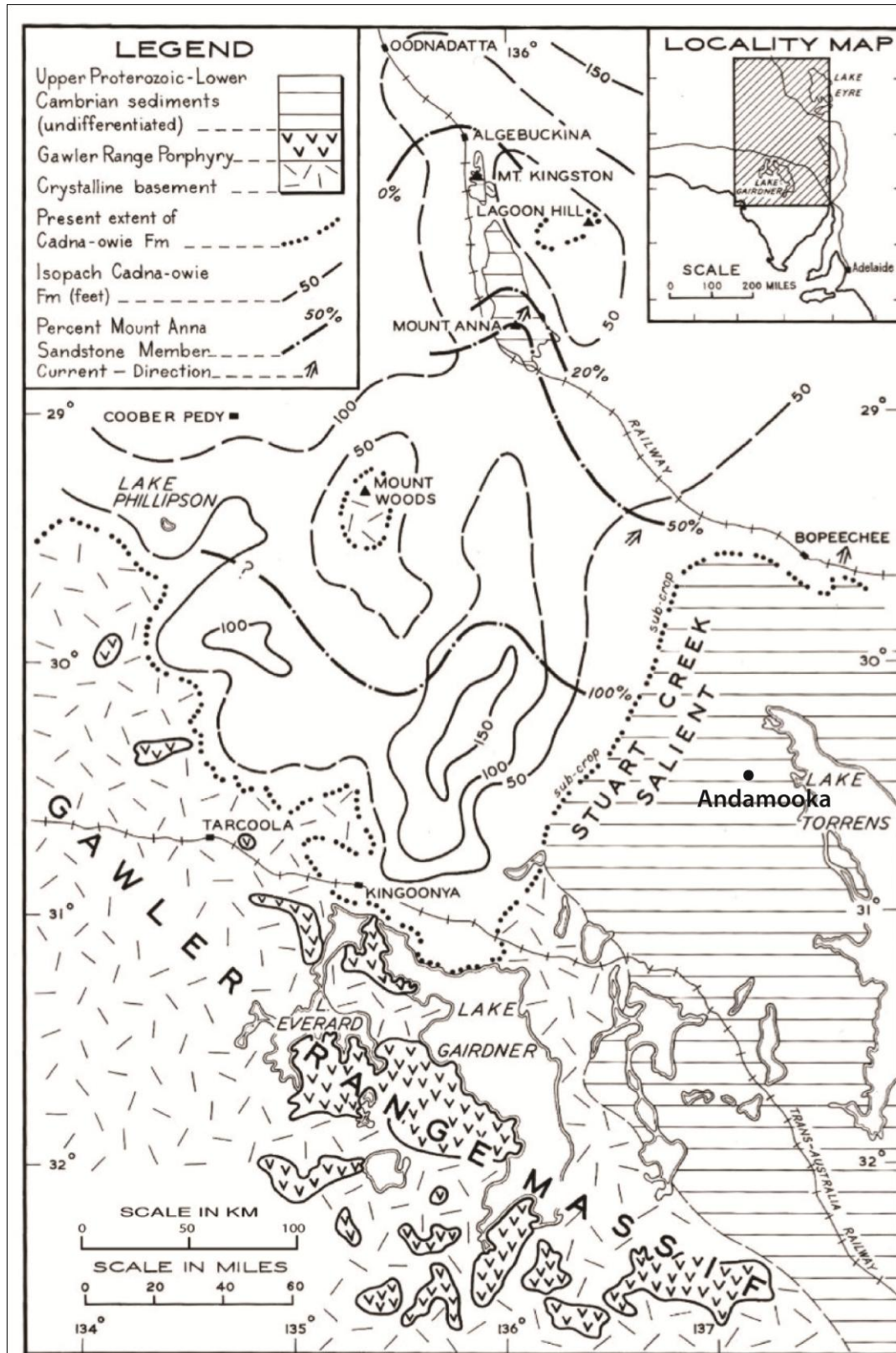


Figure 7: Type section of Alge buckina Sandstone, south-west of Alge buckina Hill (Wopfner, 1970).

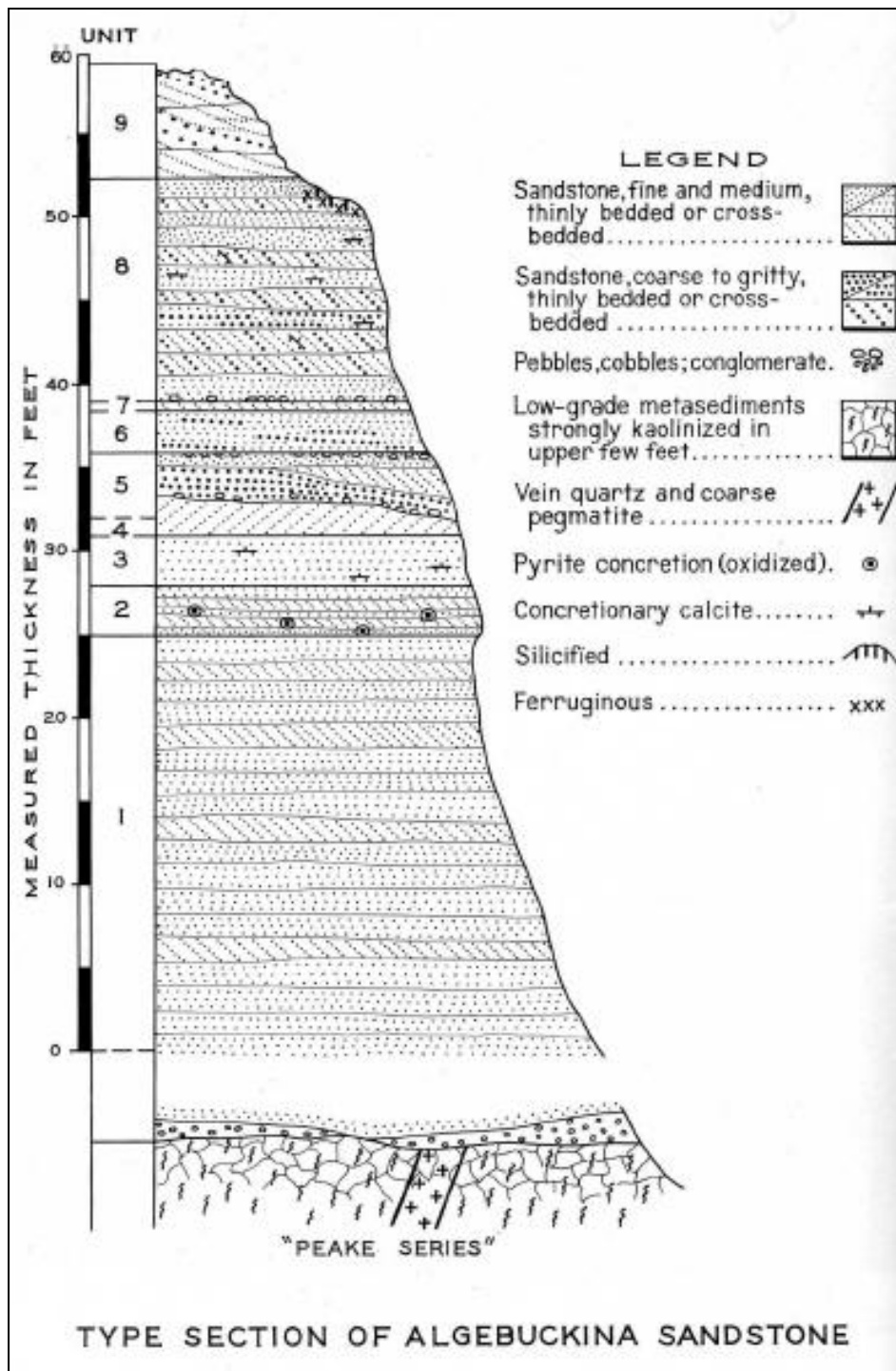


Figure 8: Type section of Cadna-owie Formation, near Algeuckina Hill (Wopfner, 1970).

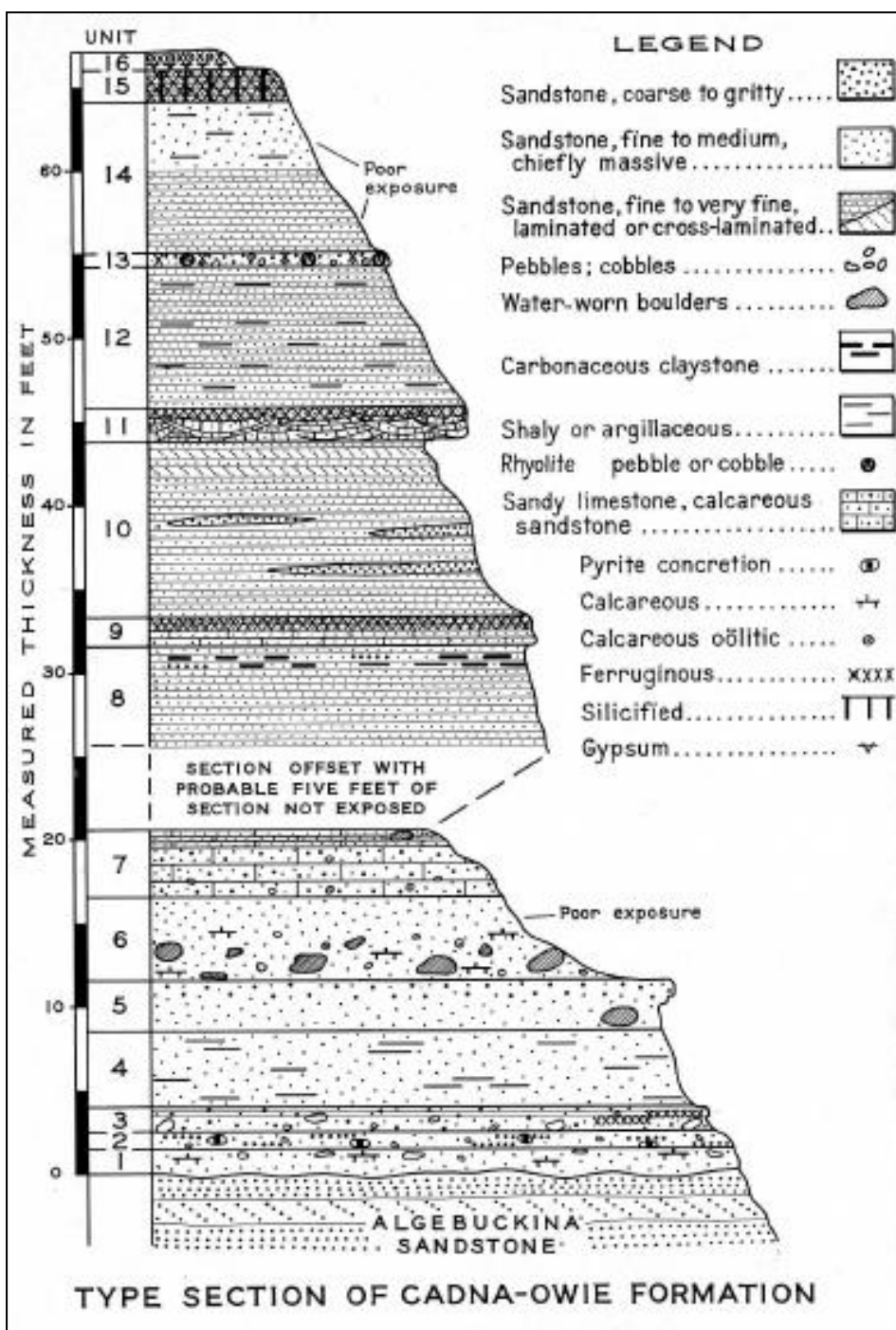


Figure 9: Comparison of previous descriptions of Mesozoic sequences at Andamooka and nearby regions.

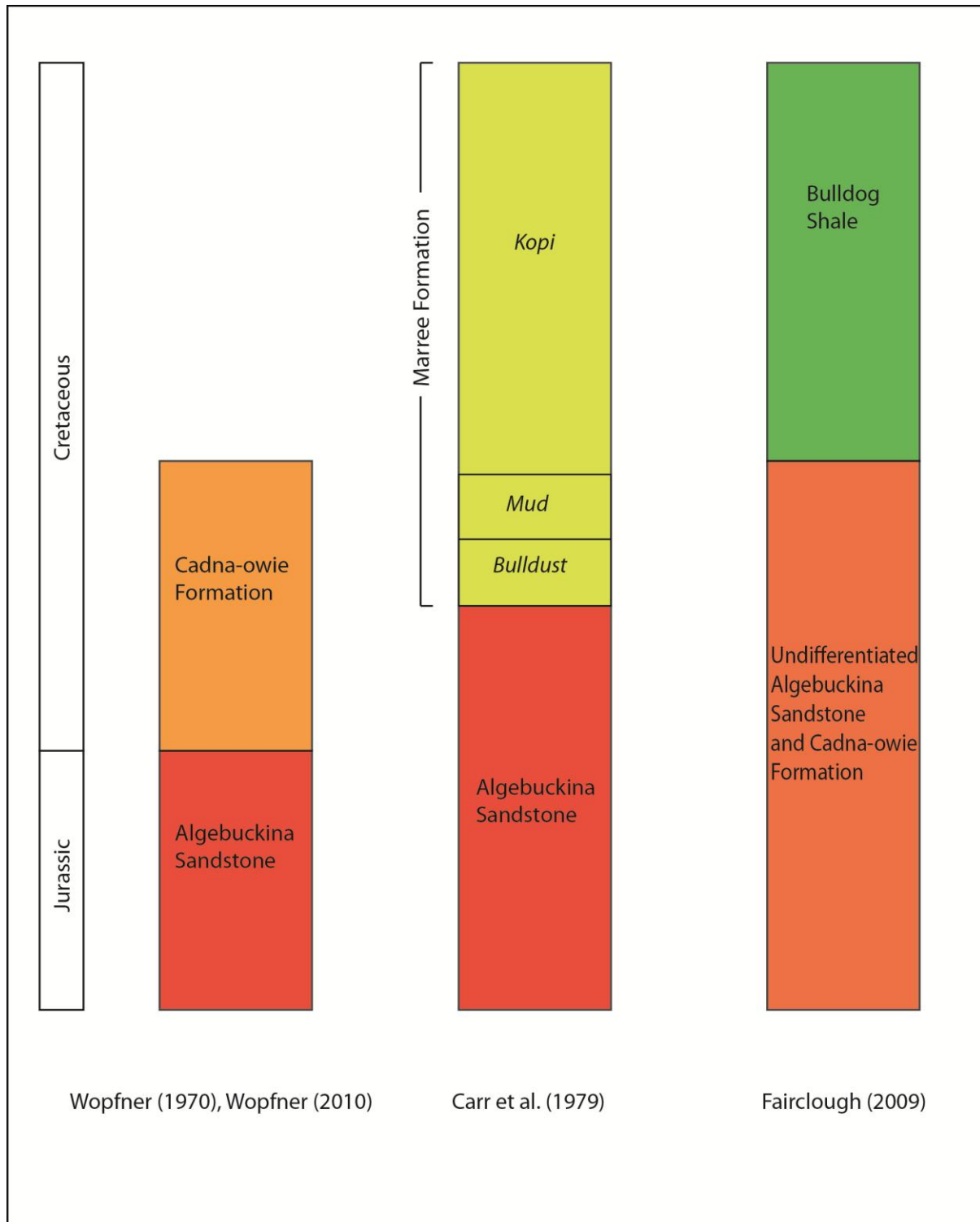


Figure 10: Stratigraphic log of profile AP1. Located at 0712173 mE 6629548 mN.

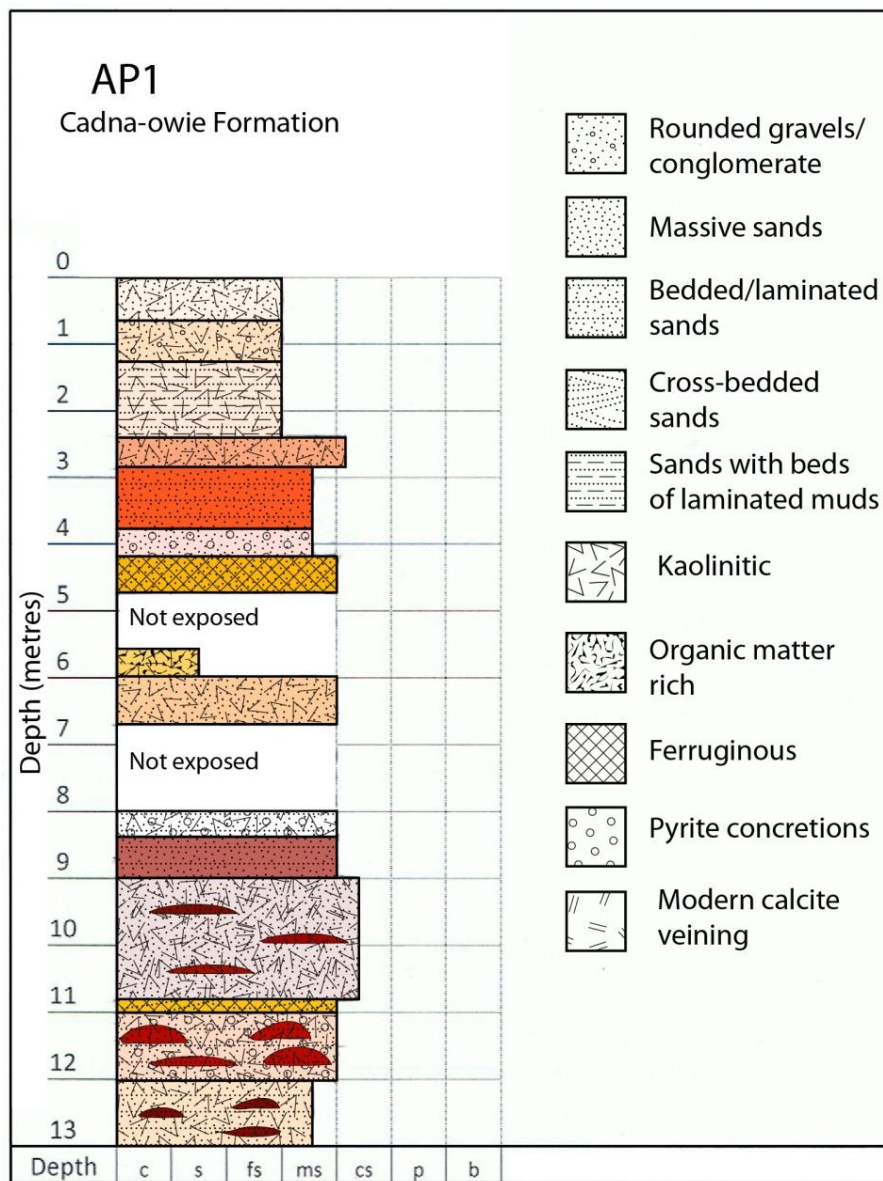


Figure 11: Stratigraphic log of profile AP2. Located at 0712155 mE 6629265 mN.

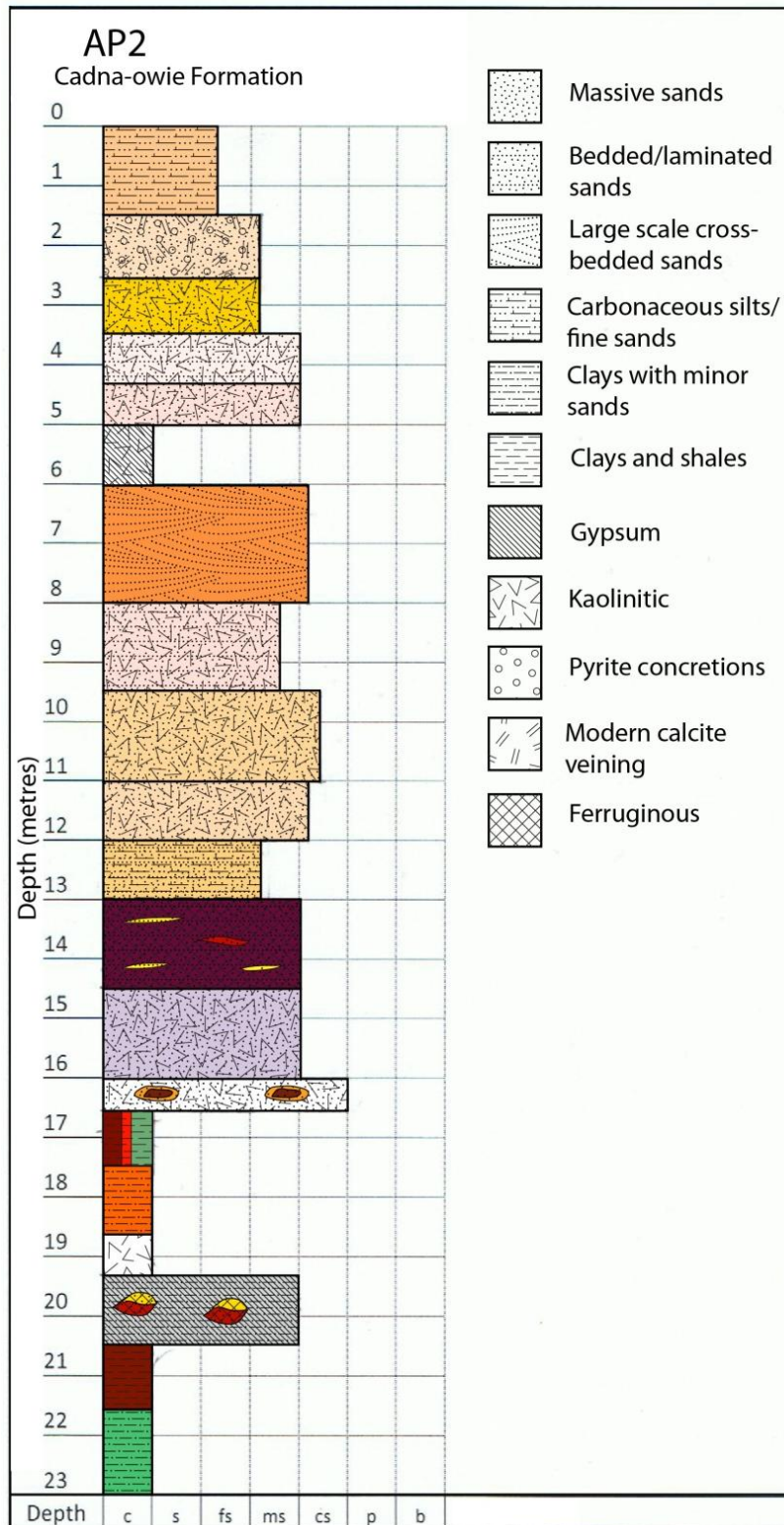


Figure 13a: Stratigraphic log of profile AP4. Located at 0714782 mE 6627140 mN.

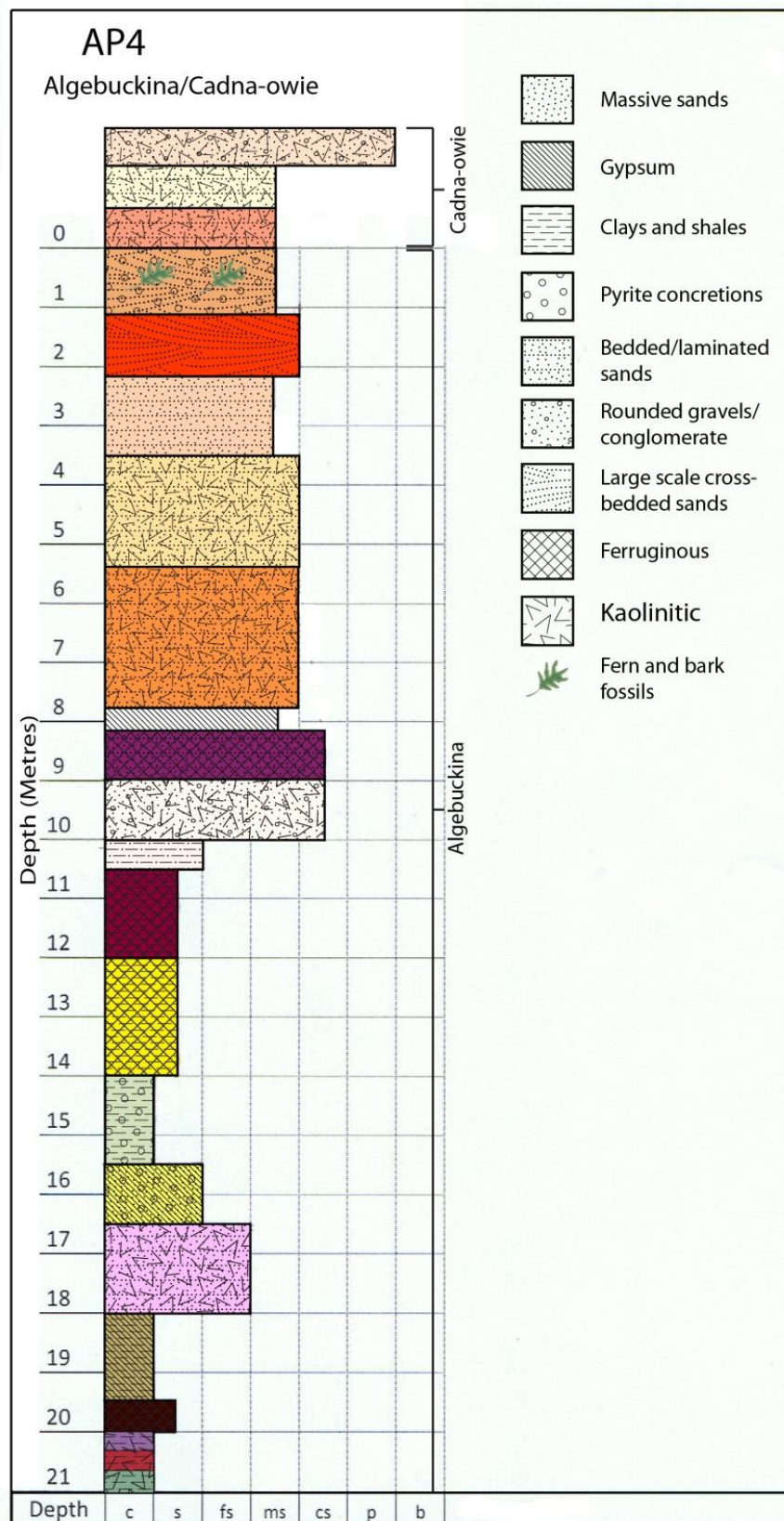


Figure 13b: Stratigraphic log of profile AP4 before amendments made by further field work. Indicates stratigraphic units that samples were taken from for geochemical analysis.

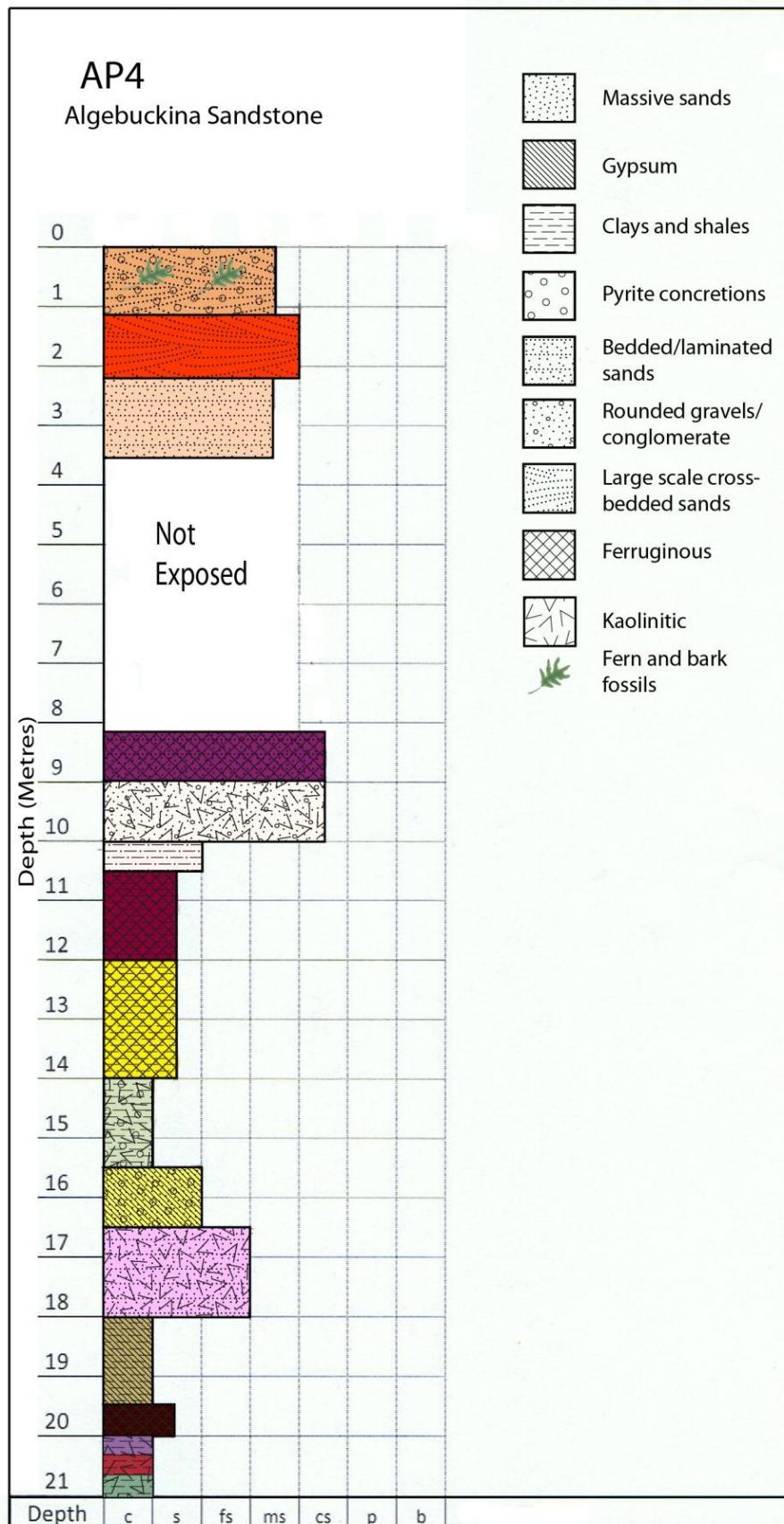


Figure 14: Stratigraphic log of profile AP5. Located at 0712142 mE 6629078 mN.

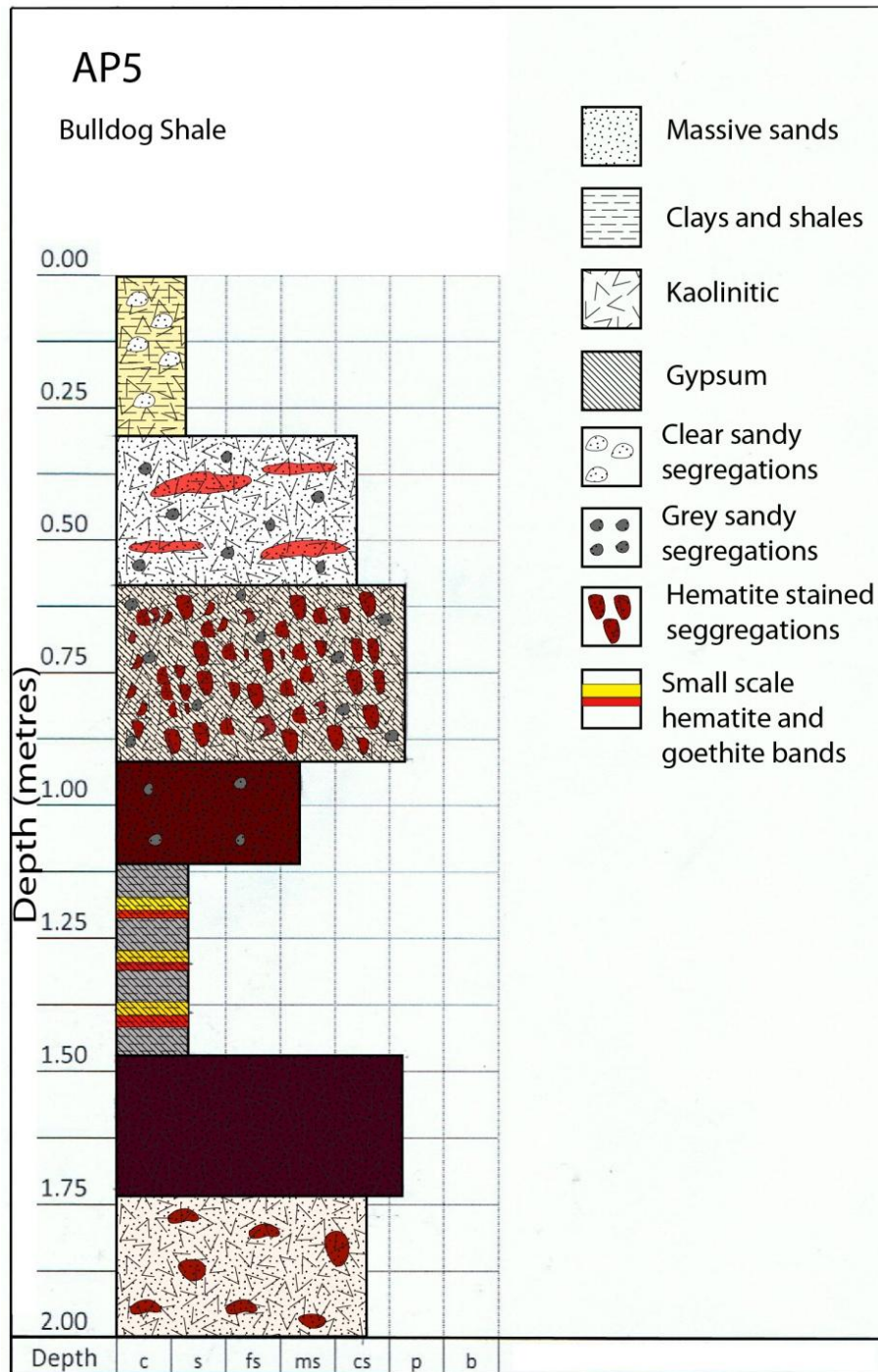


Figure 15: Stratigraphic log of profile AP6. Located at 0708845 mE 6626004 mN.

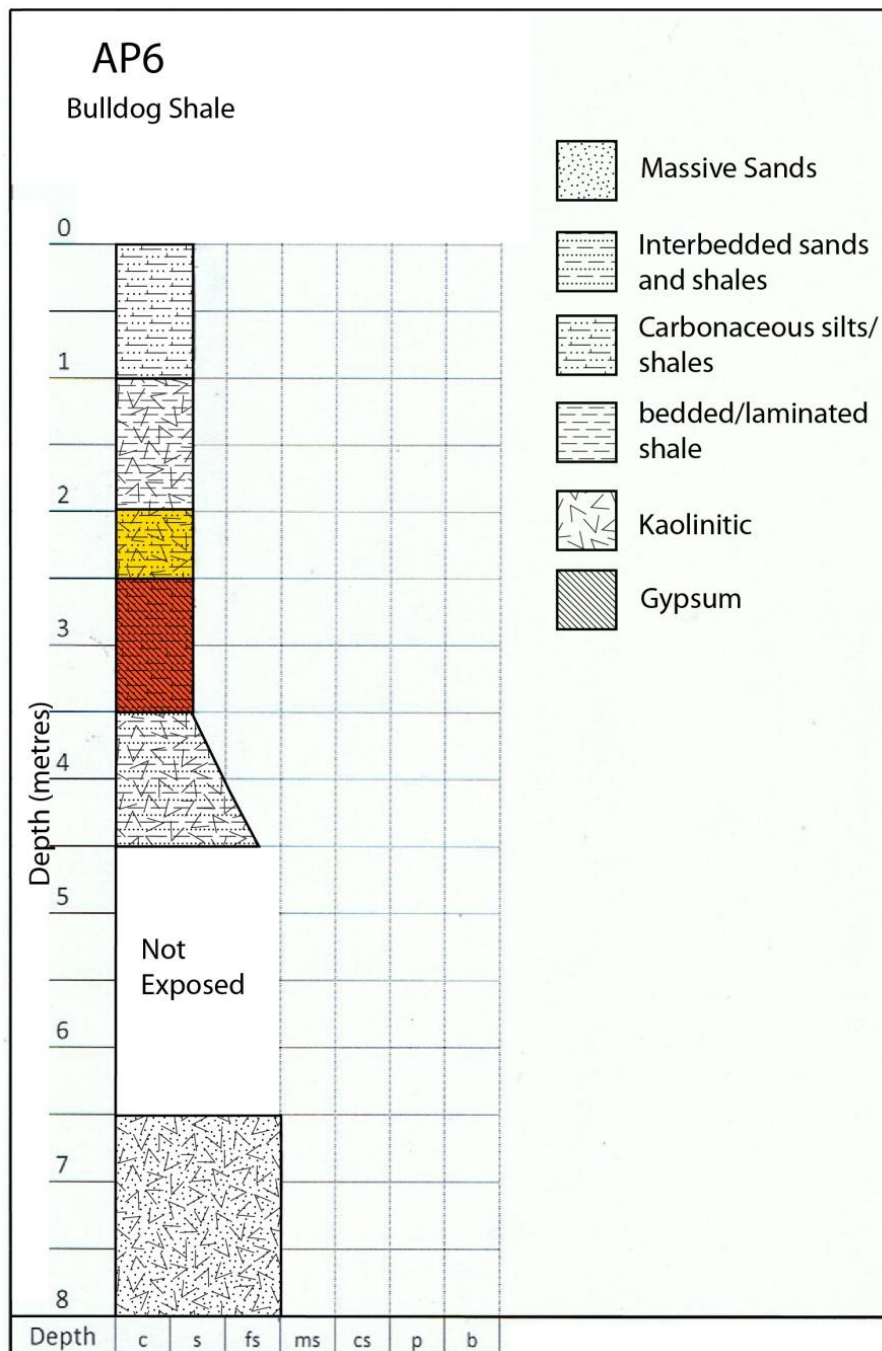


Figure 16. Geological map of study area. Includes bedding readings, faulting, cross-section line and locations of all six profiles (AP1-AP6).

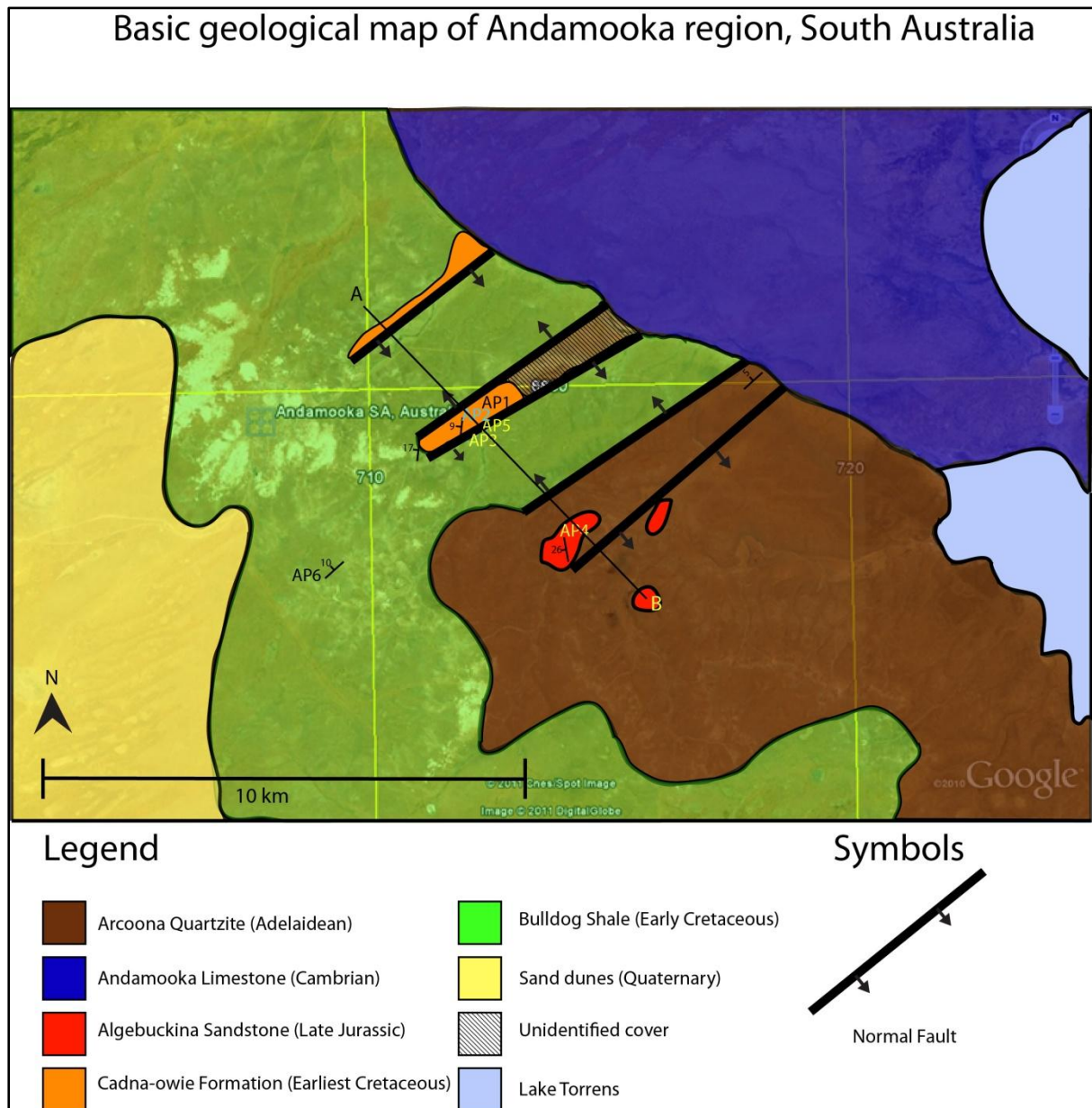


Figure 17. Cross-section of line A-B shown on geological map (Figure 16).

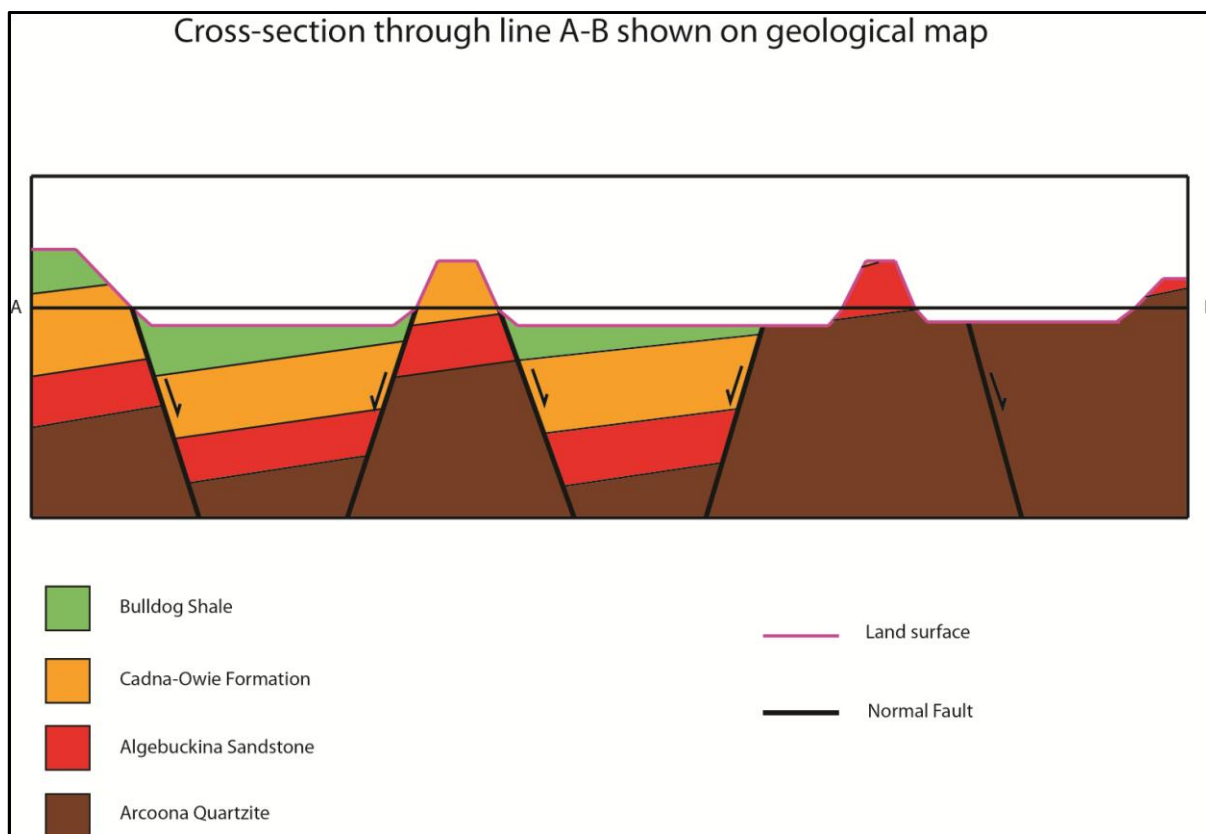
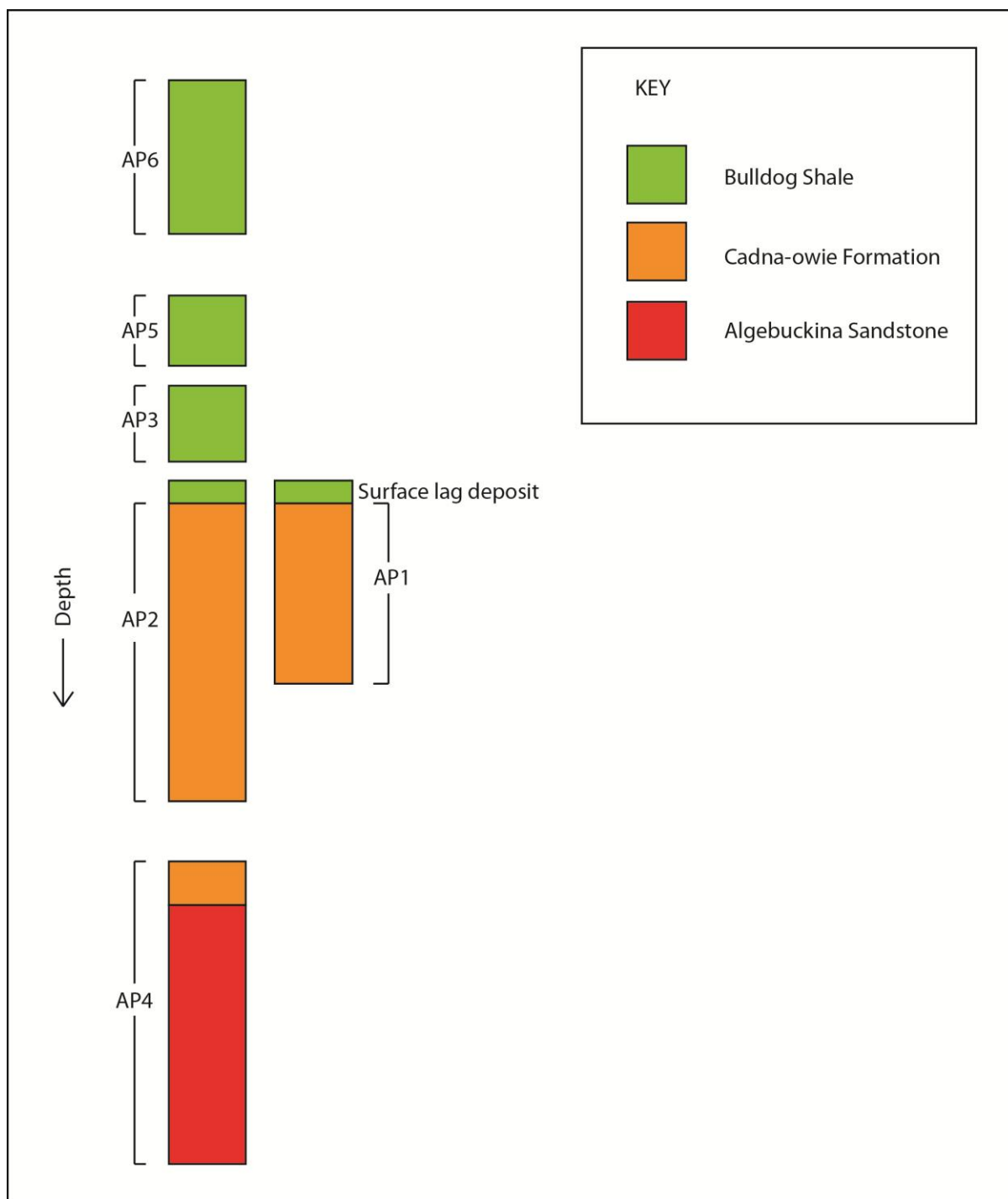


Figure 18: Schematic diagram showing the stratigraphic relationships of the six profiles (AP1-AP6) of Mesozoic sequences at Andamooka, indicating the rock formation of each profile. Gaps in between profiles indicate zones within the stratigraphy that the profile sections do not cover.



11. TABLES

Table 1: Descriptions of HyLogger mineral plots for profiles AP1-AP4. Refer to Appendices 3-6 for mineral plots.

Profile	Description
AP1:	<p>Refer to Appendix 3 for mineral plots. Plot 1 indicates a dominance of kaolinite though much of the profile except the upper part. Sulphates are present in the form of gypsum. Montmorillonite, a smectite mineral is also present in an interval within the upper half.</p> <p>Plot 2 indicates that diaspore ($\text{AlO}(\text{OH})$) is present in sample 008. Plot 2 also indicates that montmorillonite and gypsum are present in other intervals which did not show up in Plot 1.</p> <p>Hematite and goethite are present in scattered intervals throughout the profile (Plot 3).</p>
AP2:	<p>Refer to Appendix 4 for mineral plots. As there are 21 samples which make up profile AP2 sample number 021 was put in a separate chip tray to be analysed by HyLogger as each tray can only hold a maximum of 20 samples. As a result sample 021 is seen in a separate image in the figures mentioned below.</p> <p>Plot 1 shows an abundance of kaolinite throughout the profile, with minor intervals of the clay mineral montmorillonite, a member of the smectite family.</p> <p>There are minor occurrences of carbonates and sulphates throughout (Plot 2). Samples 010 and 021 contain carbonate. The carbonate occurs in the form of siderite (FeCO_3), an iron rich carbonate mineral, and magnesite (MgCO_3), a magnesium rich carbonate mineral. Sample 010 contains both siderite and magnesite, sample 021 contains just magnesite.</p> <p>Sulphates within the profile correspond to gypsum (Plot 2). Multiple smectite intervals throughout the profile occur in the form of montmorillonite and palygorskite. Some small twigs may have contaminated sample 018, shown by the presence of wood.</p> <p>Plot 3 indicates that hematite is dominant over goethite in iron rich zones; however minor occurrences of goethite are present. The sulphate mineral, jarosite ($(\text{KFe}^{3+})_3(\text{OH})_6(\text{SO}_4)$) a hydrous sulphate of potassium and iron, is present in sample 004.</p>
AP3:	<p>Refer to Appendix 5 for mineral plots. There is an abundance of kaolinite throughout (Plot 1). Goethite is abundant in the lower half, and hematite is abundant in sample 003 (Plot 2). Gypsum is abundant throughout multiple intervals (Plot 1, Plot 3).</p>

Profile	Description
AP4:	<p>Refer to Appendix 6 for mineral plots. Much of the lower region of AP4 remains unrecognised by HyLogger.</p> <p>Plot 1 shows a dominance of kaolinite in the middle and upper regions of profile AP4. Gypsum is also present.</p> <p>Plot 2 shows that gypsum occurs at several intervals throughout the profile. Smectite in the form of montmorillonite is present at the top (samples 016, 017). Some dry vegetation has contaminated sample 017.</p> <p>Goethite and hematite are present at multiple intervals throughout the profile including a main central region where sample 009 is goethite rich and sample 010 is hematite rich (Plot 3).</p>

Table 2: Discussion of notable/unusual mineral occurrences obtained by the HyLogger system. Refer to Appendices 3-6 for mineral plots.

Profile	Discussion
AP1:	Refer to Appendix 3 for mineral plots. HyLogger suggests that the extremely soft material seen in sample 008 of profile AP1 contains diaspore, an aluminium oxide hydroxide (AlO(OH)). This mineral is considered isomorphous with goethite (FeO(OH)). Since this sample lies directly below a goethite rich sample an isomorphous replacement of Fe with Al is a distinct possibility during oxidation or after oxidation.
AP2:	Refer to Appendix 4 for mineral plots. The occurrence of jarosite ($\text{KFe}^{3+}_3(\text{OH})_6(\text{SO}_4)$) in sample 004 of profile AP2 gives an indication of pH and Eh in regolith. It indicates acidic pH and high Eh (i.e. oxidising) conditions as it often forms at the redox interface during oxidation of pyrite, where sulphur is released and made available for jarosite formation (Postma, 1983). However, the measured pH of this sample was 7 (Appendix 2).
AP4:	Refer to Appendix 6 for mineral plots. It is interesting that HyLogger doesn't recognise much material from the lower region of AP4. Iron oxide is not picked up in sample 004 which geochemical analysis indicates contains around 63% iron oxide (Appendix 1). Some gypsum and kaolinite is recognised, however laboratory descriptions of the samples indicate that the region is very clay rich and contains a high level of gypsum (Appendix 2). A result like this poses serious questions about the accuracy of HyLogger, and reassures that this spectral data should only be used as a guide.

12. APPENDICES

Appendix 1: Geochemical assays. DL=Detection limit.

Analyte	SiO ₂	Al ₂ O ₃	Fe ₂ O ₃	CaO	MgO	Na ₂ O	K ₂ O	MnO	TiO ₂	P ₂ O ₅
Unit	%	%	%	%	%	%	%	%	%	%
DL	0.1	0.01	0.01	0.01	0.01	0.01	0.01	0.01	0.01	0.01
Sample										
AP2-001	63.8	17.69	1.55	0.13	1.03	2.58	3.53	<0.01	0.76	0.04
AP2-002	63.0	17.14	4.09	0.12	0.99	2.39	2.62	0.02	0.81	0.05
AP2-003	53.5	14.64	14.80	0.38	1.07	2.03	2.39	0.05	0.66	0.06
AP2-004	52.8	15.73	1.91	5.05	1.07	2.12	2.52	<0.01	0.67	0.16
AP2-005	57.1	17.75	4.39	1.18	1.15	2.77	2.61	0.01	0.70	0.04
AP2-006	59.9	19.21	3.10	0.35	1.05	2.52	2.68	0.02	0.64	0.10
AP2-007	84.8	7.14	1.34	0.09	0.29	0.84	0.29	0.03	0.11	0.02
AP2-008	83.4	4.84	3.07	1.57	0.13	0.38	0.13	0.04	0.13	0.03
AP2-009	80.9	1.76	13.55	0.91	0.09	0.04	0.06	0.09	0.07	0.09
AP2-010	95.4	1.15	0.57	0.18	0.08	0.13	0.10	<0.01	0.48	0.03
AP2-011	83.4	9.60	1.02	0.08	0.16	0.67	0.22	<0.01	0.26	<0.01
AP2-012	88.6	6.46	0.47	0.13	0.08	0.02	0.11	<0.01	0.21	<0.01
AP2-013	86.6	7.55	0.48	0.08	0.24	0.51	0.17	<0.01	0.14	<0.01
AP2-014	91.1	5.04	0.59	0.12	0.17	0.04	0.13	<0.01	0.23	0.01
AP2-015	84.9	9.11	1.32	0.06	0.13	0.50	0.10	<0.01	0.24	<0.01
AP2-016	11.2	4.65	0.40	26.98	0.06	0.17	0.08	<0.01	0.09	<0.01
AP2-017	87.0	5.81	2.54	0.08	0.11	0.34	0.18	<0.01	0.24	0.01
AP2-018	88.9	5.92	1.09	0.23	0.08	0.03	0.12	<0.01	0.32	<0.01
AP2-019	74.8	1.18	2.81	6.54	0.04	<0.01	0.06	<0.01	0.18	0.01
AP2-020	96.8	0.95	0.59	0.19	0.11	0.09	0.13	<0.01	0.51	<0.01
AP2-021	94.0	0.57	0.75	0.13	0.04	0.10	0.06	<0.01	0.84	<0.01
AP3-001	60.2	18.05	1.61	2.39	0.89	1.45	2.95	<0.01	0.79	0.05
AP3-002	57.1	15.76	3.39	3.64	0.85	1.59	2.46	<0.01	0.73	0.13
AP3-003	53.0	15.88	3.52	4.32	1.00	1.82	2.52	<0.01	0.66	0.07
AP3-004	26.3	7.69	1.87	19.45	0.37	0.41	1.11	<0.01	0.32	0.04
AP3-005	62.3	18.10	3.38	0.34	0.98	1.82	2.97	<0.01	0.80	0.15
AP3-006	57.4	18.45	4.97	0.39	1.20	2.63	2.89	<0.01	0.69	0.04
AP3-007	82.6	4.48	4.06	1.56	0.12	0.35	0.18	0.04	0.11	0.04
AP3-008	39.8	10.92	25.16	3.84	3.84	1.17	3.17	0.99	0.45	0.17
AP3-009	59.4	14.41	4.41	2.06	1.02	1.88	2.90	0.01	0.67	0.10
AP4-001	60.2	15.89	4.13	0.44	3.32	2.50	4.30	0.05	0.83	0.18
AP4-002	35.9	9.79	29.55	4.44	4.25	0.89	3.03	1.20	0.43	0.17
AP4-003	28.6	8.47	28.24	10.22	2.68	0.93	1.52	2.07	0.39	0.14
AP4-004	10.8	3.10	63.46	1.45	0.92	2.65	0.80	0.23	0.13	0.05
AP4-005	50.1	14.19	4.14	2.79	3.26	3.95	3.89	0.03	0.63	0.07
AP4-006	45.7	6.12	38.29	0.64	0.26	0.27	1.35	0.03	0.33	0.23
AP4-007	51.4	9.13	18.14	3.64	0.72	1.00	2.51	0.03	0.52	0.22
AP4-008	61.9	16.09	1.99	0.11	0.73	1.62	4.15	4.17	0.71	0.04
AP4-009	60.2	15.42	4.42	1.51	1.06	1.84	3.25	0.02	0.73	0.09
AP4-010	50.9	12.70	18.86	0.05	1.38	1.90	2.41	0.06	0.64	0.10
AP4-011	61.3	18.40	1.87	0.10	1.03	2.24	1.94	<0.01	0.56	0.15
AP4-012	87.1	5.14	0.75	0.17	0.26	1.18	0.30	0.01	0.30	0.01
AP4-013	93.5	1.59	0.99	0.69	0.04	0.05	0.12	0.01	0.15	<0.01
AP4-014	68.9	11.78	0.81	0.56	0.84	3.36	0.47	<0.01	0.24	0.01
AP4-015	87.2	2.89	0.72	0.09	0.68	1.41	0.40	<0.01	0.23	0.01
AP4-016	93.4	2.59	0.61	0.24	0.07	0.03	0.25	0.01	0.34	0.05
AP4-017	93.3	2.56	1.48	0.07	0.08	0.02	0.26	0.02	0.21	0.03

Analyte Unit	Ba %	LOI %	SUM %	TOT/C %	TOT/S %	Ba PPM	Be PPM	Co PPM	Cs PPM	Ga PPM
DL Sample	0.01	-5.11	0.01	0.02	0.02	1	1	0.2	0.1	0.5
AP2-001	0.04	9.47	100.65	0.08	0.12	377	2	2.8	6.5	19.3
AP2-002	0.08	9.55	100.86	0.10	0.16	730	2	3.6	5.2	18.0
AP2-003	0.05	10.37	99.99	0.16	0.34	406	1	5.3	4.6	16.7
AP2-004	0.07	14.76	96.92	0.06	2.77	624	<1	2.8	4.4	17.4
AP2-005	0.03	12.04	99.80	0.07	0.69	311	1	5.8	5.0	15.6
AP2-006	0.05	10.92	100.59	0.07	0.24	414	1	7.6	5.4	17.2
AP2-007	<0.01	4.90	99.87	<0.02	0.09	135	<1	5.6	0.9	3.4
AP2-008	<0.01	6.01	99.75	0.04	0.78	64	<1	17.2	0.7	4.9
AP2-009	<0.01	3.06	100.65	0.05	0.45	86	<1	3.9	0.3	3.5
AP2-010	0.01	1.96	100.09	0.05	0.08	224	<1	0.7	0.3	4.1
AP2-011	<0.01	4.97	100.38	0.07	0.06	76	<1	0.9	0.8	12.8
AP2-012	<0.01	3.13	99.23	0.04	0.05	70	<1	1.1	0.4	17.2
AP2-013	<0.01	4.60	100.39	0.05	0.02	84	<1	0.9	0.5	16.6
AP2-014	<0.01	2.66	100.07	0.08	0.03	94	<1	0.9	0.4	22.9
AP2-015	<0.01	4.50	100.83	0.03	0.03	64	<1	0.3	0.4	29.3
AP2-016	<0.01	23.91	67.58	0.04	14.94	19	<1	<0.2	0.5	9.1
AP2-017	<0.01	3.20	99.55	0.07	0.04	89	<1	0.6	1.1	28.8
AP2-018	<0.01	3.18	99.88	0.05	0.09	99	<1	0.6	0.5	56.2
AP2-019	<0.01	9.40	95.06	0.06	3.63	88	<1	0.7	0.2	14.4
AP2-020	<0.01	1.29	100.67	0.06	0.07	84	<1	0.5	0.2	6.0
AP2-021	0.02	3.52	99.99	0.05	0.04	270	<1	0.3	0.2	5.4
AP3-001	0.05	10.32	98.77	0.06	1.24	400	2	2.5	5.5	19.3
AP3-002	0.05	11.82	97.57	0.06	1.95	448	<1	4.2	5.2	17.8
AP3-003	0.04	13.99	96.81	0.07	2.46	328	1	3.4	5.1	16.4
AP3-004	0.02	20.92	78.54	0.03	10.88	167	<1	1.5	2.5	8.3
AP3-005	0.06	8.83	99.72	0.07	0.20	507	2	3.9	6.1	20.5
AP3-006	0.04	11.05	99.76	0.08	0.31	323	1	6.3	5.0	18.1
AP3-007	<0.01	5.84	99.37	0.05	0.85	68	<1	18.9	0.6	4.8
AP3-008	0.04	11.11	100.67	0.87	0.29	363	3	32.7	6.4	18.2
AP3-009	0.05	11.95	98.91	0.07	1.23	487	<1	6.0	3.5	17.3
AP4-001	0.05	8.89	100.75	0.12	0.15	459	3	23.7	9.0	20.7
AP4-002	0.04	11.19	100.90	1.04	0.09	362	3	32.2	5.9	15.3
AP4-003	0.05	16.40	99.76	2.31	0.17	399	3	29.5	5.8	15.7
AP4-004	0.01	15.33	98.96	0.13	0.87	84	2	20.2	1.5	4.1
AP4-005	0.05	16.30	99.38	0.06	1.55	384	3	13.8	9.4	20.0
AP4-006	0.03	7.57	100.79	0.17	0.16	248	12	10.9	2.8	5.8
AP4-007	0.04	11.83	99.24	0.17	1.78	326	7	22.6	4.5	12.6
AP4-008	0.16	8.00	99.67	0.12	0.06	1433	3	314.6	4.4	20.8
AP4-009	0.05	11.38	100.00	0.07	0.80	473	1	5.1	3.6	16.7
AP4-010	0.04	11.45	100.50	0.04	0.07	335	1	1.9	3.1	14.3
AP4-011	0.07	12.52	100.20	0.03	0.02	573	2	1.4	2.9	15.1
AP4-012	<0.01	5.07	100.27	<0.02	0.06	72	<1	0.8	1.0	2.6
AP4-013	<0.01	2.46	99.65	0.03	0.33	46	<1	0.4	0.4	0.7
AP4-014	0.01	12.99	99.94	0.03	0.45	126	<1	0.7	1.3	11.3
AP4-015	0.02	6.91	100.62	0.03	0.04	187	<1	1.0	0.8	5.0
AP4-016	<0.01	2.30	99.90	0.05	0.11	148	<1	0.8	0.8	4.7
AP4-017	0.02	1.85	99.90	0.14	0.03	178	<1	0.9	0.8	4.2

Analyte	Hf	Nb	Rb	Sn	Sr	Ta	Th	U	V	W
Unit	PPM	PPM	PPM	PPM	PPM	PPM	PPM	PPM	PPM	PPM
DL	0.1	0.1	0.1	1	0.5	0.1	0.2	0.1	8	0.5
Sample										
AP2-001	8.0	15.5	141.7	5	82.3	1.2	23.3	3.5	110	2.6
AP2-002	7.3	15.9	104.9	4	82.9	1.3	25.7	5.4	124	2.2
AP2-003	6.5	13.3	96.1	4	99.9	1.0	32.2	9.5	118	2.0
AP2-004	5.2	13.5	102.2	4	704.4	1.1	17.2	4.8	86	2.6
AP2-005	5.7	12.9	102.5	3	136.6	1.1	20.2	7.3	115	2.1
AP2-006	5.5	12.7	104.3	4	455.5	1.0	12.1	7.8	93	2.1
AP2-007	1.1	1.6	10.9	<1	65.9	0.1	4.2	4.4	23	<0.5
AP2-008	1.2	1.7	4.7	1	79.2	0.1	4.2	2.2	25	<0.5
AP2-009	0.9	0.8	2.3	<1	33.9	<0.1	10.7	4.1	106	<0.5
AP2-010	6.8	5.1	3.8	<1	127.9	0.5	2.6	1.1	18	0.8
AP2-011	2.3	3.3	8.2	<1	36.1	0.2	2.5	0.7	18	2.8
AP2-012	1.2	3.2	3.7	1	34.9	0.2	1.9	0.4	17	<0.5
AP2-013	1.2	2.4	4.5	1	34.3	0.2	1.8	0.3	11	<0.5
AP2-014	1.6	2.9	5.1	<1	32.5	0.2	2.4	0.5	22	<0.5
AP2-015	1.1	2.4	3.5	1	26.6	0.2	2.2	0.5	41	1.3
AP2-016	0.8	1.6	3.5	<1	253.5	0.1	1.0	0.3	11	<0.5
AP2-017	3.3	3.7	6.1	1	31.2	0.2	2.4	0.7	159	0.5
AP2-018	3.2	4.1	4.2	2	33.9	0.3	1.8	0.5	72	<0.5
AP2-019	2.2	2.3	2.3	<1	77.1	0.1	1.5	0.7	114	<0.5
AP2-020	6.8	7.1	4.0	2	27.0	0.6	2.8	0.9	36	0.9
AP2-021	6.5	10.1	1.7	3	48.2	1.0	3.7	53.2	124	1.4
AP3-001	5.8	15.7	120.3	4	142.8	1.3	25.2	6.0	96	2.7
AP3-002	5.6	14.0	99.7	4	525.3	1.1	21.7	6.5	109	2.2
AP3-003	4.2	12.9	99.5	4	179.8	1.1	15.6	6.1	93	2.5
AP3-004	2.6	6.5	48.0	2	251.8	0.5	6.5	2.8	105	1.1
AP3-005	6.4	15.9	118.5	4	559.3	1.3	22.1	6.8	118	2.4
AP3-006	5.2	13.0	110.7	4	122.6	1.1	20.9	8.1	114	2.1
AP3-007	1.0	1.5	4.3	<1	79.3	0.1	5.0	2.6	26	1.7
AP3-008	2.9	9.2	122.3	3	288.9	0.8	15.0	8.1	117	2.1
AP3-009	6.4	13.3	98.4	3	259.8	1.1	19.4	4.8	76	2.1
AP4-001	5.5	16.4	159.9	5	87.0	1.3	22.9	3.9	103	2.6
AP4-002	2.4	8.3	112.7	3	316.2	0.7	13.4	8.3	110	1.5
AP4-003	2.3	7.4	101.2	3	511.6	0.6	11.8	9.2	95	1.9
AP4-004	1.0	3.1	31.2	1	72.6	0.9	4.6	9.0	42	<0.5
AP4-005	4.0	12.7	153.6	4	125.8	1.5	20.8	2.9	101	2.3
AP4-006	3.8	6.7	42.2	2	50.7	1.3	9.4	5.2	36	1.1
AP4-007	5.5	9.7	81.0	2	151.7	1.5	13.1	4.1	83	1.3
AP4-008	6.2	13.8	112.1	4	143.7	1.3	19.7	6.2	201	1.9
AP4-009	6.5	13.6	98.0	3	206.9	1.3	21.1	5.0	66	1.6
AP4-010	5.6	12.4	83.8	3	59.6	1.2	18.5	3.8	113	1.6
AP4-011	4.2	10.6	69.3	3	148.5	1.0	10.3	2.4	55	1.6
AP4-012	5.4	4.1	9.6	<1	43.0	0.6	3.4	0.9	19	9.6
AP4-013	1.8	1.5	4.7	<1	22.4	0.5	1.6	0.6	<8	0.6
AP4-014	1.9	3.3	9.4	<1	71.2	0.4	2.5	2.7	<8	<0.5
AP4-015	2.2	3.5	7.2	<1	38.6	0.5	2.2	1.6	9	<0.5
AP4-016	5.4	3.4	7.3	<1	29.1	0.4	2.6	1.2	12	<0.5
AP4-017	3.5	2.7	8.2	<1	34.3	0.4	2.3	0.8	16	<0.5

Analyte	Zr	Y	La	Ce	Pr	Nd	Sm	Eu	Gd	Tb
Unit	PPM	PPM	PPM	PPM	PPM	PPM	PPM	PPM	PPM	PPM
DL	0.1	0.1	0.1	0.1	0.02	0.3	0.05	0.02	0.05	0.01
Sample										
AP2-001	267.8	32.8	55.1	120.5	13.55	47.4	8.70	1.63	6.80	1.10
AP2-002	276.3	29.7	43.3	88.8	9.58	33.7	5.73	0.94	4.67	0.77
AP2-003	225.4	19.8	35.7	68.1	7.17	25.2	4.01	0.64	3.27	0.55
AP2-004	186.4	18.9	103.0	159.1	14.02	44.0	6.24	1.04	4.34	0.63
AP2-005	201.1	18.3	40.8	77.2	8.05	27.3	4.43	0.73	3.43	0.55
AP2-006	200.9	16.6	97.0	127.9	10.90	31.4	4.47	0.77	3.39	0.55
AP2-007	39.8	4.5	11.1	21.9	2.41	7.7	1.37	0.22	1.05	0.16
AP2-008	39.1	4.7	8.4	14.6	1.30	5.1	1.08	0.22	1.01	0.18
AP2-009	32.3	3.5	3.2	9.9	0.80	3.2	0.78	0.16	0.74	0.12
AP2-010	251.9	5.5	5.3	10.4	1.14	4.7	0.80	0.13	0.66	0.12
AP2-011	79.6	4.6	7.0	12.8	1.33	5.0	0.83	0.15	0.80	0.13
AP2-012	40.4	3.7	5.1	8.4	0.98	3.5	0.65	0.12	0.61	0.10
AP2-013	38.4	3.1	4.6	7.9	0.88	2.9	0.58	0.10	0.55	0.09
AP2-014	50.2	3.7	5.1	9.5	1.05	3.7	0.71	0.14	0.65	0.10
AP2-015	38.4	2.5	4.3	6.7	0.76	2.8	0.50	0.10	0.47	0.07
AP2-016	28.9	1.6	3.6	6.2	0.69	2.4	0.45	0.07	0.27	0.04
AP2-017	129.6	3.7	6.0	11.5	1.29	4.1	0.86	0.15	0.73	0.11
AP2-018	130.6	3.8	5.8	10.7	1.21	4.5	0.78	0.17	0.70	0.11
AP2-019	84.8	2.7	3.2	6.7	0.74	3.0	0.53	0.09	0.42	0.07
AP2-020	245.0	7.6	9.7	15.2	1.81	6.0	1.14	0.22	1.00	0.19
AP2-021	255.0	9.3	12.8	21.2	2.43	8.8	1.37	0.25	1.08	0.22
AP3-001	205.6	34.1	55.6	117.8	13.62	51.4	10.30	1.90	8.44	1.31
AP3-002	209.1	21.2	59.4	104.8	10.82	36.2	5.60	0.89	3.99	0.65
AP3-003	159.2	17.6	39.8	74.3	8.00	26.9	4.38	0.72	3.25	0.56
AP3-004	90.9	9.3	19.5	36.2	3.65	12.5	2.02	0.35	1.56	0.28
AP3-005	218.5	23.6	67.3	117.6	12.31	39.7	5.92	0.99	4.47	0.70
AP3-006	171.3	18.2	46.1	85.6	8.87	29.5	4.69	0.77	3.53	0.59
AP3-007	39.8	4.5	7.7	14.4	1.34	4.9	1.11	0.25	1.05	0.19
AP3-008	99.2	33.2	33.9	69.6	8.41	33.4	6.48	1.29	6.42	0.98
AP3-009	213.4	20.5	41.4	77.5	8.21	27.0	4.59	0.84	3.56	0.62
AP4-001	191.7	44.9	47.7	91.4	10.82	40.5	8.60	1.75	8.86	1.39
AP4-002	82.9	31.8	31.6	63.9	7.54	30.5	6.09	1.17	5.78	0.92
AP4-003	80.6	36.6	28.0	56.7	6.94	28.1	5.63	1.22	6.16	0.92
AP4-004	32.6	20.4	13.4	29.7	3.52	15.2	2.95	0.64	3.09	0.48
AP4-005	135.4	37.1	43.1	93.9	11.11	44.6	8.35	1.63	7.20	1.08
AP4-006	121.4	53.3	14.7	34.8	4.48	22.4	6.00	1.46	8.07	1.47
AP4-007	187.4	56.9	27.5	65.1	7.92	35.7	8.67	1.96	9.62	1.72
AP4-008	209.9	50.9	45.1	120.3	13.66	58.0	12.85	2.63	10.90	1.73
AP4-009	216.8	21.9	40.6	81.1	8.08	27.6	4.61	0.85	3.85	0.64
AP4-010	189.3	16.6	27.3	50.2	4.49	14.9	2.54	0.53	2.25	0.42
AP4-011	136.8	37.2	110.0	114.6	42.57	195.2	36.30	6.21	24.04	2.76
AP4-012	185.7	6.2	7.2	14.8	1.60	5.6	1.14	0.22	1.05	0.18
AP4-013	63.0	3.1	3.7	7.3	0.77	2.9	0.55	0.09	0.54	0.09
AP4-014	68.1	3.9	7.7	17.3	1.86	7.4	1.35	0.25	0.99	0.14
AP4-015	76.1	4.0	6.0	13.1	1.36	5.5	1.00	0.20	0.88	0.13
AP4-016	192.6	5.5	5.6	12.8	1.31	5.0	1.03	0.22	0.91	0.16
AP4-017	117.5	4.2	5.9	13.3	1.37	5.2	1.04	0.20	0.88	0.14

Analyte	Dy	Ho	Er	Tm	Yb	Lu	Mo	Cu	Pb	Zn
Unit	PPM	PPM	PPM	PPM	PPM	PPM	PPM	PPM	PPM	PPM
DL	0.05	0.02	0.03	0.01	0.05	0.01	0.1	0.1	0.1	1
Sample										
AP2-001	6.51	1.14	3.31	0.50	3.23	0.45	0.1	3.9	2.9	4
AP2-002	5.04	0.96	3.03	0.48	3.10	0.46	0.4	7.2	7.1	17
AP2-003	3.52	0.66	2.11	0.34	2.22	0.35	0.7	20.6	22.4	29
AP2-004	3.47	0.67	2.08	0.33	2.13	0.32	0.3	6.8	14.3	5
AP2-005	3.19	0.62	2.02	0.34	2.20	0.31	0.8	24.4	8.5	12
AP2-006	3.32	0.63	1.92	0.30	2.00	0.28	1.2	14.6	33.4	11
AP2-007	0.95	0.16	0.47	0.07	0.50	0.06	0.5	11.8	7.7	9
AP2-008	1.02	0.19	0.56	0.09	0.51	0.08	0.6	15.7	5.4	13
AP2-009	0.75	0.13	0.40	0.06	0.36	0.05	1.2	11.8	15.8	35
AP2-010	0.91	0.18	0.63	0.11	0.69	0.11	0.1	2.3	3.0	3
AP2-011	0.79	0.16	0.50	0.08	0.56	0.08	0.1	1.5	0.6	2
AP2-012	0.71	0.13	0.44	0.06	0.41	0.07	<0.1	1.6	0.8	<1
AP2-013	0.55	0.10	0.38	0.05	0.32	0.05	<0.1	1.6	0.7	1
AP2-014	0.70	0.13	0.43	0.07	0.46	0.07	0.2	1.3	1.1	1
AP2-015	0.44	0.08	0.26	0.05	0.29	0.04	0.2	0.9	1.0	1
AP2-016	0.26	0.05	0.18	0.03	0.20	0.03	0.1	<0.1	0.2	<1
AP2-017	0.74	0.14	0.42	0.07	0.47	0.08	0.4	1.1	1.4	2
AP2-018	0.72	0.12	0.42	0.07	0.49	0.07	0.4	0.9	1.9	<1
AP2-019	0.48	0.09	0.26	0.05	0.31	0.05	3.0	2.8	1.9	9
AP2-020	1.33	0.27	0.91	0.15	1.09	0.17	0.1	1.2	2.4	<1
AP2-021	1.60	0.32	1.12	0.19	1.28	0.20	0.3	1.9	1.5	<1
AP3-001	7.29	1.29	3.60	0.53	3.43	0.48	0.3	17.3	10.4	4
AP3-002	3.90	0.71	2.25	0.38	2.27	0.34	1.5	33.9	4.7	12
AP3-003	3.48	0.61	1.91	0.31	2.04	0.30	1.3	32.2	1.9	17
AP3-004	1.76	0.34	1.03	0.16	1.20	0.16	0.5	9.9	1.6	2
AP3-005	4.44	0.82	2.42	0.37	2.54	0.38	1.1	33.8	6.8	14
AP3-006	3.53	0.66	2.11	0.31	2.13	0.33	0.8	36.9	8.6	15
AP3-007	1.08	0.19	0.62	0.08	0.53	0.08	0.6	17.6	6.3	17
AP3-008	5.44	1.07	2.85	0.41	2.53	0.38	4.1	6.2	20.8	82
AP3-009	3.72	0.73	2.30	0.34	2.23	0.33	0.2	6.4	3.9	8
AP4-001	8.19	1.53	4.54	0.63	3.80	0.54	0.2	6.9	12.0	96
AP4-002	5.23	0.95	2.81	0.40	2.43	0.36	4.9	5.6	22.8	79
AP4-003	5.19	1.03	2.90	0.39	2.47	0.37	10.7	4.0	4.4	91
AP4-004	2.74	0.52	1.42	0.19	1.15	0.16	0.5	2.2	16.3	59
AP4-005	6.16	1.20	3.32	0.50	3.05	0.44	0.1	3.6	8.7	60
AP4-006	8.89	1.88	5.33	0.76	4.31	0.64	2.0	2.5	63.0	364
AP4-007	10.05	2.07	5.86	0.88	5.27	0.78	0.7	6.1	22.6	327
AP4-008	9.52	1.80	4.72	0.68	4.21	0.58	0.8	34.4	56.3	23
AP4-009	3.75	0.78	2.33	0.35	2.32	0.35	0.3	5.9	4.2	8
AP4-010	2.71	0.60	1.78	0.30	2.01	0.29	0.2	3.5	4.9	4
AP4-011	12.13	1.57	3.44	0.44	2.70	0.34	<0.1	2.4	1.9	4
AP4-012	1.05	0.20	0.65	0.10	0.73	0.11	<0.1	1.1	2.6	<1
AP4-013	0.52	0.10	0.32	0.05	0.33	0.05	0.2	1.0	0.9	<1
AP4-014	0.74	0.14	0.43	0.06	0.44	0.07	0.2	1.3	0.4	<1
AP4-015	0.74	0.14	0.46	0.07	0.44	0.07	0.3	2.2	1.4	<1
AP4-016	0.93	0.19	0.59	0.09	0.67	0.10	0.2	3.6	4.4	<1
AP4-017	0.79	0.15	0.46	0.06	0.46	0.07	0.3	2.8	3.4	2

Analyte	Ni	As	Cd	Sb	Bi	Ag	Au	Hg	Tl	Se
Unit	PPM	PPM	PPM	PPM	PPM	PPM	PPB	PPM	PPM	PPM
DL	0.1	0.5	0.1	0.1	0.1	0.1	0.5	0.01	0.1	0.5
Sample										
AP2-001	2.0	1.3	<0.1	<0.1	<0.1	<0.1	1.8	<0.01	0.1	<0.5
AP2-002	3.6	5.3	<0.1	0.1	0.3	<0.1	1.8	<0.01	<0.1	5.1
AP2-003	7.4	36.2	<0.1	0.2	0.5	<0.1	1.7	<0.01	<0.1	39.8
AP2-004	3.4	3.2	<0.1	0.1	0.3	<0.1	1.5	<0.01	<0.1	6.2
AP2-005	8.1	10.8	<0.1	0.2	0.3	<0.1	2.0	<0.01	<0.1	18.9
AP2-006	6.0	8.6	<0.1	0.2	0.1	<0.1	0.6	<0.01	0.1	3.7
AP2-007	4.9	3.7	<0.1	<0.1	0.2	<0.1	<0.5	<0.01	0.3	0.9
AP2-008	9.1	4.3	<0.1	<0.1	<0.1	<0.1	1.0	<0.01	<0.1	0.9
AP2-009	9.5	12.4	<0.1	0.3	0.3	<0.1	<0.5	<0.01	0.1	2.6
AP2-010	0.8	0.9	<0.1	<0.1	<0.1	<0.1	<0.5	<0.01	<0.1	<0.5
AP2-011	1.0	1.0	<0.1	<0.1	<0.1	<0.1	6.4	<0.01	<0.1	<0.5
AP2-012	0.9	0.6	<0.1	<0.1	<0.1	<0.1	2.4	<0.01	<0.1	<0.5
AP2-013	0.5	<0.5	<0.1	<0.1	<0.1	<0.1	1.4	<0.01	<0.1	<0.5
AP2-014	0.4	<0.5	<0.1	<0.1	<0.1	<0.1	1.5	<0.01	<0.1	<0.5
AP2-015	0.4	2.2	<0.1	<0.1	<0.1	<0.1	0.9	<0.01	<0.1	0.8
AP2-016	<0.1	1.0	<0.1	<0.1	<0.1	<0.1	0.6	<0.01	<0.1	<0.5
AP2-017	0.8	9.7	<0.1	<0.1	0.3	<0.1	<0.5	<0.01	<0.1	0.9
AP2-018	0.5	1.9	<0.1	<0.1	0.2	<0.1	1.3	<0.01	<0.1	0.6
AP2-019	0.6	11.3	<0.1	<0.1	0.1	<0.1	0.7	<0.01	<0.1	0.8
AP2-020	0.6	<0.5	<0.1	<0.1	<0.1	<0.1	2.3	<0.01	<0.1	<0.5
AP2-021	0.4	1.9	<0.1	<0.1	<0.1	<0.1	<0.5	<0.01	<0.1	<0.5
AP3-001	3.2	<0.5	<0.1	<0.1	0.3	<0.1	1.4	<0.01	<0.1	<0.5
AP3-002	8.2	4.6	<0.1	0.2	0.6	<0.1	1.7	<0.01	<0.1	2.5
AP3-003	8.2	4.4	<0.1	0.1	0.2	<0.1	1.1	0.01	<0.1	1.8
AP3-004	2.0	3.1	<0.1	0.2	<0.1	<0.1	2.4	<0.01	<0.1	1.2
AP3-005	8.4	4.3	<0.1	0.2	0.6	<0.1	1.1	<0.01	<0.1	2.5
AP3-006	10.3	12.2	<0.1	0.2	0.3	<0.1	2.1	<0.01	<0.1	18.2
AP3-007	10.5	3.8	<0.1	<0.1	0.1	<0.1	0.6	<0.01	<0.1	0.7
AP3-008	71.4	13.0	1.3	0.5	0.4	<0.1	1.1	<0.01	0.5	0.9
AP3-009	3.9	4.6	<0.1	0.2	0.3	<0.1	<0.5	<0.01	<0.1	1.8
AP4-001	70.3	1.8	<0.1	<0.1	0.4	<0.1	0.7	<0.01	0.1	<0.5
AP4-002	72.6	16.6	2.0	0.5	0.4	<0.1	0.5	<0.01	0.5	1.2
AP4-003	72.1	2.5	3.8	0.1	0.3	<0.1	<0.5	<0.01	2.2	1.0
AP4-004	55.6	2.9	0.4	<0.1	0.1	<0.1	3.0	<0.01	<0.1	3.6
AP4-005	60.8	6.5	<0.1	0.2	0.5	<0.1	2.3	<0.01	<0.1	1.0
AP4-006	56.9	29.9	0.1	1.0	0.4	<0.1	0.6	<0.01	0.2	1.5
AP4-007	102.6	11.9	<0.1	0.5	0.3	<0.1	4.8	0.02	<0.1	5.0
AP4-008	14.5	4.3	<0.1	<0.1	0.5	<0.1	4.9	<0.01	11.3	0.8
AP4-009	3.8	6.5	<0.1	0.1	0.3	<0.1	<0.5	<0.01	<0.1	1.2
AP4-010	3.0	3.5	<0.1	0.1	0.3	<0.1	1.0	<0.01	<0.1	1.9
AP4-011	3.2	1.4	<0.1	<0.1	0.1	<0.1	<0.5	<0.01	<0.1	0.5
AP4-012	1.1	0.5	<0.1	<0.1	<0.1	<0.1	1.9	<0.01	<0.1	<0.5
AP4-013	1.0	0.7	<0.1	<0.1	<0.1	<0.1	<0.5	<0.01	<0.1	<0.5
AP4-014	0.7	0.9	<0.1	<0.1	<0.1	<0.1	0.7	<0.01	<0.1	<0.5
AP4-015	0.5	0.9	<0.1	<0.1	<0.1	<0.1	0.5	<0.01	<0.1	0.8
AP4-016	0.8	<0.5	<0.1	<0.1	<0.1	<0.1	<0.5	<0.01	<0.1	0.6
AP4-017	1.4	1.0	<0.1	<0.1	<0.1	<0.1	1.8	<0.01	<0.1	<0.5

Appendix 2: Sample descriptions in order from profile AP1 to AP6. Porosity measured on a scale of 0 to 2 from laboratory observations.

Sample	Grain size	Grain shape	Quartz grains	Sorting	Porosity	Weathering features	Description
AP1-001 Location: 0712244 6629519	FS-MS	Rounded to sub-rounded	"	Mod	1	Minor secondary ferruginisation tends to follow bedding/lamination planes.	Kaolin rich (5%) sandstone with minor patches of secondary ferruginisation. Bedding exists, but not well defined.
	pH	Colour	Sedimentary structures	Fabric	Rock strength		
	6.5	White + pale pink/purple	Poorly bedded. Laminations preserved	some primary retained	Very low		
Sample	Grain size	Grain shape	Quartz grains	Sorting	Porosity	Weathering features	Description
AP1-002 Location: 0712244 6629519	MS	Rounded	"	Mod-poor	1	Minor secondary ferruginisation tends to follow bedding/lamination planes.	Kaolin rich (5%) sandstone with patches of secondary ferruginisation. Bedding exists, but not well defined. Some black pyrite concretions present.
	pH	Colour	Sedimentary structures	Fabric	Rock strength		
	7	red-pink	Poorly bedded. Laminations preserved	some primary retained	Low		
Sample	Grain size	Grain shape	Quartz grains	Sorting	Porosity	Weathering features	Description
AP1-003 Location: 0712244 6629519	MS	Rounded to sub-rounded	"	Mod	1	Secondary ferruginisation in the form of hematite and goethite. Red and yellow bands tend to be separate.	Kaolin rich (5%) sandstone with bands of secondary ferruginisation causing strong discolouration. Bedding exists, but not well defined. White kaolin-rich veins are present.
	pH	Colour	Sedimentary structures	Fabric	Rock strength		
	8	yellow/red-orange	Slight low angle cross-laminations	slightly retained	Low		
Sample	Grain size	Grain shape	Quartz grains	Sorting	Porosity	Weathering features	Description
AP1-004 Location: 0712244 6629519	MS	Rounded to sub-rounded	"	Mod-well	1	Secondary ferruginisation in the form of hematite and goethite. Red and yellow bands tend to be separate.	Pale grey sandstone with reduced kaolin content of the matrix compared with 001-003. Modern calcite veining is present.
	pH	Colour	Sedimentary structures	Fabric	Rock strength		
	7	Pale grey	bedding very poorly defined	Some retained	Very low		
Sample	Grain size	Grain shape	Quartz grains	Sorting	Porosity	Weathering features	Description
AP1-005 Location: 0712244 6629519	MS-CS	Rounded	"	Mod	1	Secondary ferruginisation in the form of hematite causing some red discolouration.	Bedded sandstone, with significant hematite stained lenses.
	pH	Colour	Sedimentary structures	Fabric	Rock strength		
	7.5	Pink-red	Bedding exists	Bedding retained	Low		
Sample	Grain size	Grain shape	Quartz grains	Sorting	Porosity	Weathering features	Description
AP1-006 Location: 0712244 6629519	MS	Rounded to sub-rounded	"	Mod	1	Very kaolinitic and white in colour.	Kaolin-rich (5-10%) sandstone. Some black pyrite concretions present. Quite 'blocky' in nature.
	pH	Colour	Sedimentary structures	Fabric	Rock strength		
	7.5	White	Minor bedding	Retained	Very low		

Sample	Grain size	Grain shape	Quartz grains	Sorting	Porosity	Weathering features	Description
AP1-007 Location: 0712217 6629545	MS	Rounded to sub-rounded	"	Mod	1	Kaolinised somewhat.	Well consolidated, kaolin rich sandstone.
	pH	Colour	Sedimentary structures	Fabric	Rock strength		
	7.5	brown-orange/white-purple	-	not observed	Low		
Sample	Grain size	Grain shape	Quartz grains	Sorting	Porosity	Weathering features	Description
AP1-008 Location: 0712217 6629545	C-S	-	MS-Rounded	-	0	Very loose, soft and moist material.	Very fine and loose material, with abundant organic matter (roots). Forms lumps or nodules. Some quartz grain clasts are present.
	pH	Colour	Sedimentary structures	Fabric	Rock strength		
	9.5	Yellow-light brown	-	No fabric	Very low		
Sample	Grain size	Grain shape	Quartz grains	Sorting	Porosity	Weathering features	Description
AP1-009 Location: 0712217 6629545	MS	Rounded	"	Well	1	This unit is a yellow goethite stained ferruginous band within the stratigraphy.	Thin ferruginous layer (50 cm) (goethite) of sandstone. Quite 'blocky' in nature.
	pH	Colour	Sedimentary structures	Fabric	Rock strength		
	8.5	yellow	Elongate flute casts present	Minor	Low		
Sample	Grain size	Grain shape	Quartz grains	Sorting	Porosity	Weathering features	Description
AP1-10 Location: 0712173 6629548	FS-MS	Sub-angular	"	Mod-poor	1	Secondary ferruginisation causing red (hematite) staining.	A firm and well consolidated blocky sandstone. Secondary ferruginisation is present, often banded. Hematite also occurs in fractures within rock. Kaolinite is present. Minor pyrite concretions present.
	pH	Colour	Sedimentary structures	Fabric	Rock strength		
	7	White + red patches	bedding poorly defined	well retained	Mod-high		
Sample	Grain size	Grain shape	Quartz grains	Sorting	Porosity	Weathering features	Description
AP1-011 Location: 0712173 6629548	FS-MS	Sub-rounded to sub-angular	"	Mod-poor	1	Strong red (hematite) staining from secondary ferruginisation.	A well consolidated sandstone, however slightly powdery in nature. Prominent red (hematite) discolouration. Kaolinite is present.
	pH	Colour	Sedimentary structures	Fabric	Rock strength		
	7.5	Red	Minor bedding	Well retained	Mod		
Sample	Grain size	Grain shape	Quartz grains	Sorting	Porosity	Weathering features	Description
AP1-012 Location: 0712173 6629548	MS + CS	angular + rounded	"	very poor	1	Secondary ferruginisation causing red (hematite) staining.	A firm red (hematite stained) sandstone with a medium sand and coarse sand fraction. Medium sand is rounded, coarse sand is angular. Kaolinite is present (5%).
	pH	Colour	Sedimentary structures	Fabric	Rock strength		
	8.5	Red-pale pink	-	not observed	low + hard		

Sample	Grain size	Grain shape	Quartz grains	Sorting	Porosity	Weathering features	Description
AP1-13 Location: 0712173 6629548	FS	Sub-angular	"	Well	1	Kaolinised somewhat.	A light coloured kaolinitic sandstone with beds of brittle, fine, laminated mud, which form sheet like structures.
	pH	Colour	Sedimentary structures	Fabric	Rock strength		
	8	Pale white-brown	Some bedding	Some retained	Mod		
Sample	Grain size	Grain shape	Quartz grains	Sorting	Porosity	Weathering features	Description
AP1-014 Location: 0712173 6629548	FS	Rounded to sub-rounded	"	Mod	1	Kaolinitic. Some concretionary lumps of kaolinite.	A kaolinitic sandstone with organic material (roots) and some rounded quartz pebbles (1-2 cm).
	pH	Colour	Sedimentary structures	Fabric	Rock strength		
	8	Pale white/pinky brown	-	not observed	Low		
Sample	Grain size	Grain shape	Quartz grains	Sorting	Porosity	Weathering features	Description
AP1-015 Location: 0712173 6629548	FS	Sub-rounded	"	Well	1	Some goethite rich nodules.	very loose sandy and kaolinitic material. Some consolidated angular lumps have formed. Goethite is present, as well as minor hematite in patches.
	pH	Colour	Sedimentary structures	Fabric	Rock strength		
	8	White-pale light brown	-	not observed	Low		

Sample	Grain size	Grain shape	Quartz grains	Sorting	Porosity	Weathering features	Description
AP2-001 Location: 0712273 6629231	C	-	MS- Rounded	-	0	Red (hematite) mottles.	Green clay with red mottles. Minor medium sand clasts.
	pH	Colour	Sedimentary structures	Fabric	Rock strength		
	6.5	Green-grey	-	Slight	Very low		
Sample	Grain size	Grain shape	Quartz grains	Sorting	Porosity	Weathering features	Description
AP2-002 Location: 0712273 6629231	C	-	-	-	0	Purple-red hematite staining.	Purple clay.
	pH	Colour	Sedimentary structures	Fabric	Rock strength		
	7	Purple-red	Small scale laminations (5 mm)	Slight	Very low		
Sample	Grain size	Grain shape	Quartz grains	Sorting	Porosity	Weathering features	Description
AP2-003 Location: 0712273 6629231	C	-	MS- Rounded	Poor	1	Hematite and goethite bands have formed by secondary ferruginisation.	Clay mixed with rounded sands. Some harder iron-rich concretions, which are more sandy in nature. A mixture of clear quartz grains and red, hematite stained quartz grains. Gypsum is present.
	pH	Colour	Sedimentary structures	Fabric	Rock strength		
	5	Orange-red/brown to green	Minor laminations	Slight	Low		
Sample	Grain size	Grain shape	Quartz grains	Sorting	Porosity	Weathering features	Description
AP2-004 Location: 0712273 6629231	C	-	-	-	0	Kaolinised.	A white layer of clay containing relatively high levels of Ca (5.05%) and Mg (1.07%). Kaolin rich.
	pH	Colour	Sedimentary structures	Fabric	Rock strength		
	7	White + brown	-	Slight	Low		
Sample	Grain size	Grain shape	Quartz grains	Sorting	Porosity	Weathering features	Description
AP2-005 Location: 0712273 6629231	C	-	FS-Sub- rounded	-	0-1	Hematite and goethite staining	Clay rich unit with minor fine sands. Gypsum present, causing elevated Ca concentration.
	pH	Colour	Sedimentary structures	Fabric	Rock strength		
	6	Orange	Bedded + minor cross-bedding.	Retained	Low		
Sample	Grain size	Grain shape	Quartz grains	Sorting	Porosity	Weathering features	Description
AP2-006 Location: 0712230 6629227	C	-	-	-	0	Small scale ferruginisation/ redox boundaries.	A clay with small scale redox boundaries. i.e. Purple colours meet green colours with a red band at the boundary between green and purple. Form the shape of paleo-groundwater flows.
	pH	Colour	Sedimentary structures	Fabric	Rock strength		
	6	Green to purple + red	-	-	Low		

Sample	Grain size	Grain shape	Quartz grains	Sorting	Porosity	Weathering features	Description
AP2-007 Location: 0712230 6629227	CS	Rounded	"	Mod	2	Small scale ferruginisation/redox boundaries.	Kaolin rich sandstone with small scale redox boundaries which follow paleo-groundwater flows. Colours range from dark purple to pale green, with orange at the boundaries between these colours.
	pH	Colour	Sedimentary structures	Fabric	Rock strength		
	5.5	White green	-	-	Low		
Sample	Grain size	Grain shape	Quartz grains	Sorting	Porosity	Weathering features	Description
AP2-008 Location: 0712230 6629227	MS	Rounded to sub-rounded	"	Well	1	Kaolinised. Very weak.	Loose medium sands.
	pH	Colour	Sedimentary structures	Fabric	Rock strength		
	8	Purple white	-	-	Very low		
Sample	Grain size	Grain shape	Quartz grains	Sorting	Porosity	Weathering features	Description
AP2-009 Location: 0712230 6629227	MS	Sub-rounded to sub-angular	"	Mod	1	Prominent ferruginisation and iron staining.	This well consolidated unit forms a bench like structure on side of hill. A sandy ferricrete. Sands cemented together by iron-rich cement which also contains kaolinite.
	pH	Colour	Sedimentary structures	Fabric	Rock strength		
	6.5	Purple + red/yellow	Bedding + laminations	Well retained	Mod-high		
Sample	Grain size	Grain shape	Quartz grains	Sorting	Porosity	Weathering features	Description
AP2-010 Location: 0712173 6629254	FS + MS	Sub-rounded to sub-angular	"	Poor-mod	1	-	Fine sand with a mixture of purple sand grains and clear sand grains. Minor silicification.
	pH	Colour	Sedimentary structures	Fabric	Rock strength		
	7	Light brown	Some bedding/laminations	Well retained	High		
Sample	Grain size	Grain shape	Quartz grains	Sorting	Porosity	Weathering features	Description
AP2-011 Location: 0712173 6629254	MS	Sub-rounded to sub-angular	"	Poor	1	Highly weathered and loose.	Sandy material with kaolinite. Some harder lumps present.
	pH	Colour	Sedimentary structures	Fabric	Rock strength		
	6	White/pinky brown	sedimentary layer	-	Low		
Sample	Grain size	Grain shape	Quartz grains	Sorting	Porosity	Weathering features	Description
AP2-012 Location: 0712155 6629265	MS-CS	Rounded to sub-rounded	"	Mod	1	Highly weathered.	Consolidated rounded sands with kaolinite.
	pH	Colour	Sedimentary structures	Fabric	Rock strength		
	8.5	Light brown to orange	sedimentary layer	Slight	Mod		

Sample	Grain size	Grain shape	Quartz grains	Sorting	Porosity	Weathering features	Description
AP2-013 Location: 0712155 6629265	FS	Sub rounded	"	Mod	1	Highly weathered and kaolinitic.	Kaolinitic sands with minor kaolinite veins.
	pH	Colour	Sedimentary structures	Fabric	Rock strength		
	7.5	Pale pink	Bedded	Well retained	Mod		
Sample	Grain size	Grain shape	Quartz grains	Sorting	Porosity	Weathering features	Description
AP2-014 Location: 0712155 6629265	MS	Rounded to sub-rounded	"	Mod	1	Kaolinised.	Sandstone with kaolinite. A coarse, angular sand fraction is also present.
	pH	Colour	Sedimentary structures	Fabric	Rock strength		
	8.5	Orange	Large scale cross-bedding	Well retained	Mod-high		
Sample	Grain size	Grain shape	Quartz grains	Sorting	Porosity	Weathering features	Description
AP2-015 Location: 0712155 6629265	MS+FS	Rounded to sub-rounded	"	Mod	1	Kaolinised.	Similar to 013. Probably part of the same stratigraphic unit. Kaolinitic sands.
	pH	Colour	Sedimentary structures	Fabric	Rock strength		
	7.5	Pale pink	-	Slight	Mod		
Sample	Grain size	Grain shape	Quartz grains	Sorting	Porosity	Weathering features	Description
AP2-016 Location: 0712155 6629265	C	-	-	-	0-1	-	This is a gypsum layer within the sequence. May have formed in a fracture. Gypsum shards with minor kaolinite.
	pH	Colour	Sedimentary structures	Fabric	Rock strength		
	8.5	White/milky clear	-	-	Low		
Sample	Grain size	Grain shape	Quartz grains	Sorting	Porosity	Weathering features	Description
AP2-017 Location: 0712148 6629275	MS	Sub rounded	"	Mod-well	1	Small scale ferruginisation (hematite).	Kaolinitic sandstone.
	pH	Colour	Sedimentary structures	Fabric	Rock strength		
	7	White + red pink	-	-	Mod		
Sample	Grain size	Grain shape	Quartz grains	Sorting	Porosity	Weathering features	Description
AP2-018 Location: 0712148 6629275	MS	Rounded to sub-rounded	"	Mod-well	1	Minor redox zones. Hematite and goethite staining.	Well consolidated sandstone retaining bedding and highly fractured. Stronger unit than surroundings. Kaolinite present.
	pH	Colour	Sedimentary structures	Fabric	Rock strength		
	7	White pink orange	Bedded	Well retained	Mod		

Sample	Grain size	Grain shape	Quartz grains	Sorting	Porosity	Weathering features	Description
AP2-019 Location: 0712148 6629275	FS-MS	Rounded to sub-rounded	"	Well	0-1	Goethite staining.	Well consolidated sandstone. Kaolinite present. Surface is quite pitted.
	pH	Colour	Sedimentary structures	Fabric	Rock strength		
	6.5	Yellow	-	-	Mod		
Sample	Grain size	Grain shape	Quartz grains	Sorting	Porosity	Weathering features	Description
AP2-020 Location: 0712148 6629275	FS-MS	Sub rounded	"	Poor	1	-	Fine sand with kaolinite. Pyrite concretions are present. Carbonaceous in places.
	pH	Colour	Sedimentary structures	Fabric	Rock strength		
	8.5	Pale pink	-	-	Mod		
Sample	Grain size	Grain shape	Quartz grains	Sorting	Porosity	Weathering features	Description
AP2-021 Location: 0712148 6629275	S-FS	Sub rounded	FS-Sub rounded	Mod	1	Small scale ferruginisation (hematite).	Carbonaceous, well consolidated and laminated silt to sand. Some parts are silty, some sandy. Strong fizzing with HCl.
	pH	Colour	Sedimentary structures	Fabric	Rock strength		
	9	Pale brown	laminations preserved	Well retained	Mod		

Sample	Grain size	Grain shape	Quartz grains	Sorting	Porosity	Weathering features	Description
AP3-001 Location: 0712167 6629035	C	-	-	-	0	Slight hematite mottling.	A green clay with abundant gypsum. Minor hematite mottles present.
	pH	Colour	Sedimentary structures	Fabric	Rock strength		
	8.5	Green	Minor laminations	Slight	Very low		
AP3-002 Location: 0712167 6629035	C	-	FS-Rounded	-	0-1	Prominent hematite mottling.	A red clay with abundant gypsum. Prominent hematite mottling present. Minor rounded fine sand present.
	pH	Colour	Sedimentary structures	Fabric	Rock strength		
	6.5	Red	laminations preserved	Slight	Very low		
AP3-003 Location: 0712167 6629035	C	-	-	-	0	Minor hematite mottling.	A geothite stained yellow clay with abundant gypsum.
	pH	Colour	Sedimentary structures	Fabric	Rock strength		
	8	Yellow	Minor cross-laminations	Slight	Very low		
AP3-004 Location: 0712167 6629035	C	-	-	-	0	Minor hematite mottling.	Grey-green gypsum-rich clay.
	pH	Colour	Sedimentary structures	Fabric	Rock strength		
	7.5	Grey green	Minor laminations	Slight	Very low		

Sample	Grain size	Grain shape	Quartz grains	Sorting	Porosity	Weathering features	Description
AP4-001 Location: 0714824 6627173	C	-	-	-	0-1	Highly weathered.	Green fine grained shaley mud. Well laminated, and tends to break along lamination planes. Some organic matter (roots) present.
	pH	Colour	Sedimentary structures	Fabric	Rock strength		
	7.5	Green	Laminations	Well retained	Very low		
Sample	Grain size	Grain shape	Quartz grains	Sorting	Porosity	Weathering features	Description
AP4-002 Location: 0714824 6627173	C	-	-	-	0-1	Hematite stained.	Red fine grained chaley mud. Well laminated, however tends to form angular blocky structures rather than breaking along lamination plane into sheets. Organic matter is present (roots).
	pH	Colour	Sedimentary structures	Fabric	Rock strength		
	9	Red	laminations preserved	Moderate	Low		
Sample	Grain size	Grain shape	Quartz grains	Sorting	Porosity	Weathering features	Description
AP4-003 Location: 0714824 6627173	C	-	-	-	0-1	Hematite stained.	Purple fine grained shaley mud. Slight laminations preserved. Organic matter present (roots).
	pH	Colour	Sedimentary structures	Fabric	Rock strength		
	9	Purple	Minor laminations	Moderate	Low		
Sample	Grain size	Grain shape	Quartz grains	Sorting	Porosity	Weathering features	Description
AP4-004 Location: 0714806 6627165	C-S	-	-	-	0-1	Ferruginous.	A small layer within the stratigraphy containing 63% iron oxide. Extremely ferruginous.
	pH	Colour	Sedimentary structures	Fabric	Rock strength		
	9	Dark red + yellow	Minor laminations	Slight	Mod		
Sample	Grain size	Grain shape	Quartz grains	Sorting	Porosity	Weathering features	Description
AP4-005 Location: 0714806 6627165	C	-	-	-	1	Highly weathered and loose.	Very unconsolidated and weathered material. Gypsum is present.
	pH	Colour	Sedimentary structures	Fabric	Rock strength		
	8	Medium brown	Slight bedding	Slight	Very low		
Sample	Grain size	Grain shape	Quartz grains	Sorting	Porosity	Weathering features	Description
AP4-006 Location: 0714806 6627165	FS	Sub-rounded to sub-angular	"	Mod	1	Prominent secondary ferruginisation, mainly hematite, but minor goethite.	A well cemented and hard layer, which has been affected by secondary ferruginisation.
	pH	Colour	Sedimentary structures	Fabric	Rock strength		
	7.5	Purple	Laminations and bedding	Well retained	High		

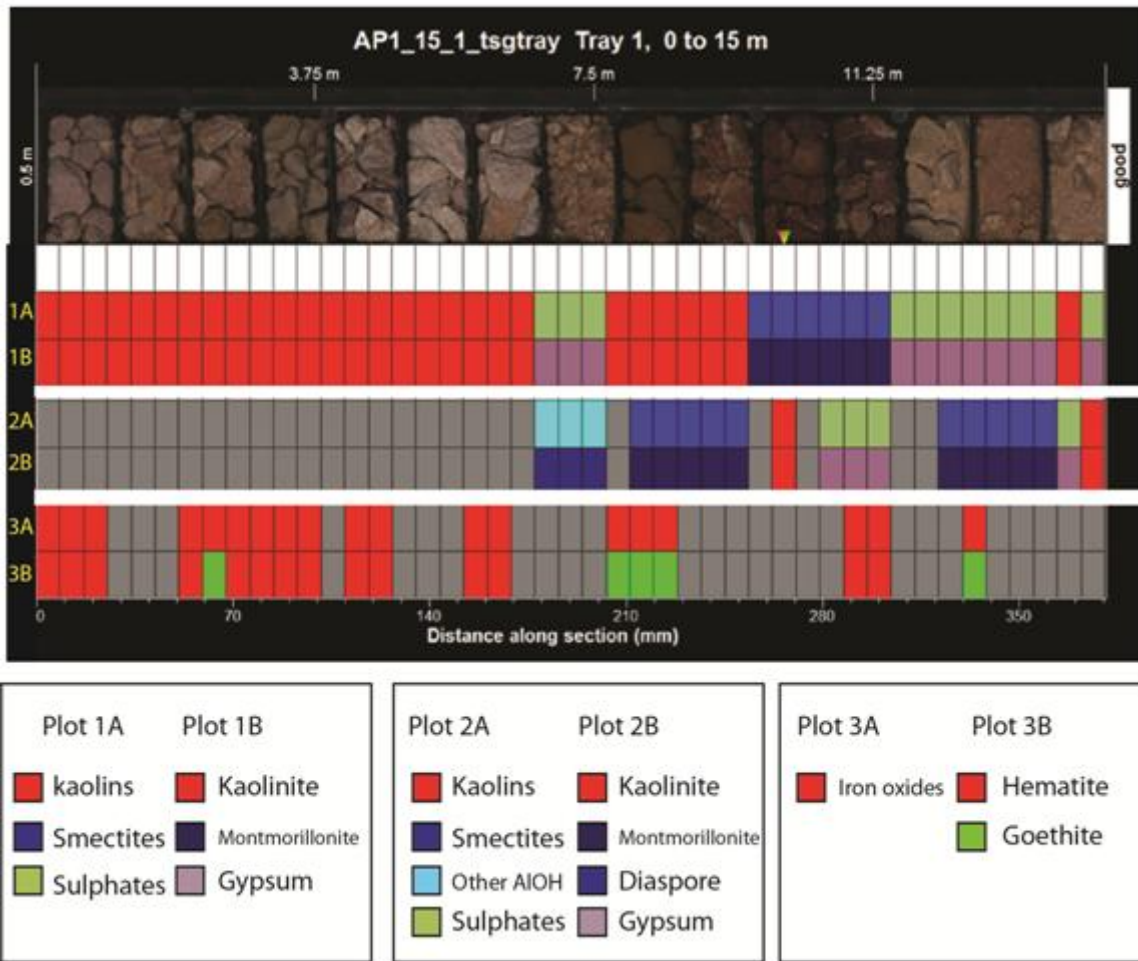
Sample	Grain size	Grain shape	Quartz grains	Sorting	Porosity	Weathering features	Description
AP4-007 Location: 0714805 6627159	FS + C	Sub- rounded to sub-angular	FS-Sub- rounded/an gular	Mod-poor	1	Highly weathered.	Fine sand embedded in a clay matrix. Geothite staining has occurred. Minor pyrite concretions present. Gypsum present.
	pH	Colour	Sedimentary structures	Fabric	Rock strength		
	8.5	Yellow	-	-	Very low		
Sample	Grain size	Grain shape	Quartz grains	Sorting	Porosity	Weathering features	Description
AP4-008 Location: 0714799 6627149	C	-	-	-	0-1	Highly weathered.	Fine grained kaolin rich shale. Black colour on throughout parts of the rock. High Mn content and high Ba content, indicated black colour attributed to "black hematite'.
	pH	Colour	Sedimentary structures	Fabric	Rock strength		
	7.5	Pale grey green + black	Laminated	Slight	Low		
Sample	Grain size	Grain shape	Quartz grains	Sorting	Porosity	Weathering features	Description
AP4-009 Location: 0714790 6627142	C-S	-	-	-	1	Goethite stained.	Prominent yellow (goethite stained) band within the stratigraphy. Clay-rich.
	pH	Colour	Sedimentary structures	Fabric	Rock strength		
	8.5	Yellow	-	-	Very low		
Sample	Grain size	Grain shape	Quartz grains	Sorting	Porosity	Weathering features	Description
AP4-010 Location: 0714786 6627140	C-S	-	-	-	0-1	Hematite stained.	Prominent purple (hematite stained) band within the stratigraphy. Clay-rich, significantly firmer than 009.
	pH	Colour	Sedimentary structures	Fabric	Rock strength		
	6	Purple	-	Slight	Low- mod		
Sample	Grain size	Grain shape	Quartz grains	Sorting	Porosity	Weathering features	Description
AP4-011 Location: 0714782 6627140	S	-	-	-	0-1	Highly weathered.	Weaker than the overlying units. Silty material with veins containing hematite and geothite. Hematite and geothite are restricted to these vein structures. Kaolin-rich.
	pH	Colour	Sedimentary structures	Fabric	Rock strength		
	6.5	White grey	Bedding + laminations	Well retained	Mod- low		
Sample	Grain size	Grain shape	Quartz grains	Sorting	Porosity	Weathering features	Description
AP4-012 Location: 0714782 6627140	MS-CS	Rounded to sub- rounded	"	Poor	2	Moderately weathered.	Kaolin-rich rounded sandstone with minor rounded quartz pebble clasts. Conglomeritic texture. Some pure kaolinite indurations also present.
	pH	Colour	Sedimentary structures	Fabric	Rock strength		
	6	White grey	Slight bedding	Slight	Mod		

Sample	Grain size	Grain shape	Quartz grains	Sorting	Porosity	Weathering features	Description
AP4-013 Location: 0714782 6627140	MS-CS	Rounded	"	Mod-well	1	Moderately weathered.	Sandy with hematite, kaolin cement. Gypsum present. Small veins containing kaolinite.
	pH	Colour	Sedimentary structures	Fabric	Rock strength		
	8	Purple white	Bedding + laminations	Moderate	Mod-high		
Sample	Grain size	Grain shape	Quartz grains	Sorting	Porosity	Weathering features	Description
AP4-014 Location: 0714782 6627129	MS-FS	Sub-rounded	"	Mod	1.5	Moderately weathered.	Kaolinitic sandstone. Minor hematite in veins/fractures.
	pH	Colour	Sedimentary structures	Fabric	Rock strength		
	5.5	Pale pink	Minor cross-laminations	Slight	Mod		
Sample	Grain size	Grain shape	Quartz grains	Sorting	Porosity	Weathering features	Description
AP4-015 Location: 0714782 6627129	MS	Rounded to sub-rounded	"	Mod	1.5	-	Sandstone with minor kaolinite. Red, hematite cementation coats sand grains. Bedding well preserved.
	pH	Colour	Sedimentary structures	Fabric	Rock strength		
	6.5	Red	Minor bedding + laminations	Well retained	Mod-high		
Sample	Grain size	Grain shape	Quartz grains	Sorting	Porosity	Weathering features	Description
AP4-016 Location: 0714782 6627129	FS-MS	Sub-rounded	"	Mod-poor	1	Very minor hematite staining.	Well consolidated clean sandstone. Well bedded, containing large scale cross-bedding. Interbeds of finer and coarser sands. Minor silicification, and preserved fern and bark fossils.
	pH	Colour	Sedimentary structures	Fabric	Rock strength		
	5	Light brown, red	Well bedded. Minor laminations	Well retained	High		
Sample	Grain size	Grain shape	Quartz grains	Sorting	Porosity	Weathering features	Description
AP4-017 Location: 0714785 6627135	FS-MS	Sub-rounded	"	Mod-poor	1	Very minor hematite staining.	Same as sample 016, except contains surface pyrite concretions.
	pH	Colour	Sedimentary structures	Fabric	Rock strength		
	5	Light brown, red	Well bedded. Minor laminations	Well retained	High		

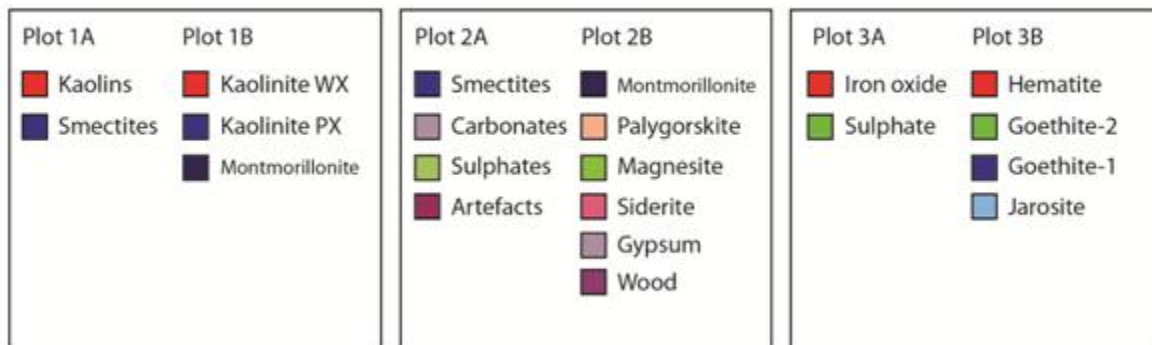
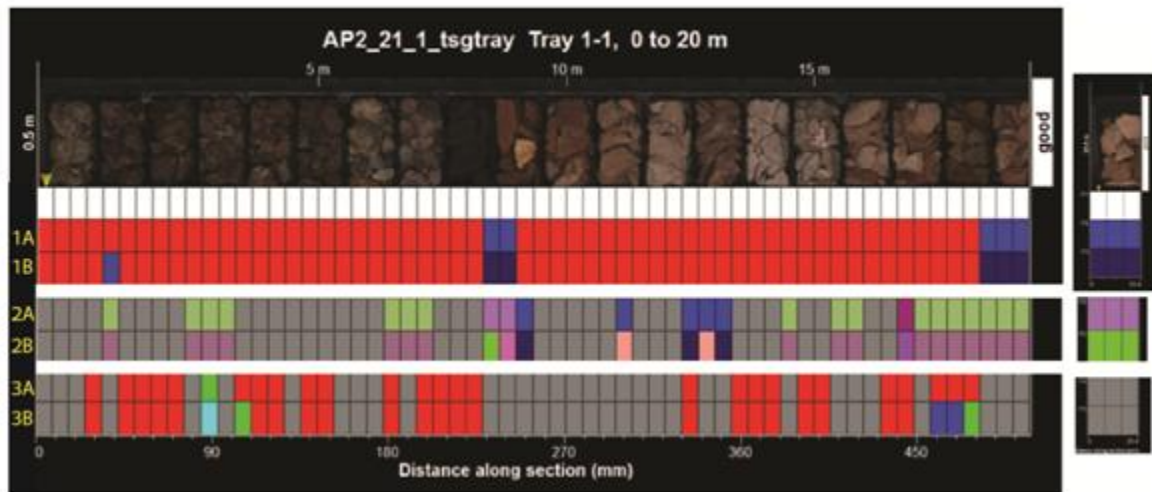
Sample	Grain size	Grain shape	Quartz grains	Sorting	Porosity	Weathering features	Description
AP5-001 Location: 0712142 6629078	MS-CS	Rounded to sub-rounded	"	Mod-poor	1	Minor hematite staining.	Kaolin-rich with varying sand content from 5% to 90%. Kaolin makes up the matrix.
	pH	Colour	Sedimentary structures	Fabric	Rock strength		
	6	Pale cream + red	-	-	Mod		
Sample	Grain size	Grain shape	Quartz grains	Sorting	Porosity	Weathering features	Description
AP5-002 Location: 0712142 6629078	MS-CS + VCS	Sub-rounded	"	Mod	1.5	Hematite stained.	Clear sands coated and cemented together by hematite stained kaolinite.
	pH	Colour	Sedimentary structures	Fabric	Rock strength		
	6.5	Dark red	-	-	Very low		
Sample	Grain size	Grain shape	Quartz grains	Sorting	Porosity	Weathering features	Description
AP5-003 Location: 0712142 6629078	C + FS	-	FS- Sub rounded	Mod	1	Red (hematite) stained segregations and yellow (geothite stained) segregations.	Shale/clay with very minor sand fraction. Small scale hematite stained and geothite stained segregations.
	pH	Colour	Sedimentary structures	Fabric	Rock strength		
	5.5	Grey	Slight layering	Slight	Mod-low		
Sample	Grain size	Grain shape	Quartz grains	Sorting	Porosity	Weathering features	Description
AP5-004 Location: 0712142 6629078	FS-MS	Sub-angular to sub-rounded	"	Mod	1.5	Minor hematite staining.	Kaolinitic sands with minor hematite cementation.
	pH	Colour	Sedimentary structures	Fabric	Rock strength		
	5.5	Red	-	Not observed	Low		
Sample	Grain size	Grain shape	Quartz grains	Sorting	Porosity	Weathering features	Description
AP5-005 Location: 0712142 6629078	FS-VCS	Sub-angular to sub-rounded	"	Very poor	1.5	Hematite mottles. Lots of segregations.	A mixture of kaolin-rich segregations, gypsum-rich parts, sand-rich segregations.
	pH	Colour	Sedimentary structures	Fabric	Rock strength		
	6	Pale cream + red	-	Slight	Mod		
Sample	Grain size	Grain shape	Quartz grains	Sorting	Porosity	Weathering features	Description
AP5-006 Location: 0712142 6629078	MS-CS	Sub-angular to sub-rounded	"	Poor	1.5	Highly mottled. Lots of segregations.	A clay matrix, with segregations of pure kaolinite, grey quartz, clear quartz with kaolin cement, and hematite stained quartz.
	pH	Colour	Sedimentary structures	Fabric	Rock strength		
	7.5	grey purple	Slight bedding	Slight	Mod		
Sample	Grain size	Grain shape	Quartz grains	Sorting	Porosity	Weathering features	Description
AP5-007 Location: 0712142 6629078	C	-	MS-sub-rounded	-	0-1	Highly weathered.	Mostly kaolinite, with a very minor sand fraction.
	pH	Colour	Sedimentary structures	Fabric	Rock strength		
	7	Pale cream	-	-	Very low		

Sample	Grain size	Grain shape	Quartz grains	Sorting	Porosity	Weathering features	Description
AP6-001 Location: 0708845 6626004	FS	Sub- rounded	"	Well	1	Minor secondary ferruginisation (red and yellow staining)	Kaolinitic sands.
	pH	Colour	Sedimentary structures	Fabric	Rock strength		
	5.5	White	-	-	Mod		
Sample	Grain size	Grain shape	Quartz grains	Sorting	Porosity	Weathering features	Description
AP6-002 Location: 0708845 6626004	C-S	-	FS-rounded	Mod	0-1	Minor hematite staining. Highly kaolinitic.	Highly fractured and bedded shale with minor hematite staining in places. Fines up from a fine sand to shale.
	pH	Colour	Sedimentary structures	Fabric	Rock strength		
	6.5	White	Bedding (2-5 cm)	Well retained	Mod- high		
Sample	Grain size	Grain shape	Quartz grains	Sorting	Porosity	Weathering features	Description
AP6-003 Location: 0708845 6626004	C-S	-	-	-	0	Red (hematite) staining is present in fractures. Highly kaolinitic.	Carbonaceous shale, with gypsum and hematite staining in fractures.
	pH	Colour	Sedimentary structures	Fabric	Rock strength		
	6	White + red	Bedded	Mod	Mod		
Sample	Grain size	Grain shape	Quartz grains	Sorting	Porosity	Weathering features	Description
AP6-004 Location: 0708845 6626004	C-S	-	-	-	0	Yellow (goethite) staining especially in fractures. Highly kaolinitic.	Carbonaceous shale, with gypsum and goethite staining in fractures.
	pH	Colour	Sedimentary structures	Fabric	Rock strength		
	6	White + yellow	Bedded	Mod	High		
Sample	Grain size	Grain shape	Quartz grains	Sorting	Porosity	Weathering features	Description
AP6-005 Location: 0708845 6626004	C-S	-	-	-	0	Minor hematite and goethite staining. Highly kaolinitic.	highly fractured shale which is well bedded.
	pH	Colour	Sedimentary structures	Fabric	Rock strength		
	7	White	Bedded	Mod	Mod- high		
Sample	Grain size	Grain shape	Quartz grains	Sorting	Porosity	Weathering features	Description
AP6-006 Location: 0708845 6626004	C-S	-	-	-	0	Highly kaolinitic.	Well bedded, carbonaceous shale.
	pH	Colour	Sedimentary structures	Fabric	Rock strength		
	7	White	Well bedded	Mod	Mod- high		

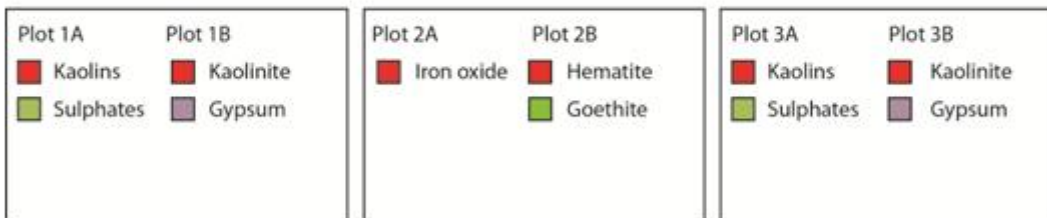
Appendix 3: HyLogger mineral plots for profile AP1. Depth (m) increases from the base to the top of the profile.



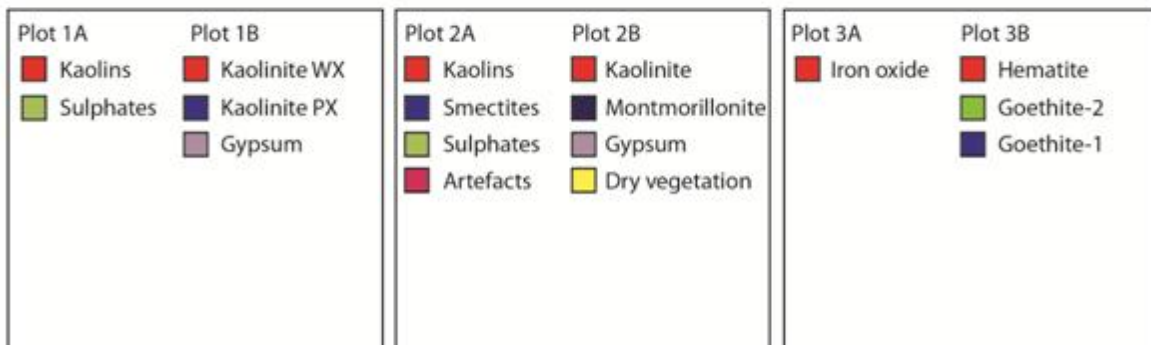
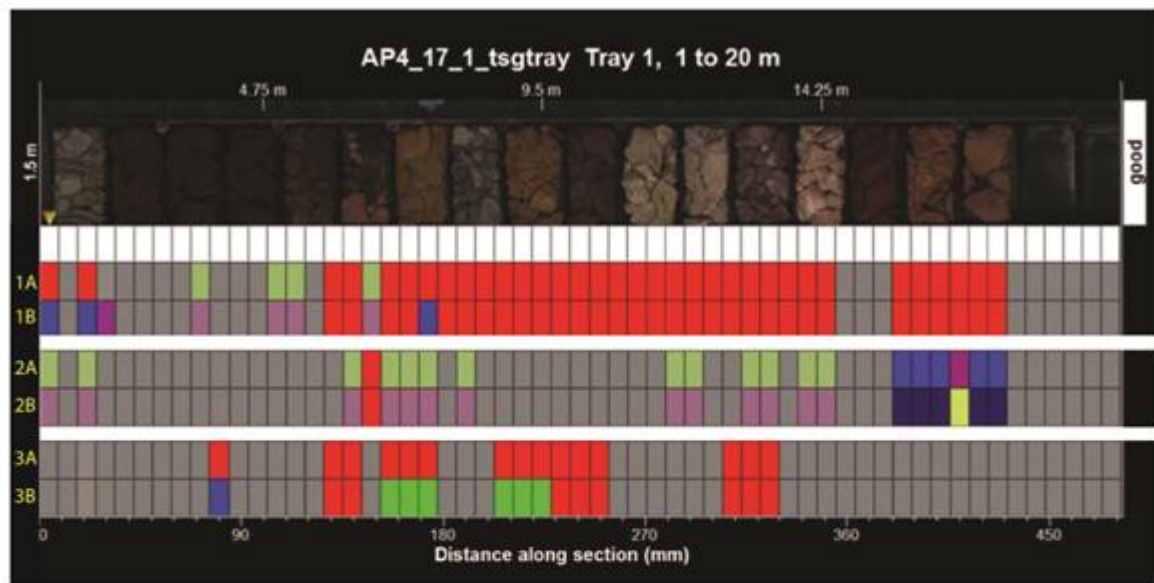
Appendix 4: HyLogger mineral plots for profile AP2. Depth (m) increases from the base to the top of the profile.



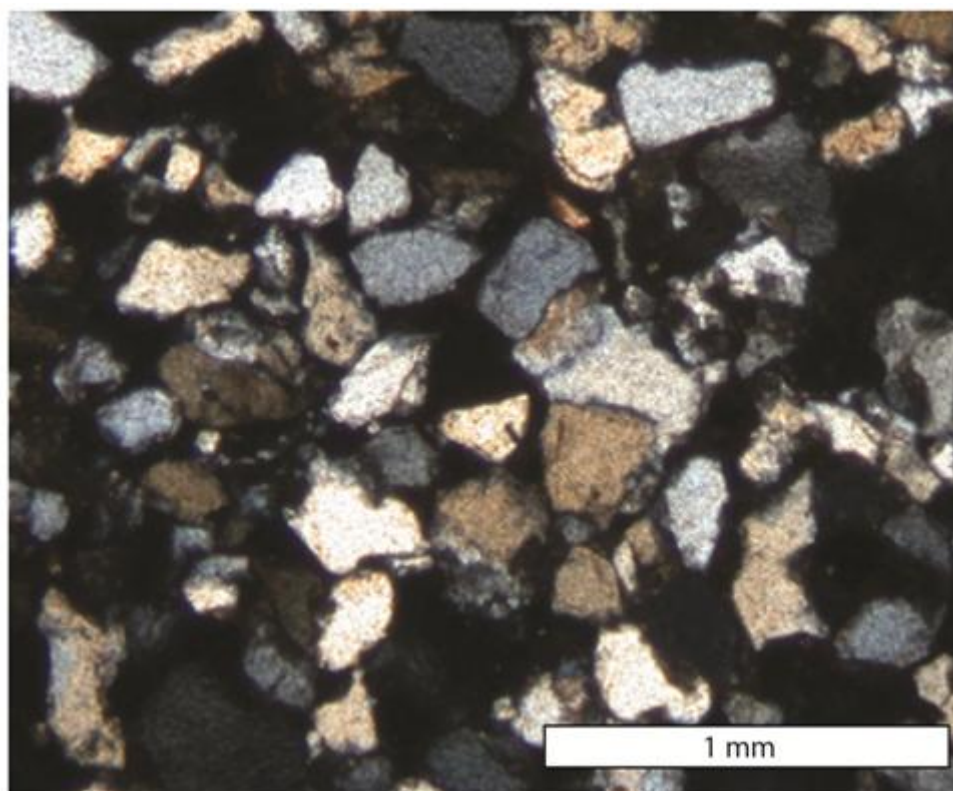
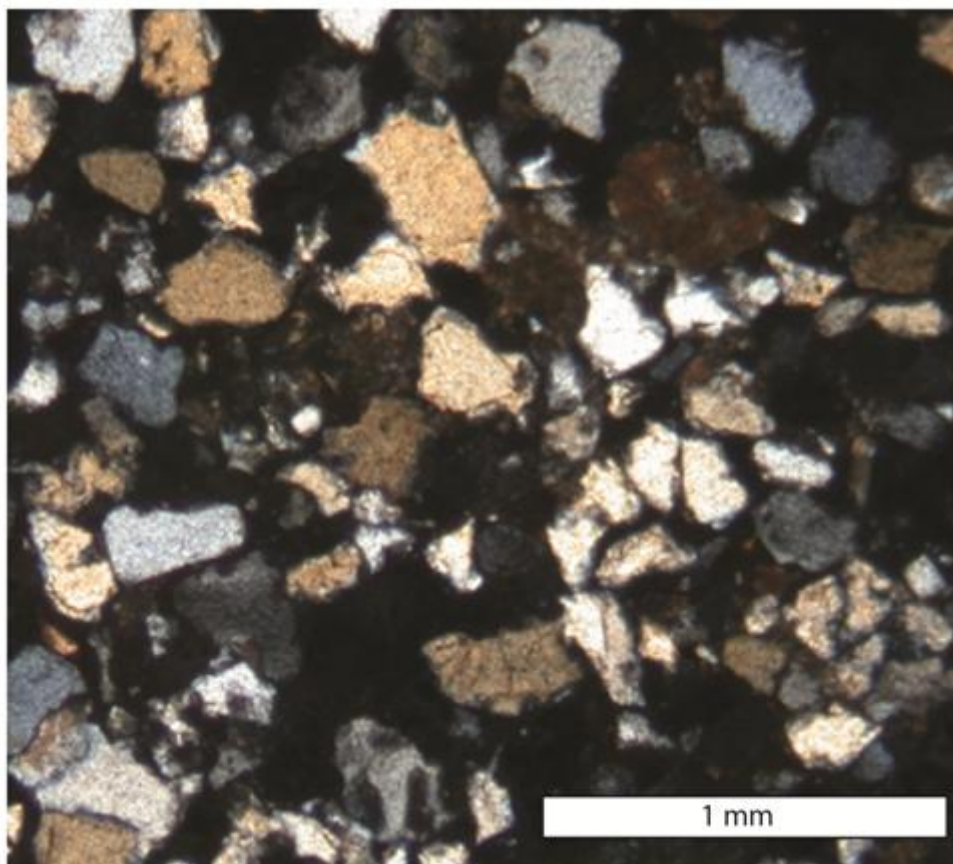
Appendix 5: HyLogger mineral plots for profile AP3. Depth (m) increases from the base to the top of the profile.



Appendix 6: HyLogger mineral plots for profile AP4. Depth (m) increases from the base to the top of the profile.



Appendix 7: Images of thin section of sample AP4-016 using petrographic microscope under cross-polarised light.



Appendix 8: Top: The ferricrete layer at depth 14 m in profile AP2. Bottom: Image showing lateral offset of profile AP2 above the ferricrete layer at depth 14 m.



Appendix 9: Photograph of profile AP3 exposed section.



Appendix 10: Photograph of profile AP4 exposed section.



Appendix 11: Fern and bark fossil imprints at the top of profile AP4.



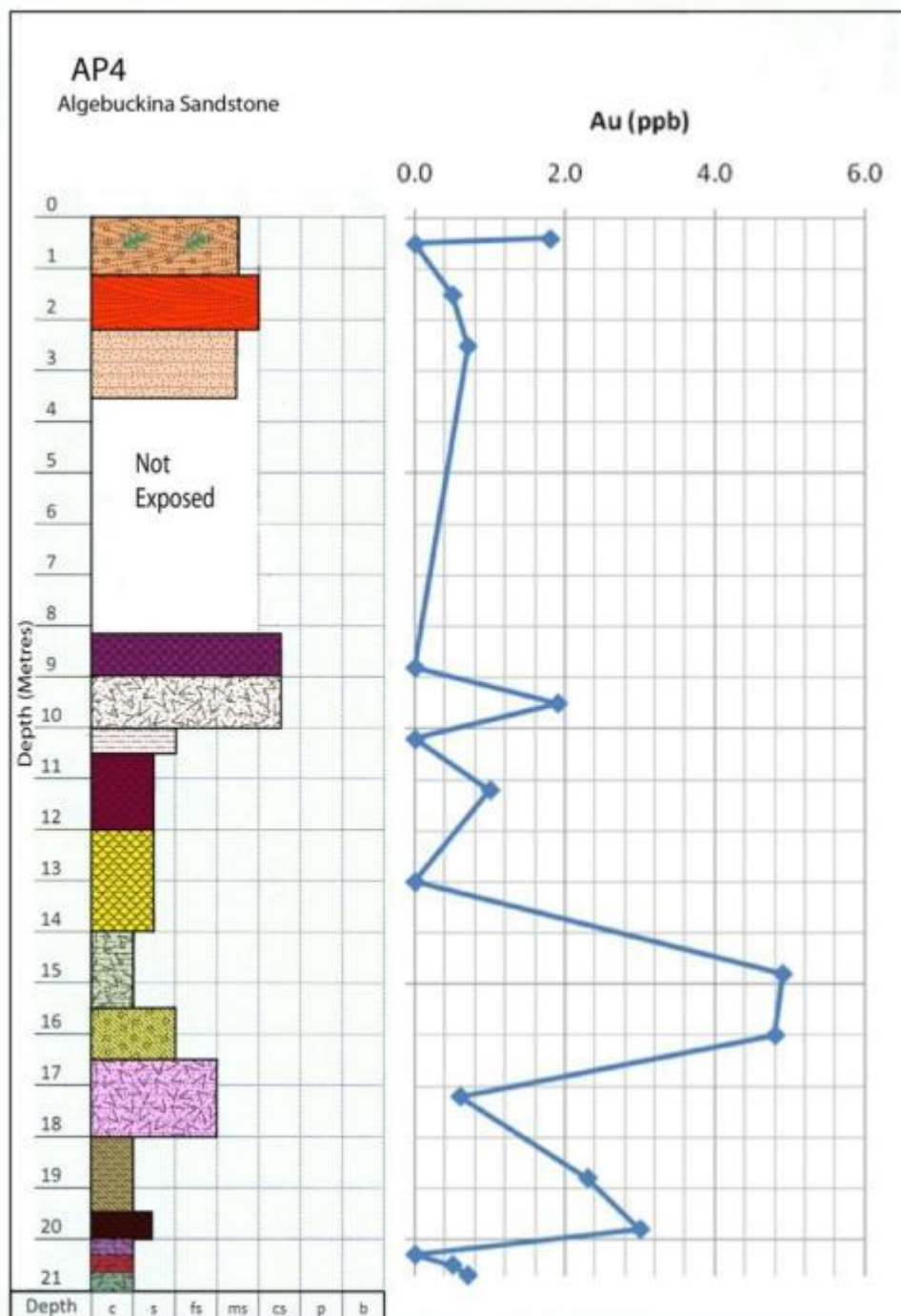
Appendix 12: Photograph of profile AP5 exposed section.



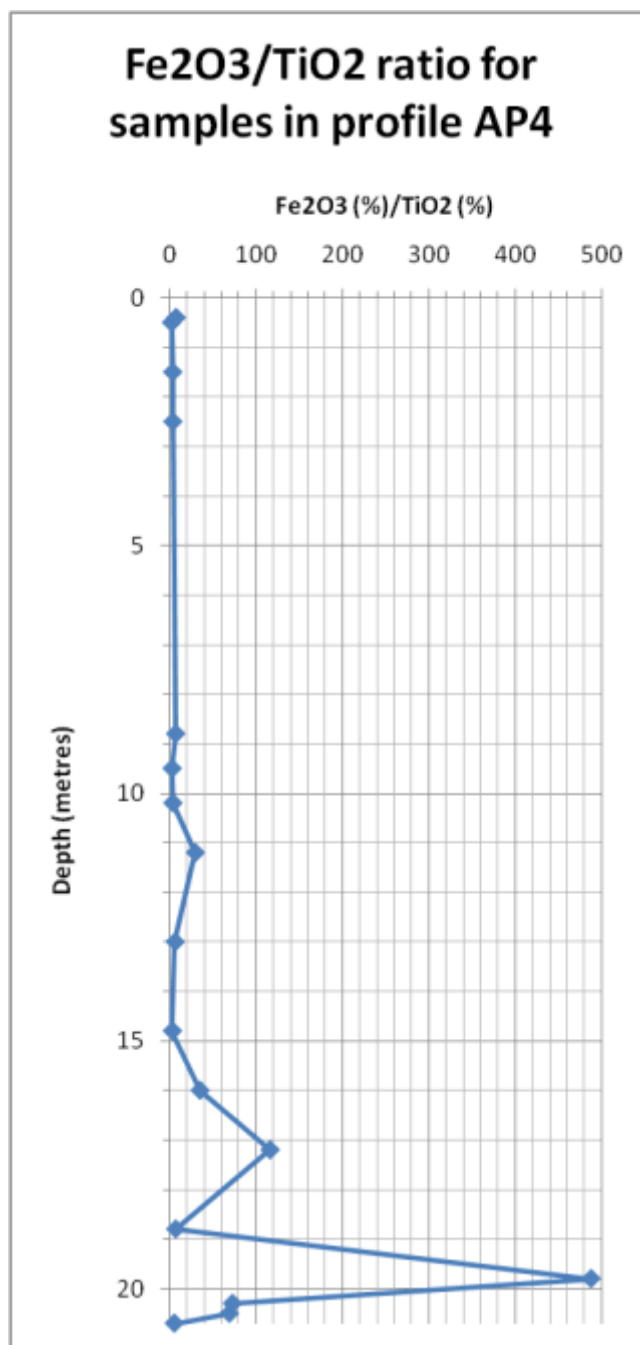
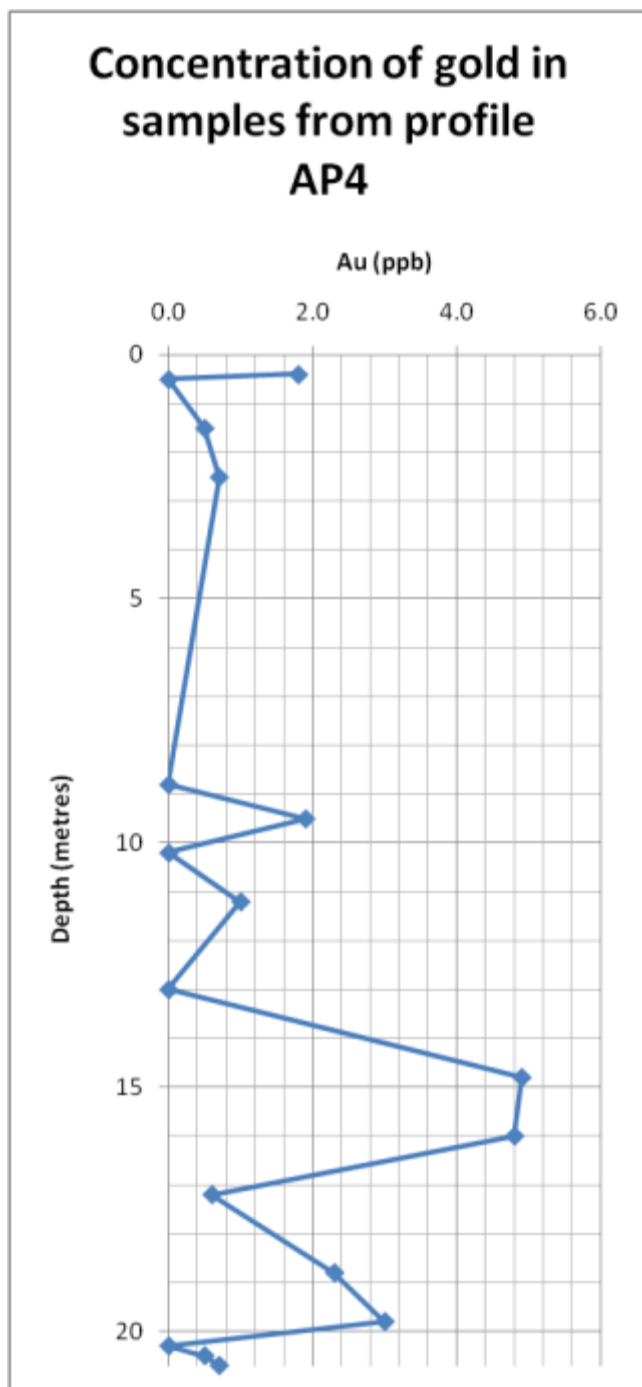
Appendix 13: Photograph of profile AP6 exposed section.



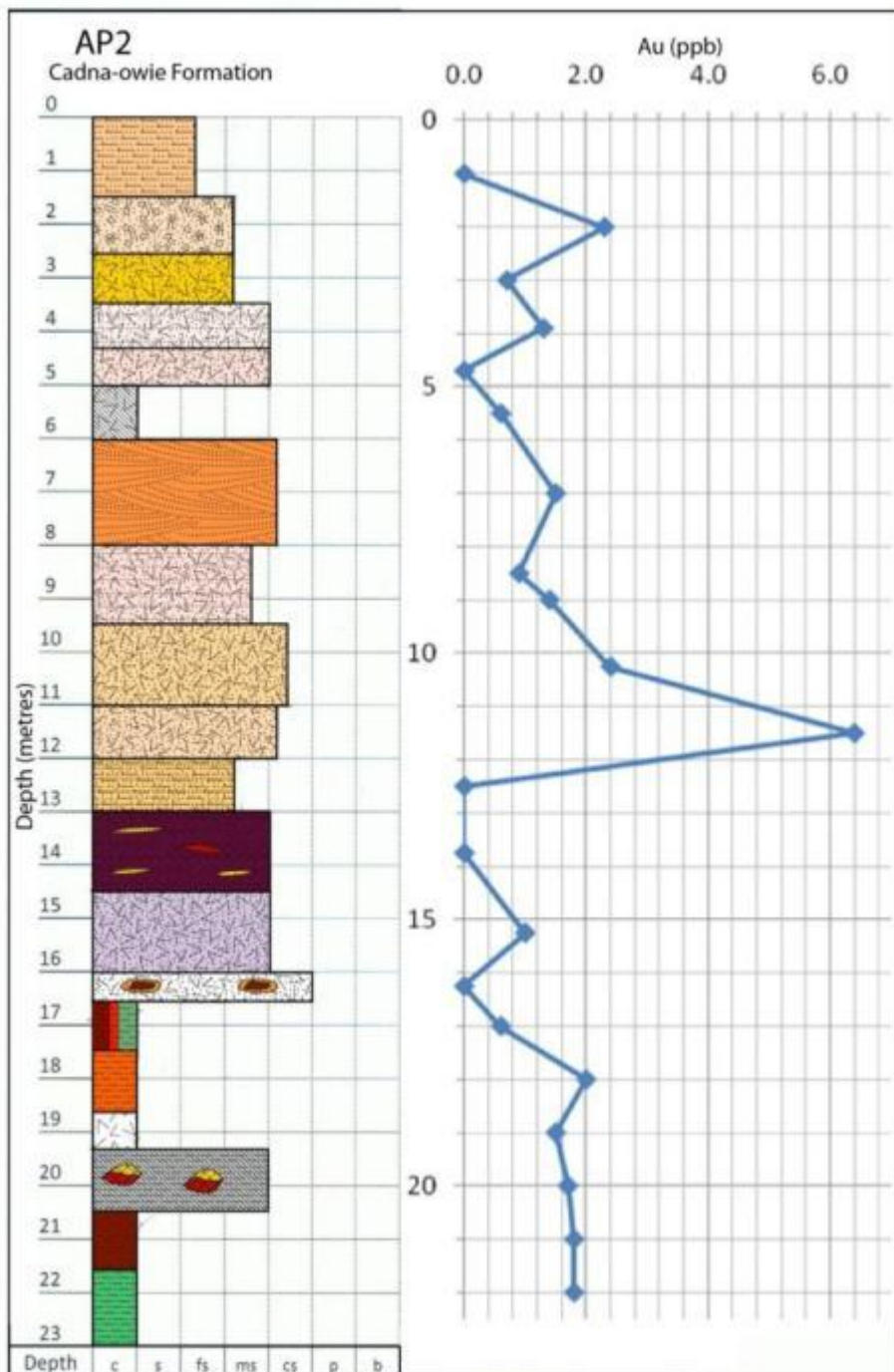
Appendix 14: Stratigraphic log of profile AP4 with concentration of gold in samples taken from profile. Indicates a gold anomaly within the lower third of the profile. Refer to Figure 13b for stratigraphic log legend.



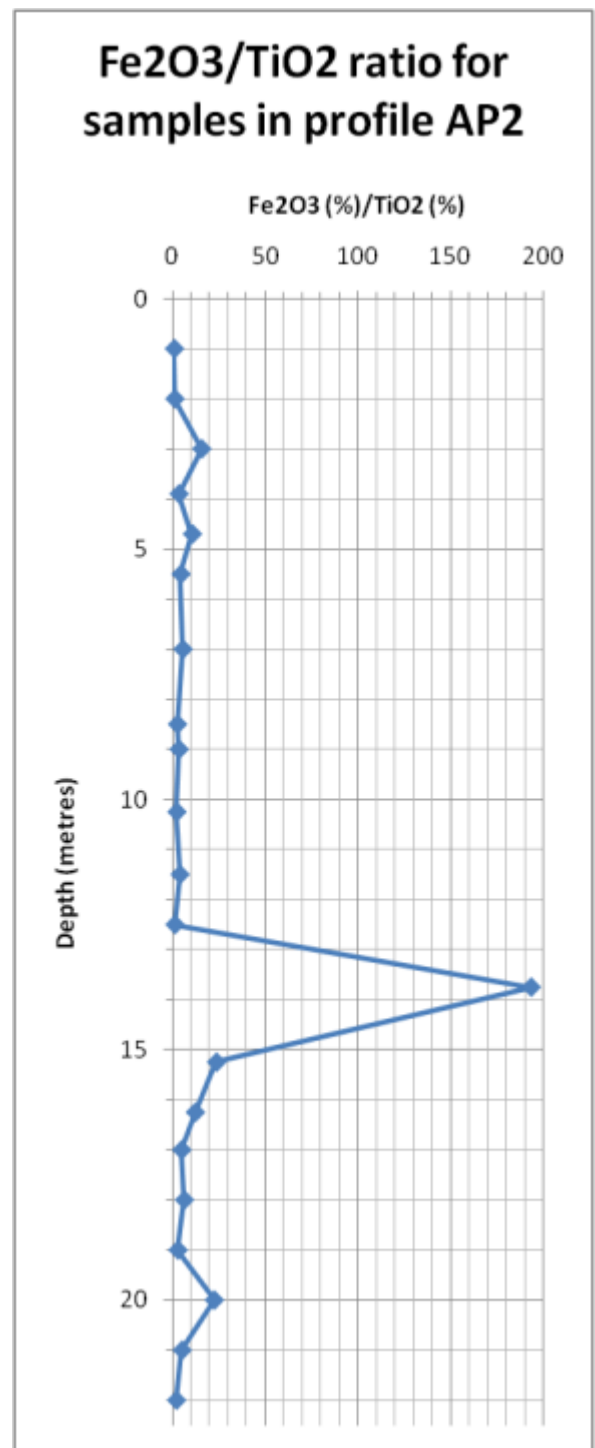
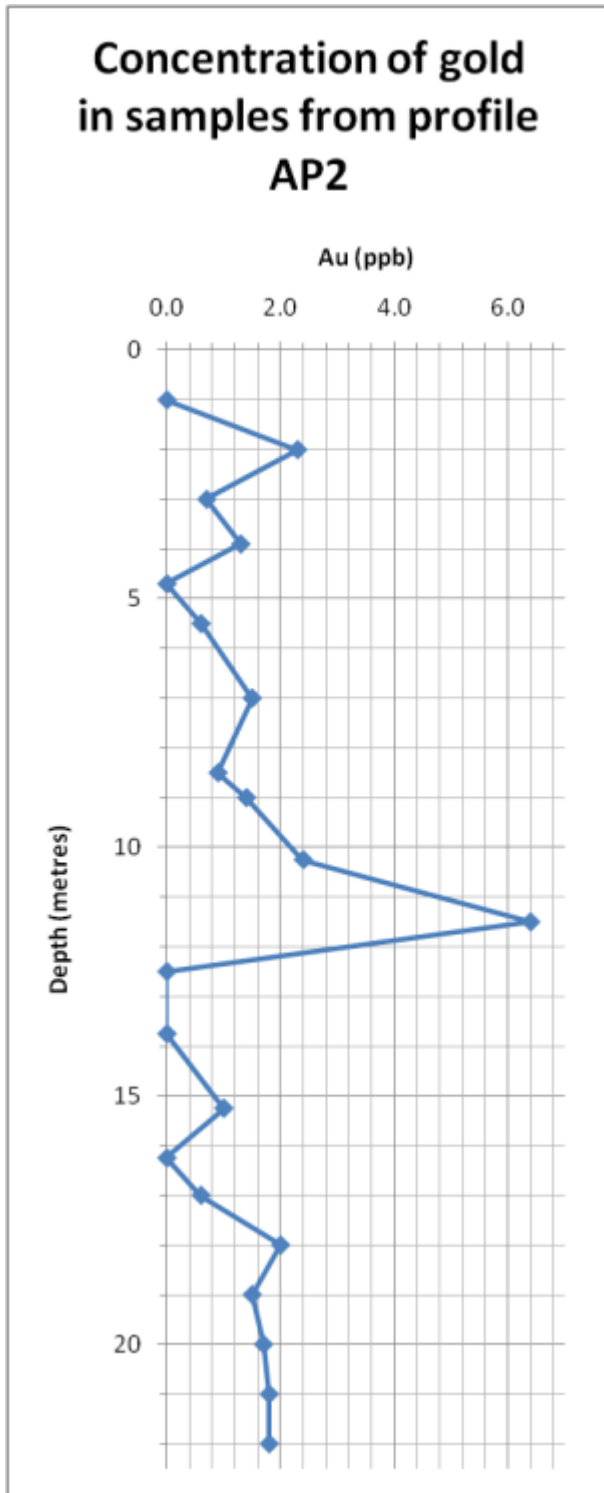
Appendix 15: Concentration of gold in samples from profile AP4 and Fe₂O₃/TiO₂ ratios of samples. Indicates that anomalous gold values do not correspond with ferruginous zones.



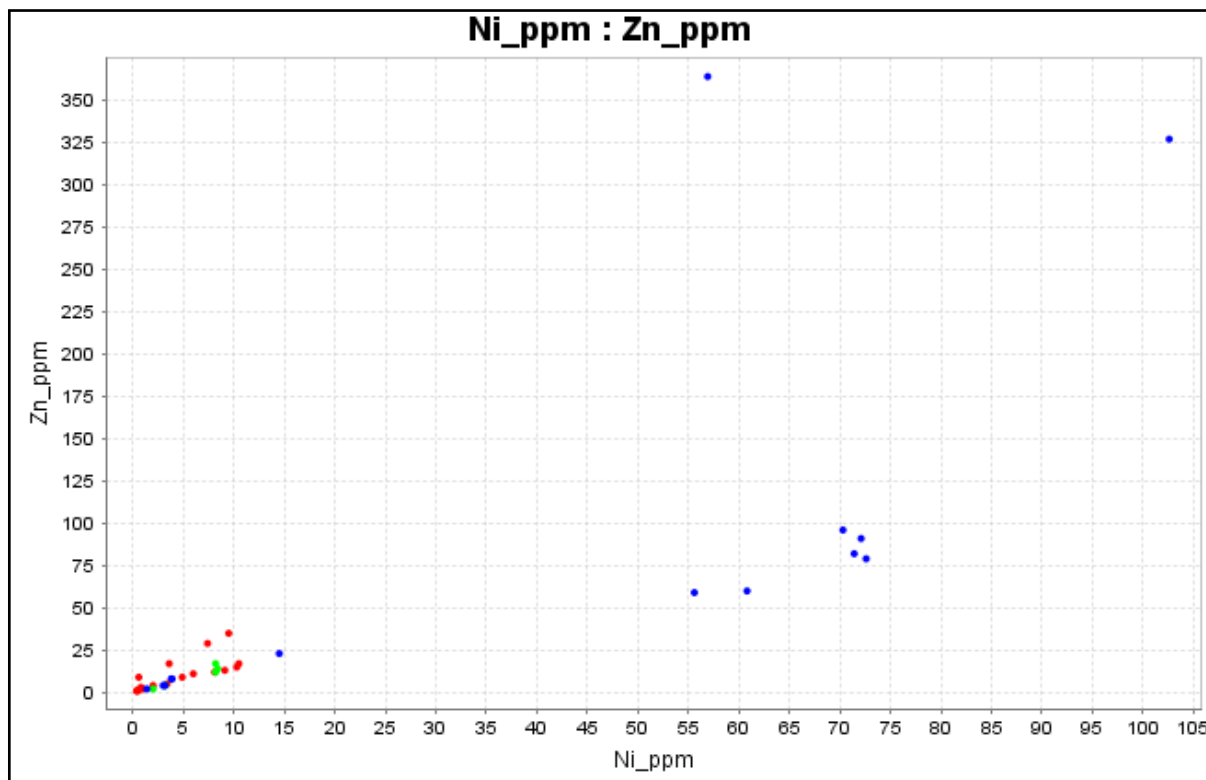
Appendix 16: Stratigraphic log of profile AP2 with concentration of gold in samples taken from profile. Refer to Figure 11 for stratigraphic log legend.



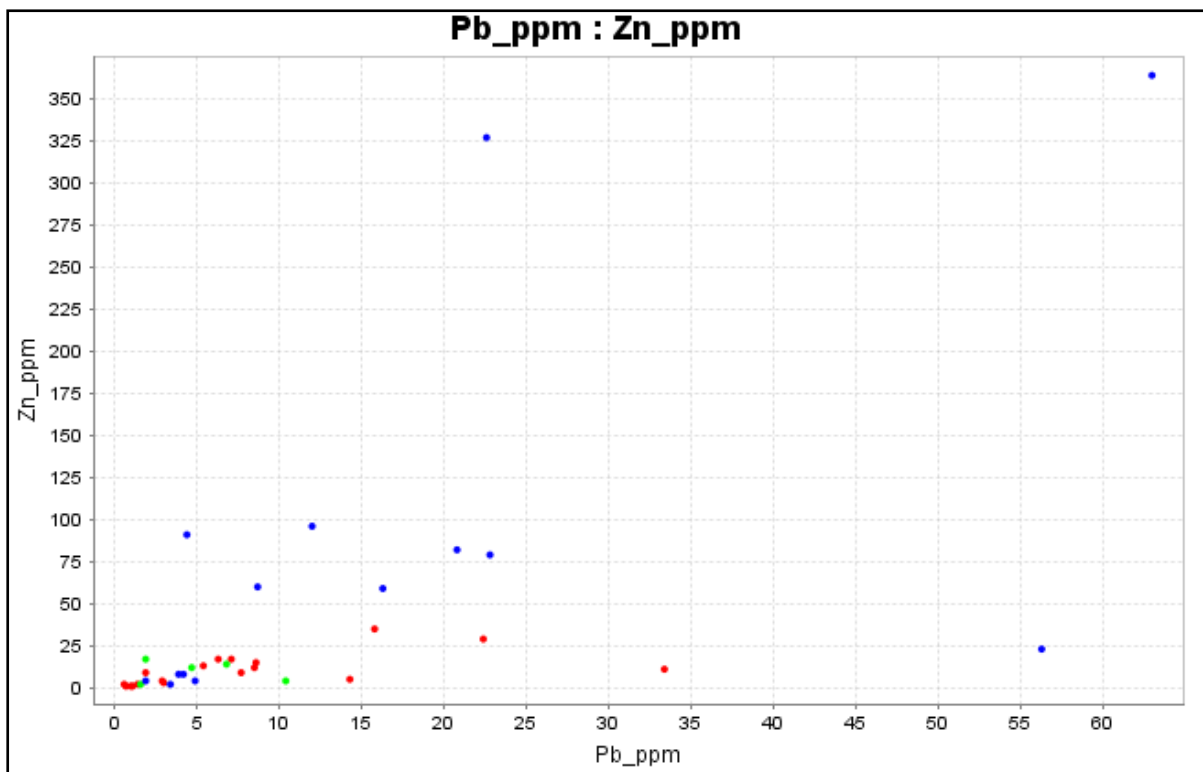
Appendix 17: Concentration of gold in samples from profile AP2 and Fe₂O₃/TiO₂ ratios of samples. Indicates no prominent relationship between gold and ferruginous zones.



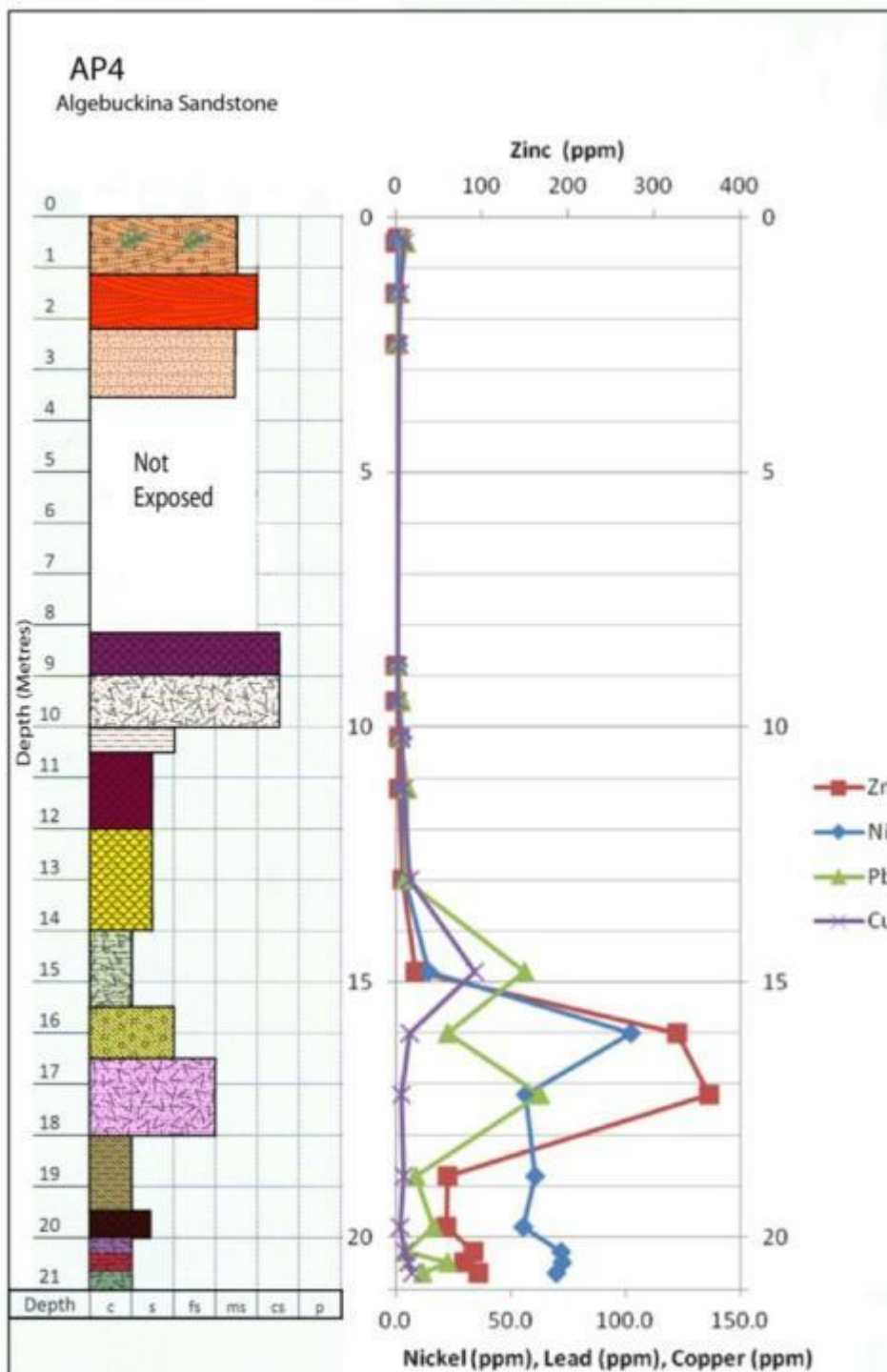
Appendix 18: Plot of concentrations of nickel vs. zinc of all samples assayed. Red: samples from profile AP2, green: samples from profile AP3, blue: samples from profile AP4.



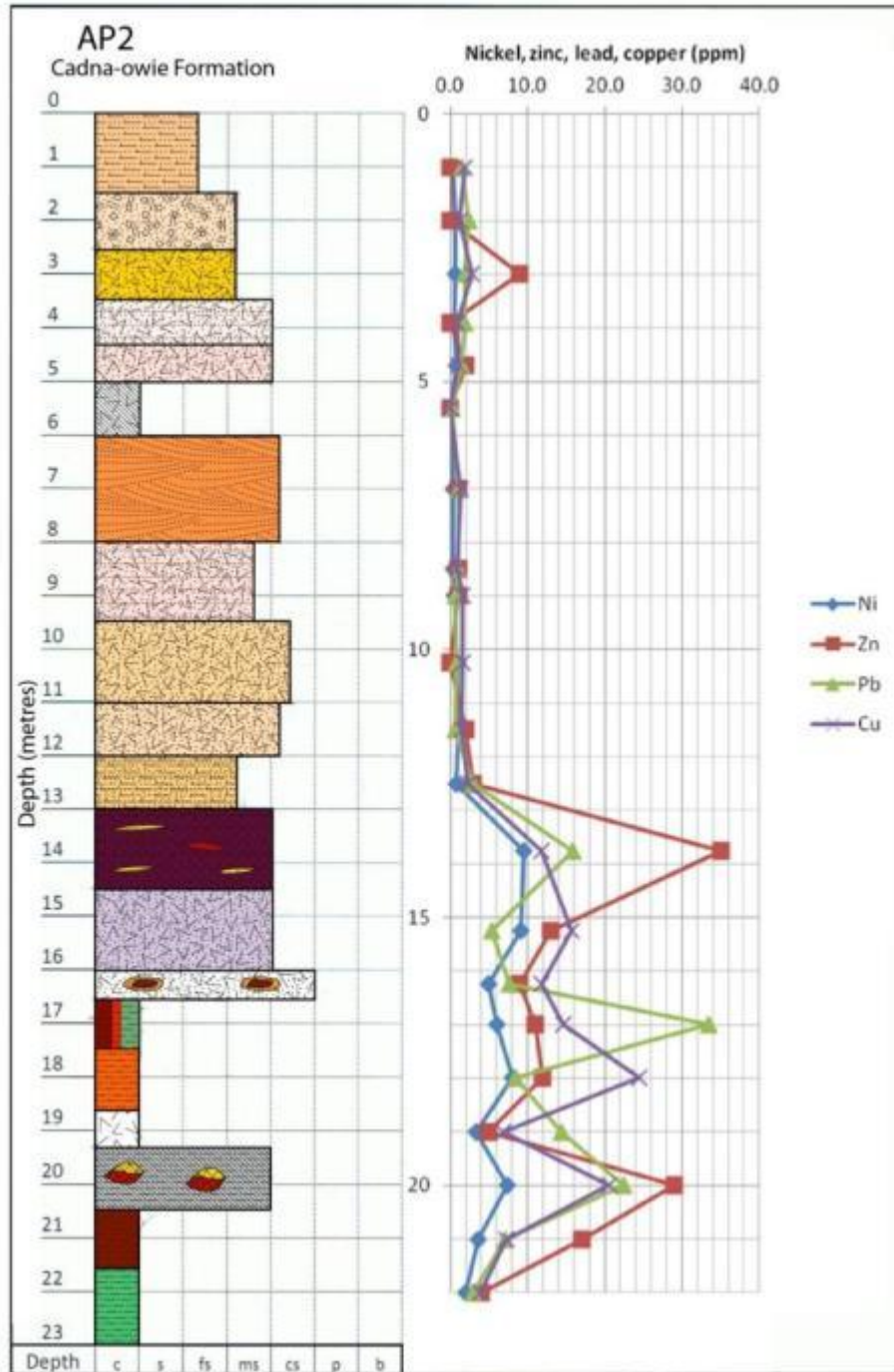
Appendix 19: Plot of concentrations of lead vs. zinc of all samples assayed. Red: samples from profile AP2, green: samples from profile AP3, blue: samples from profile AP4.



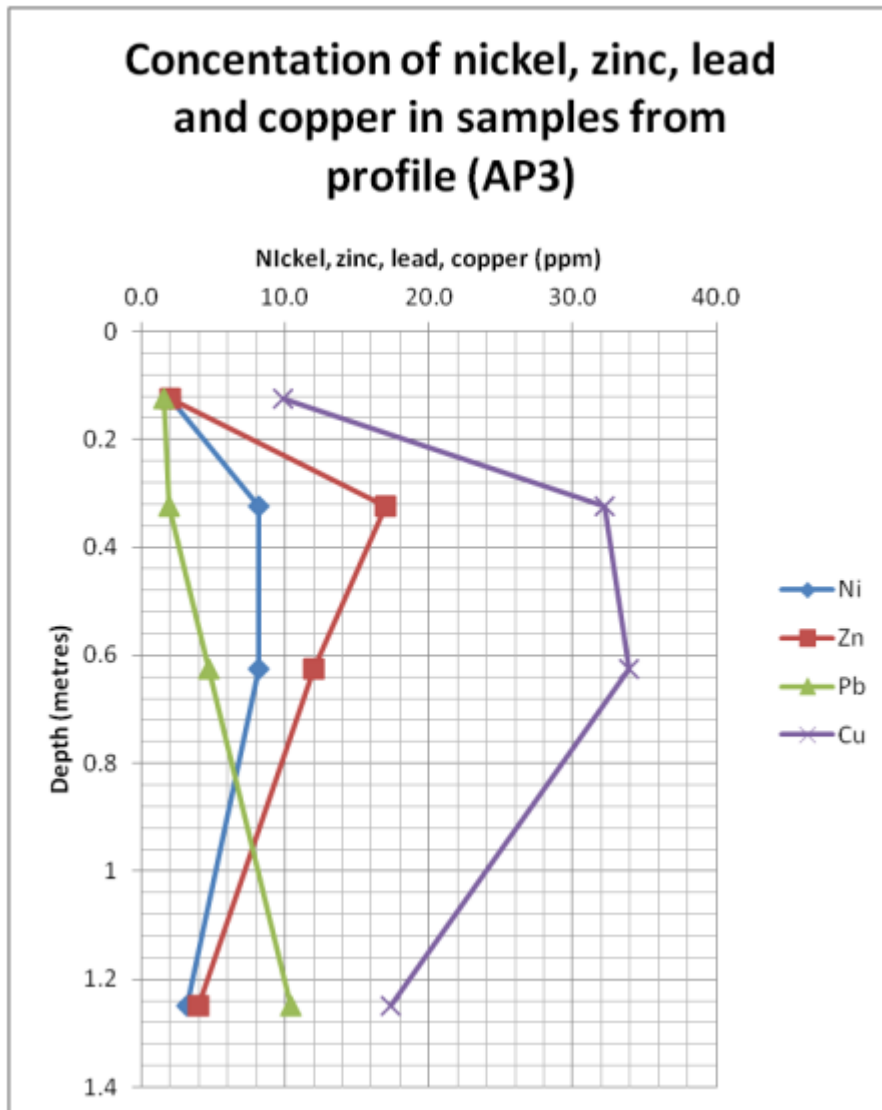
Appendix 20: Stratigraphic log of profile AP4 and concentrations of zinc, nickel, lead and copper in samples. Indicates a zinc, nickel, lead, copper anomaly in the basal region of the Algebuckina Sandstone. Refer to Figure 13b for stratigraphic log legend.



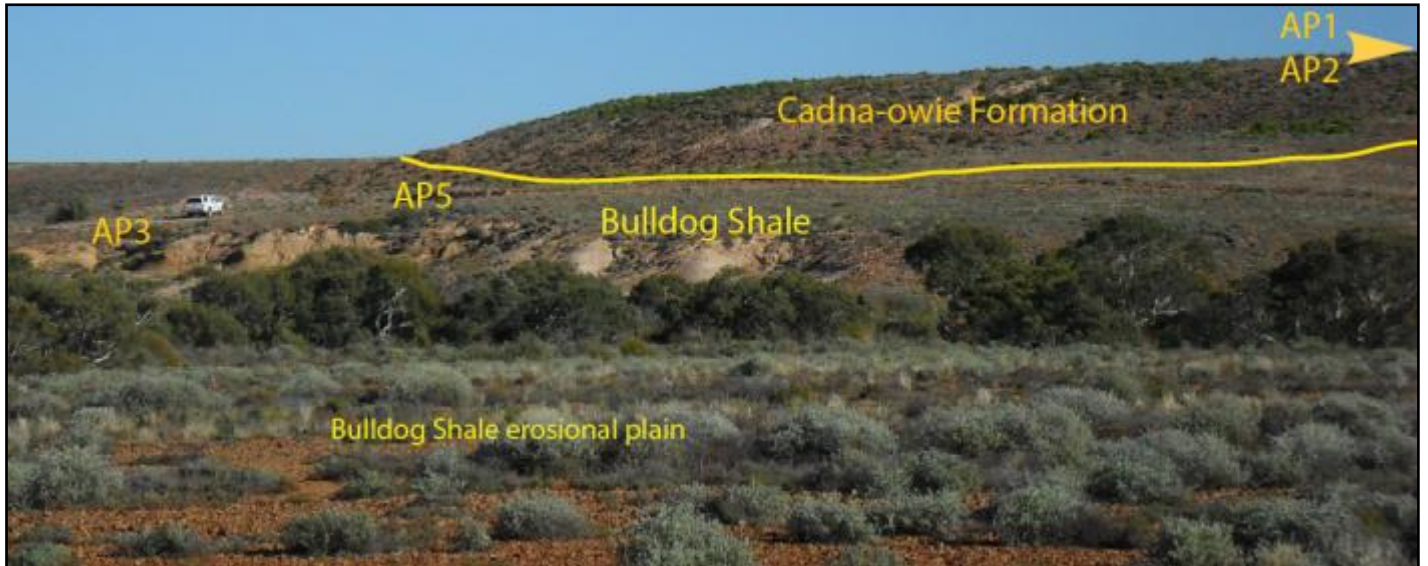
Appendix 21: Stratigraphic log of profile AP2 and concentrations of nickel, zinc, lead and copper. Indicates an anomaly of nickel, zinc, lead and copper at and below the ferruginous zone. Refer to Figure 11 for stratigraphic log legend.



Appendix 22: Concentrations of nickel, zinc, lead and copper in samples from profile AP3. Indicates some anomalous copper values, and copper is more abundant than nickel, lead and zinc unlike profiles AP1 and AP2.



Appendix 23: Annotated photograph (facing towards the west) showing Cadna-owie Formation and Bulldog Shale field relationship, near Blue Dam (east of Andamooka).



Appendix 24: Typical horizontally-bedded exposure of Arcoona Quartzite. Located at 0715769 mE 6627544 mN.



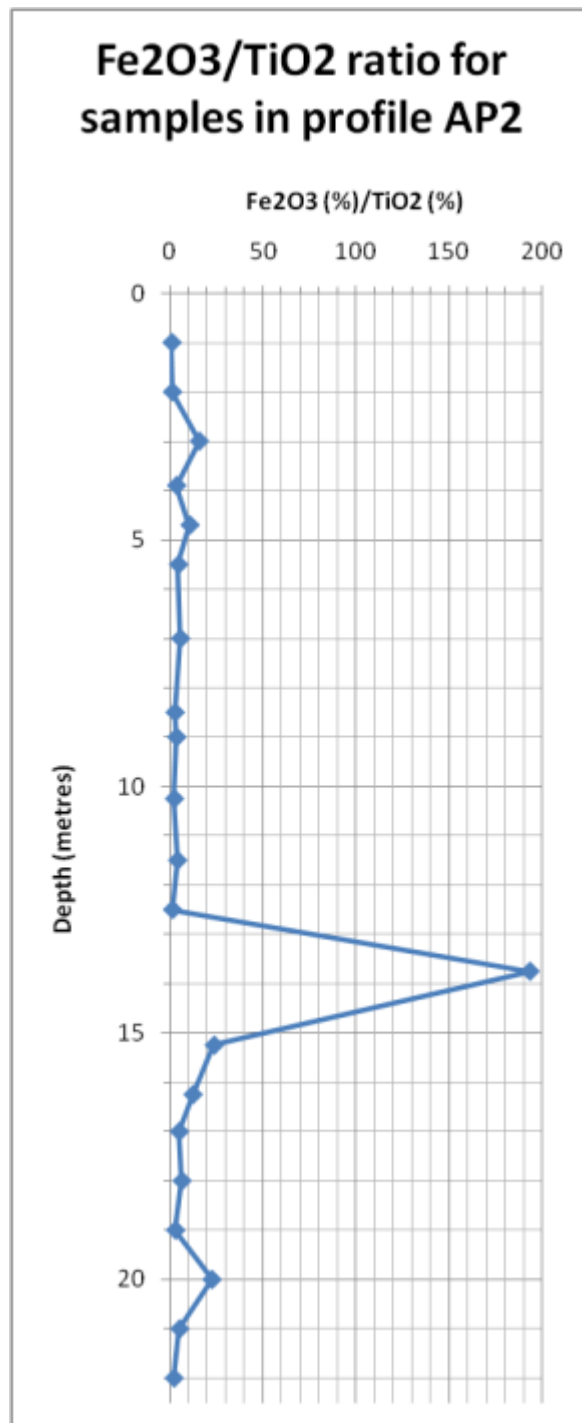
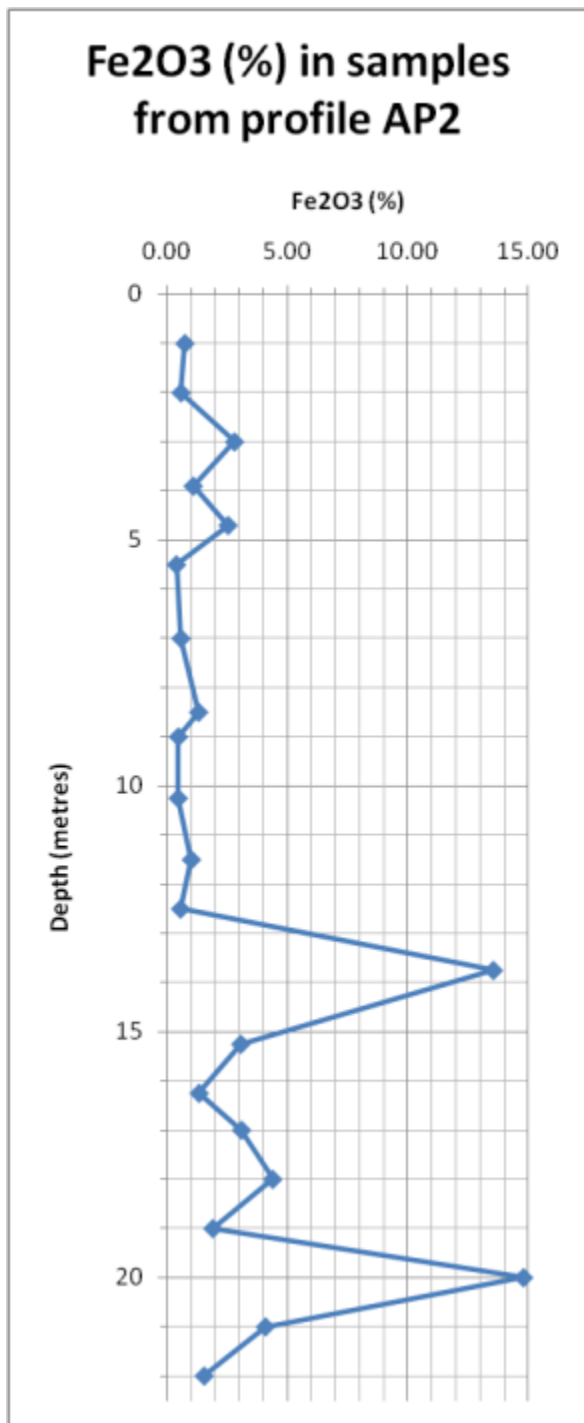
Appendix 25: Highly fractured and folded exposure of Arcoona Quartzite in a fault zone. Located at 0715115 mE 6627901 mN.



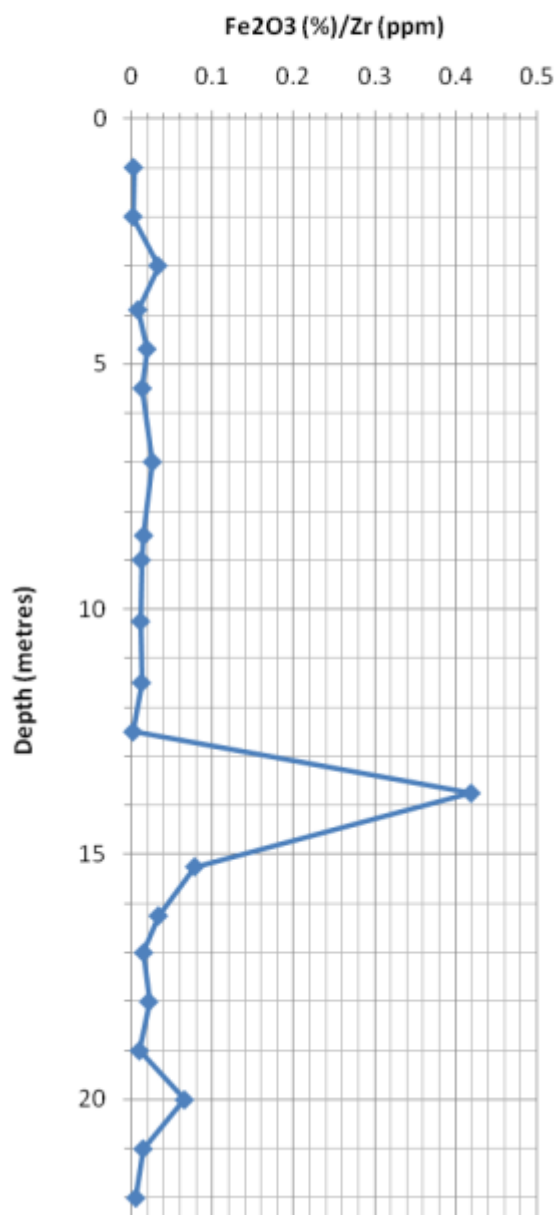
Appendix 26: Bedding readings taken from exposures around Andamooka.

Location (mE, mN)	Rock Unit	Reading
0717443, 6630077	Arcoona Quartzite	05/312
0712238, 6629253	Cadna-owie Formation	06/279
0712238, 6629253	Cadna-owie Formation	04/297
0712238, 6629253	Cadna-owie Formation	10/282
0712238, 6629253	Cadna-owie Formation	16/249
0712148, 6629275	Cadna-owie Formation	10/274
0711638, 6628958	Cadna-owie Formation	07/269
0711638, 6628958	Cadna-owie Formation	18/284
0708845, 6626004	Bulldog Shale	10/310
0714762, 6627101	Algebuckina Sandstone	22/210
0714762, 6627101	Algebuckina Sandstone	18/230
0714762, 6627101	Algebuckina Sandstone	34/311
0714762, 6627101	Algebuckina Sandstone	58/201
0714762, 6627101	Algebuckina Sandstone	30/230

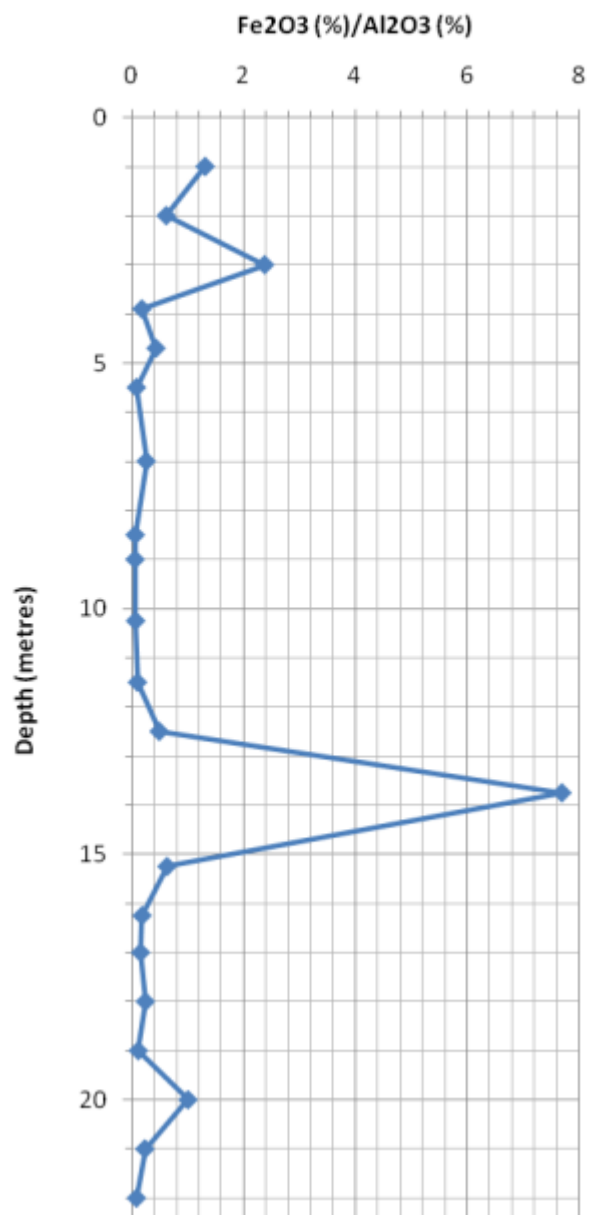
Appendix 27: Plots of Fe_2O_3 concentration, $\text{Fe}_2\text{O}_3/\text{TiO}_2$, $\text{Fe}_2\text{O}_3/\text{Zr}$ and $\text{Fe}_2\text{O}_3/\text{Al}_2\text{O}_3$ against depth for samples from profile AP2.



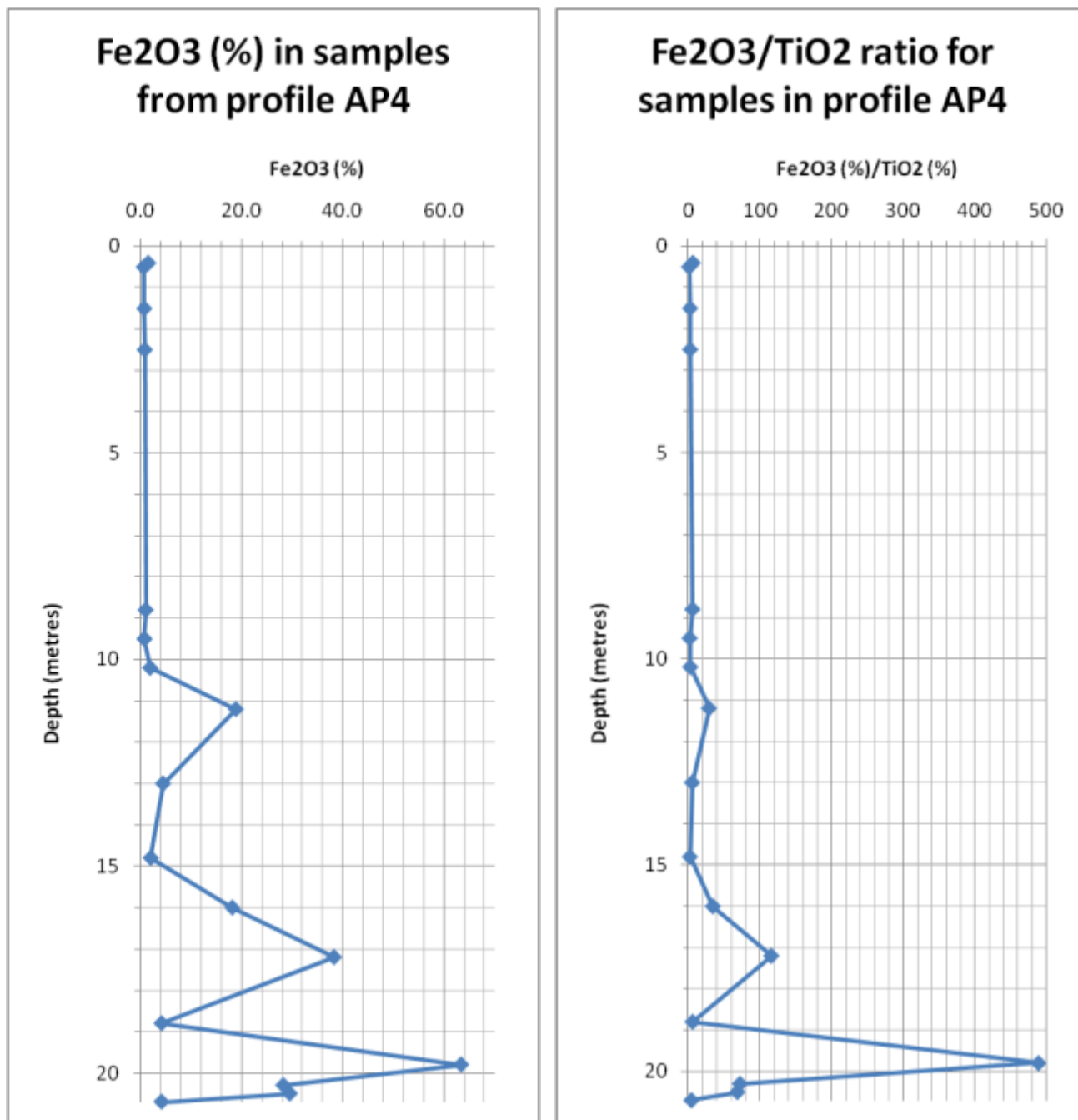
Fe₂O₃/Zr ratio for samples in profile AP2



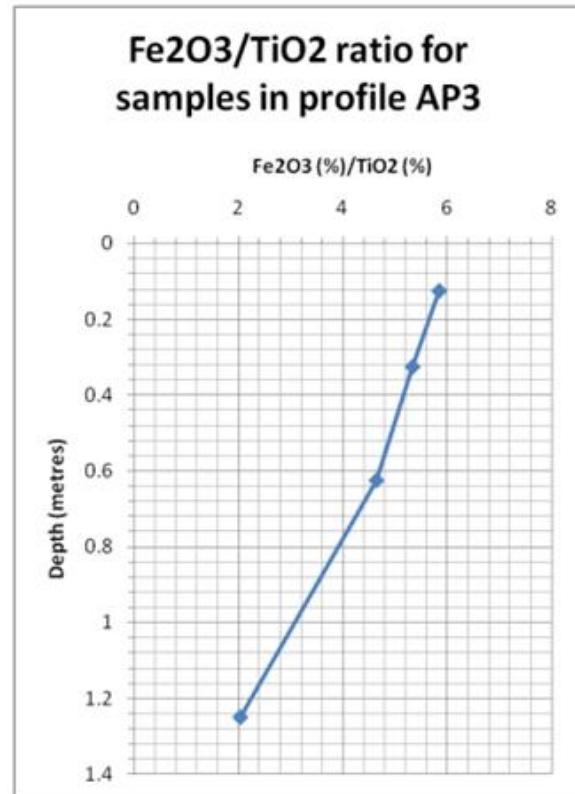
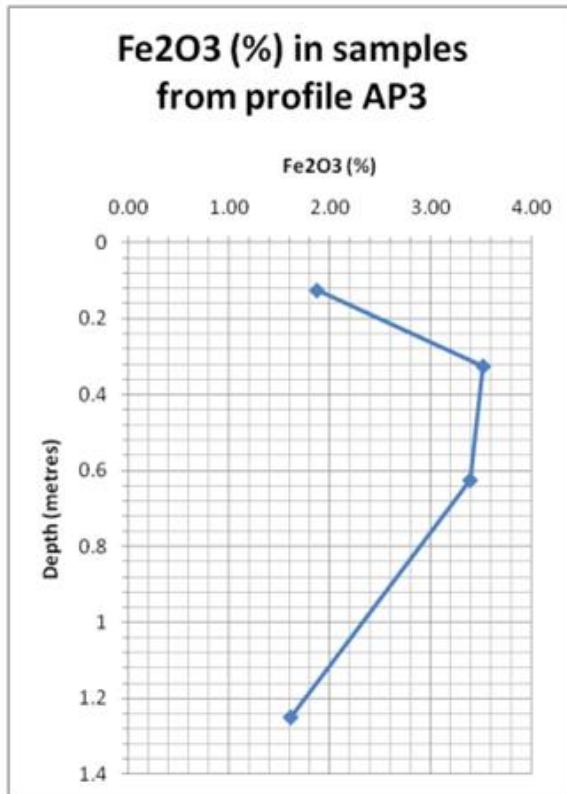
Fe₂O₃/Al₂O₃ ratio for samples in profile AP2



Appendix 28: Plots of Fe_2O_3 concentration and $\text{Fe}_2\text{O}_3/\text{TiO}_2$ against depth for samples from profile AP4.



Appendix 29: Plots of Fe_2O_3 concentration and $\text{Fe}_2\text{O}_3/\text{TiO}_2$ against depth for samples from profile AP3.



Appendix 30: The ferricrete layer of the Cadna-owie Formation, as seen in profile AP2 (Figure 11). Unit is seen in multiple regions within the study area indicating it is laterally extensive.



Appendix 31: Lag deposit of silicified conglomerate containing rounded quartzite pebbles. Located on the land surface above profile AP2.



Appendix 32: Hematite and goethite in fractures within the Bulldog Shale.



Appendix 33: Iron cementation on fracture surface of Arcoona Quartzite, in faulted region. Located at 0715115 mE 6627901 mN.

